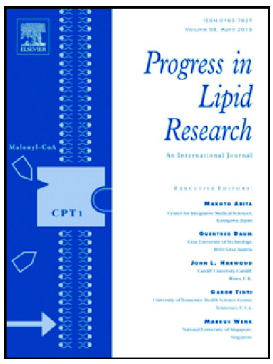

Structure, function, and regulation of thioesterases

Crystall Swarbrick, Jeffrey D. Nanson, Edward I. Patterson, Jade K. Forwood

PII: S0163-7827(20)30016-3

DOI: https://doi.org/10.1016/j.plipres.2020.101036

Reference: JPLR 101036

To appear in: *Progress in Lipid Research*

Received date: 25 February 2020

Revised date: 30 April 2020

Accepted date: 1 May 2020

Please cite this article as: C. Swarbrick, J.D. Nanson, E.I. Patterson, et al., Structure, function, and regulation of thioesterases, *Progress in Lipid Research* (2020), https://doi.org/10.1016/j.plipres.2020.101036

STRUCTURE, FUNCTION, AND REGULATION OF THIOESTERASES

Swarbrick, Crystall M.D.[a], Nanson, Jeffrey D.[b], Patterson, Edward I.[c], and Forwood, Jade K.[d#]

[a] Institute for Glycomics, Griffith University, Southport, Queensland, 4222 Australia.
[b] School of Chemistry and Molecular Biosciences, Institute for Molecular Bioscience, and Australian Infectious Diseases Research Centre, University of Queensland, Brisbane, Queensland, 4072 Australia.
[c] Departments of Vector Biology and Tropical Disease Biology, Liverpool School of Tropical Medicine, Liverpool L3 5QA, UK
[d] School of Biomedical Sciences, Charles Sturt University, Boorooma Street, Wagga Wagga, New South Wales, Australia.

[#]To whom correspondence should be addressed: Jade K. Forwood, School of Biomedical Sciences, Wagga Wagga, Australia, Tel: (+61) 7-69332317; Fax: (+61) 7-69332587; E-mail: jforwood@csu.edu.au.

Keywords: Thioesterase, Hydrolase, Coenzyme A, Fatty acyl-CoA, Hotdog domain, Regulation

CONTENTS

ABSTRACT

Thioesterases are present in all living cells and perform a wide range of important biological functions by catalysing the cleavage of thioester bonds present in a diverse array of cellular substrates. Thioesterases are organised into 25 families based on their sequence conservation, tertiary and quaternary structure, active site configuration, and substrate specificity. Recent structural and functional characterisation of thioesterases has led to significant changes in our understanding of the regulatory mechanisms that govern enzyme activity and their respective cellular roles. The resulting dogma changes in thioesterase regulation include mechanistic insights into ATP and GDP-mediated regulation by oligomerisation, the role of new key regulatory regions, and new insights into a conserved quaternary structure within TE4 family members. Here we provide a current and comparative snapshot of our understanding of thioesterase structure, function, and regulation across the different thioesterase families.

1. INTRODUCTION

Thioesterases are a large superfamily of enzymes that play important cellular roles. They catalyse the cleavage of thioester bonds that are present in a wide range of activated fatty acyl-coenzyme A (CoA) substrates, acyl-carrier proteins (ACPs), glutathione, and other cellular molecules (**Figure 1**). CoA-bound substrates are found as intermediates in many cellular biosynthesis pathways, including β-oxidation and synthesis of fatty acids, steroid synthesis, mevalonate and ketogenesis pathways, and include molecules such as acetyl-CoA, malonyl-CoA, acetoacetyl-CoA, propionyl-CoA, and arachidonoyl-CoA. In addition to these CoA-bound fatty acid substrates and cleaved reaction products being important intermediates and indicators of biological pathways, over-accumulation of these compounds can be toxic to the cell [1-8]. The toxicity of these acyl-CoA products can be reduced by binding to acyl-CoA binding proteins and membranes, and has been reviewed in [9]. Additionally, recent evidence has pointed towards acyl-CoA thioesterases playing a role in metabolic diseases, and as targets for management of obesity, diabetes, and non-alcoholic fatty liver disease [10].

Due to their widespread distribution, varied subcellular localisation (particularly in isoforms and spliced variants), vast substrates, and long history since their initial discovery in the 1950s [11, 12], one challenge in the thioesterase literature has been devising a consistent nomenclature for describing and categorising these enzymes. To better understand the structural and catalytic similarities shared within these enzymes, a classification system was devised whereby thioesterases were grouped into families based on sequence conservation, tertiary structure, active site configuration and catalytic mechanism [13]. Thioesterase families (TE) 1-13, and 24-25 are active against sulfhydryl bonds within fatty acyl-CoAs, TE14-19 cleave bonds between acyl-ACPs, TE20 and TE21 are protein-acyl hydrolases, and TE22 and 23 are glutathione-acyl hydrolases (**Figure 2**). Structurally, these families share common folds and oligomerisation states, which bring together requisite, but often varied active site configurations. Families TE4-15, and 24-25 possess a hotdog fold domain [13], with either single or double domains within their primary structure that self-associate to form higher order complexes. These hotdog domain thioesterases are found in both prokaryotes and eukaryotes (**Figure 3**). Families TE2 and TE16-22 contain an α/β hydrolase fold (**Figure 2**), are predominantly monomeric, and are found in both prokaryote and eukaryotes (**Figure 3**). The remaining families form three unrelated folds, NagB (TE1), Flavodoxin (TE3) and Lactamase (TE23) (**Figure 2**), and have evolved to perform the same catalytic function as hotdog and α/β hydrolase folds, representing examples of both

convergent and divergent evolution [14]. Moreover, the presence of domain duplication in a number of TE families is suggestive of a gene duplication event, whereby genes which were once in separate reading frames have been combined to form a single open reading frame containing multiple domains [15].

New insights into the regulatory mechanisms of thioesterase families have been elucidated recently through structural and molecular approaches. Here, we provide a snapshot of the structural and functional elements that govern thioesterase biology, including new mechanisms of regulation and focus on areas where our understanding has been challenged through recent literature reports.

2. STRUCTURE, FUNCTION, AND REGULATION OF THIOESTERASE FAMILIES

2.1. Hotdog fold thioesterases

The hotdog domain is the most common structural fold within the TE superfamily, present within TE4-15, 24 and 25 thioesterase families. The fold is comprised of an α-helix (representing the 'sausage' of the hotdog domain) surrounded by an antiparallel β-sheet (forming the 'bun'). The fold was first described in 1996 [16] for the *Escherichia coli* β-hydroxydecanoyl thiol ester dehydrase FabA, and there are now currently >85 depositions in the Protein Data Bank. The active site configurations and oligomerisation states vary considerably within thioesterases containing hotdog folds (described below). The active site is often found at the dimer interface of two hotdog domains, mediated through either intra- or inter-domain interactions depending on the domain organisation.

2.1.1 Acyl-CoA thioesterases

TE4 Family

Members of the TE4 thioesterase family, also known as TesB, acyl-CoA thioesterase II, and ACOT8 thioesterases, exhibit substrate specificity for short- to long-chain acyl-CoA, palmitoyl-CoA, and choloyl-CoA substrates [17-19]. TE4 thioesterases contain a conserved double hotdog fold, and structures have been solved from both prokaryotes *E. coli* (PDB 1C8U; [20]), *Yersinia pestis* (PDB 4QFW; [17]), *Mycobacterium avium* (PDB 3RD7; [21]), *Mycobacterium. marinum* (PDB 3U0A; [21]), *M. avium subsp. paratuberculosis* (PDB 4R9Z; [22]) and eukaryotes *Saccharomyces cerevisiae* (PDB 1TBU; [23]). Both prokaryotes and eukaryotes encode fused double hotdog domains (**Figure 3**), with a topology of α1-β1-β2-α2-β3-β4-β5-β6-*α3-β7-β8-α4-β9-β10-β11-β12*, where the hotdog domain boundary is indicated by italics (**Figure 4**). Active site residues within TE4 family members, confirmed through structure-guided mutagenesis, are conserved and comprised of an Asp located in the middle of the α4-helix, and Gln and Thr on β-strands 9 and 12, respectively [20] (**Figure 4**).

New insights into a conserved and unique quaternary structure within TE4 family members was reported in 2015 [17]. An octamer of hotdog domains (or tetramer of the double hotdog domain protomers) was identified in the TesB from *Y. pestis* (PDB 4QFW) and confirmed using a range of biophysical and structural approaches including analytical ultracentrifugation, size exclusion chromatography, small angle X-ray scattering data, mutagenesis, and X-ray crystallography. The same arrangement was identified in *E. coli* (PDB 1C8U), and *M. marinum* (PDB 3U0A). All members possess the Asp active site residue within a π-helix, centrally located in the α4-helix in

the second hotdog domain. An additional, distinctive structural feature of TE4 members is that they lack the C-terminal α-helix which is commonly found in other TE families.

The most functionally characterised TE4 eukaryotic family member is ACOT8. This enzyme localises to peroxisomes within humans, mice, and rats, where it is speculated to play a role in the catabolism of long-chain fatty acids (β-oxidation) [18] and branched-chain fatty acids [19]. ACOT8 expression is also increased in hepatocellular carcinoma development, possibly through lipolysis altering cellular levels of non-esterified fatty acids [24]. Subsequent knockdown of ACOT8 resulted in inhibited cell growth, which could be rescued by the addition of the non-esterified fatty acid myristic acid [24]. Prior to this report, a link between ACOT8 and metastatic lung cancer was proposed by Jung, Kim [25], however, whether over-expression is caused by, or results in the differences in tumor cell phenotype remains to be established. That ACOT8 is located in the peroxisome and has broad activity against short, medium and long acyl-CoAs, trihydroxycoprostanoyl-CoA and hydroxymethyl-glutaryl-CoA, with greatest activity levels for CoA esters of primary bile acids choloyl-CoA and chenodeoxycholoyl-CoA suggests that ACOT8 is a regulator of peroxisomal lipid metabolism [26]. These activities suggest ACOT8 can play a role in regulating bile acid formation and excretion, control the β-oxidation of a range of acyl-CoA metabolites, and regulate intracellular levels of free CoASH. Regulation of ACOT8 by binding of peroxisome proliferator activated receptor α (PPARα) to the promoter region provides a link between lipid metabolism and bile acid production [26]. Within mammals, the regulation of fatty acid concentrations is controlled by a range of transcription factors, with a number of these identified through binding and regulation studies including PPARs, sterol regulatory element binding protein-1c (SREBP-1c), and hepatic nuclear factors (HNF-4α and γ) [27]. PPARα is a key regulator of lipid metabolism [28]. PPARα is part of a steroid hormone nuclear receptor family, consisting of PPARα, PPARγ and PPARδ, which act as transcription factors regulating the expression of target genes by binding with promoter regions [29]. Finally, Liu *et al*. [30] showed ACOT8 interaction with the product of the HIV *Nef* gene may play a role in the down-regulation of CD4 during HIV infection. More recently, molecular characterisation of the ACOT8: HIV-1 Nef interaction was studied through *in silico* structural predictions and confirmed using *in vitro* functional assays [31]. It was shown that ACOT8 regions Arg^{45}-Phe^{55} and Arg^{86}-Pro^{93} were involved in Nef binding, with Lys^{91} playing a critical role in the interaction and when bound to ACOT8 degradation of Nef may be reduced.

TE5 Family

In contrast to members of the TE4 family, TE5 thioesterases (also known as thioesterase III, ybaW or FadM) are found solely in bacteria (**Figure 3**). They exhibit substrate specificity for long-chain acyl-CoA's and 3,5-tetradecadienoyl-CoA [32], and possess a single hotdog fold domain. To date, the structure of only one member from this family has been solved, FadM from *E. coli* (PDB 1NJK; [33]). This structure remains to be published, and since this limits our knowledge of the structural features of this family, here we provide a brief preliminary analysis of the deposited structure. The secondary structural elements of this enzyme are arranged in the topology β1-α1-α2-α3-β2-β3-β4-β5-α4 (**Figure 5**). The active site residues have not been formally tested, however the highly conserved Asp^{13} is predicted to be involved in catalysis based on structural superposition of related thioesterases (**Figure 5**) [13]. This family contains a single hotdog domain that likely associates as a "face-to-face" tetramer of hotdog domains

(**Figure 5**) based on the binding interface analysis (PISA [34]), and structural homology with other tetrameric hotdog thioesterases.

The function of FadM was first identified through deletion experiments in *E. coli* involving TesA and TesB [35]. These deletion mutants, when grown on oleate were shown to excrete 3,5-cis-tetradecadienoic acid, establishing that presence of a long-chain thioesterase other than TesA and TesB. When *E. coli* was grown using oleic acid as the sole carbon source, 90% of the oleic acid was completely metabolised by β-oxidation, and the remaining 10% only partially degraded to 3,5-cis-tetradecadienoyl-CoA. FadM prevents the accumulation of 3,5-cis-tetradecadienoyl-CoA, which cannot be further metabolised by β-oxidation, by hydrolysing 3,5-cis-tetradecadienoyl-CoA to 3,5-cis-tetradecadienoic acid which is subsequently released into the growth medium. It is proposed that the removal of 3,5-cis-tetradecadienoyl-CoA is required to prevent sequestration of CoA, and/or alleviate inhibition of enzymes controlling β-oxidation [32].

Regulation of *FadM* expression occurs through transcriptional regulation by the fatty acid global regulator, FadR [36]. The binding of FadR to a 17 bp promoter region immediately preceding the *FadM* gene has been shown to directly repress protein expression [36]. When fatty acids are the sole carbon source, long-chain acyl-CoA species (C16 and C18) bind the acyl-CoA binding domain of FadR, inducing conformational changes in the DNA binding domains, displacing it from the promoter and allow transcription and fatty acid metabolism to proceed [36, 37]. It is also worth noting that FadR transcription regulator has also been shown to activate the fatty acid synthesis promoter *fabH* which controls expression of the fatty acid biosynthesis operon *fabHDG* making FadR a regulator of both fatty acid degradation and synthesis [38].

TE6 Family

Family members of TE6 thioesterases have been well characterised both structurally and functionally. Members include ACOT7 (BACH, ACH1, ACT, CTE-II, LACH), ACOT11 (BFIT, Them2, STARD14), ACOT12 (STARD15) and YciA. TE6 thioesterases exhibit broad substrate specificity, ranging from short (C2; [39]) to long (C20:4; [4])-chain saturated fatty-acyl CoA's. A clear distinction exists in the domain organisation between prokaryotic and eukaryotic homologues. Prokaryotic TE6 thioesterases, exemplified by structures from *Campylobactor jejuni* (PDB 3D6L; [40]), *Haemophilus influenzae* (PDB 1YLI) and *Neisseria meningitidis* (PDB 5V3A, 5SZZ, 5SZY, 5TO2 and 5SZU; [39]), contain a single hotdog domain, whilst eukaryotic family members contain two fused hotdog fold domains, with representative structures determined from mouse ACOT7 (PDB 2Q2B, 2V1O; [4], 2QQ2; [41], 4ZV3; [42]) and ACOT12 (PDB 4MOB, 4MOC, 3B7K; [43]). The secondary structure topology is arranged as β1-α1-β2-β3-β4-β5 for prokaryotes and β1-α1-β2-β3-β4-β5-α2-*β6-α3-β7-β8-β9-β10-α4* for eukaryotes, where the second hotdog domain is in italics (**Figure 6**). A consensus active site for TE6 family members remains to be established, in part due to the differences in domain architecture. From mutagenesis studies and structural alignments of both prokaryote and eukaryote TE6 members, an Asp residue located on the central α-helix (α1 in prokaryotes, and α1 or α3 in eukaryotes), appears to be critical for catalysis (**Figure 6**). Eukaryotes also require an Asn for catalysis, located on a loop region connecting β1 and α1. Despite these differences in domain organisation and duplication, superposition of structures originating from prokaryotic and eukaryotic TE6 members highlight a conserved biological assembly (**Figure 6**) (see also below). The first eukaryotic TE6 member to be resolved structurally was Acot7 [4]. The N- and C- thioesterase

domains, both solved independently, formed the same hexameric quaternary structure [4]. Since the N- and C-terminal hotdog domains formed highly similar hexameric arrangements ("trimer of double hotdog dimers"), a model of the full-length protein was generated by superimposing and alternating the domains. The full-length model satisfied biophysical data including analytical ultracentrifugation, size exclusion chromatography, chemical crosslinking and mass-spectrometry [4]. The full-length structure revealed two non-identical putative active sites, and through mutagenesis, it was shown that one of two possible active sites was responsible for catalysis and comprised of Asn^{24} and Asp^{213}. The other non-conserved putative active site had no effect on thioesterase activity when residues Glu^{39} and Thr^{198} were mutated to Ala. This half-of-sites activity has been described subsequently in other TE6 members and across TE family members, however the cellular role remains to be elucidated [4].

The cellular roles of ACOT7 have been investigated using a range of approaches. The enzyme is expressed highly in the brain [44] (giving rise to its synonym brain acyl-CoA hydrolase (bACH)). In mouse conditional knockout trials, upon fasting, mice express a phenotype concurrent with neurodegeneration, and alterations in behaviour and physiology such as hypermetabolism, hepatic steatosis, dyslipidemia and behavioural hyperexcitability [45]. Other studies have established that ACOT7 is the predominant source of thioesterase activity in the brain, providing neurons the capacity to regulate fatty acid metabolism [45]. The enzyme is also highly over-expressed in activated macrophages and displays specificity for arachidonoyl-CoA. Here, ACOT7 releases arachidonic acid [4], the precursor for prostaglandins and eicosanoids [46], where it may supplement the well-characterised PLA_2-mediated pathway for inflammation. In support of this role, a recent report has established that overexpression of ACOT7 in mesenteric lymph nodes mediates a fat-induced inflammatory response [47].

The structural and functional role of ACOT12 has also been reported [48]. Together with ATP-citrate lyase [49] and cytosolic acetyl-CoA synthetase [50], ACOT12 regulates cytosolic levels of acetyl-CoA. Over-expression of ACOT12 has been characterised in the liver of mice [51], rats [52] and humans [53], where acetyl-CoA plays an important role in fatty acid synthesis [54, 55] and production of signalling molecules [56, 57]. The recent crystal structure of ACOT12 has highlighted a domain switching event in the hotdog domains when compared with ACOT7 [43]. This may result in reversal of the active site architecture, with the Asp active site residue located on the α-helix of the N-terminal hotdog domain, and Asn harboured within the C-terminal domain [43]. Interestingly, ACOT12 also contains a steroidogenic acute regulatory domain (START domain), positioned at the C-terminus to the two fused hotdog domains (**Figure 7**). START domains have been shown to function in binding and transport of lipids between membranes, and contain a deep lipid-binding pocket, shielding the lipid from the aqueous environment. A full length model of the ACOT12 was established through superposition of overlapping regions between the thioesterase domains of ACOT12, and the START domain of ACOT11, allowing analysis of the interactions between the START domain and thioesterase domains [43]. The structural basis for ACOT12 regulation was also elucidated in the same study, providing clarity in the literature regarding the mechanism of regulation of TE6 members. ACOT12 and ACOT11, both reciprocally regulated by ADP and ATP, were thought to be regulated by nucleotide-induced changes in the oligomeric assembly of the hotdog domains. ACOT12 was believed to be monomeric (and inactive) in the presence of ADP, and an active dimer and tetramer in the presence of ATP [51-53, 58, 59]. Similarly, ACOT11 was believed to

exist as an inactive monomer, with ATP binding inducing an active dimer formation [60]. However, the structure of ACOT12 revealed the oligomeric state is unaltered in the absence or presence of nucleotides. In both ligand bound and unbound forms, ACOT12 was a trimer of double hotdogs, similar to all TE6 thioesterases [43]. Rather than disruption of the quaternary structure, the mechanism of regulation occurred through two regulatory regions within the thioesterase domains. When bound to ADP, the C-terminal α-helix is constrained by these regulatory loop regions which tether the C-terminal α-helix (**Figure 7**). Upon binding with ATP, the γ-phosphate prevents the C-terminal helix from being locked through these regulatory domains. Since flexibility of the C-terminal α-helix is important for activity, the switch between ADP and ATP bound forms establish a structural basis for regulation [43].

Closely related to ACOT12, ACOT11 shares 55% sequence identity and similar domain architecture. The function of ACOT11 in brown adipose tissue was described recently in a double knockout mouse model, where ACOT11-deficient mice were shown to be resistant to obesity and associated diet-induced inflammation in white adipose tissue, displayed increases in energy expenditure, and diminished endoplasmic reticulum (ER) stress [61]. These observations were attributed to ACOT11 function in conserving calories by decreasing energy consumption within brown adipose tissue, a role that in conditions of nutritional excess promotes obesity and the production of excess non-esterified fatty acids which act to promote inflammation, insulin resistance and ER stress [60, 61].

The function of prokaryote TE6 members have also been well characterised. The YciA-type thioesterases have been investigated from both *E. coli* and *H. influenzae*, and show substrate specificity for a broad range of fatty acyl-CoAs including short, medium and long-chain acyl-CoAs. These functional studies, which in addition to the co-location of these genes within operon clusters have led to putative roles in membrane biogenesis during division, or insertion of transporter proteins [62, 63]. Despite encoding only single hotdog domains in the primary structure, prokaryote TE6 members form the same quaternary architecture as eukaryotic TE6 thioesterases [63] (**Figure 6**). An interesting corollary of prokaryote and eukaryote thioesterases containing one and two hotdog domains, respectively, in the primary structure, is that prokaryotic TE6 members contain six identical active sites, whilst eukaryote thioesterases contain non-identical active sites. Despite this, many TE6 enzymes characterised to date appear to utilise half of potential active sites. For example, in eukaryotes TE6 family members such as ACOT7 and ACOT12, half of the potential active sites are catalytically active, while the structurally related (but sequence disparate) site, is catalytically inactive [4]. In contrast, TE6 thioesterases from prokaryotes achieve a similar half-of-sites reactivity through a different mechanism since they are comprised of a single hotdog domain, and all six of the putative active sites are identical. Within related hotdog families several crystal structures have shown only half of the domains contain CoA, despite all domains containing equivalent active site configurations (PDBs: 4MOB, 4MOC [43], 3B7K, 4ZV3). Moreover, other single hotdog domain TE family members also exhibit CoA bound at only a fraction of the sites (PDBs 4R4U [17], 4ZRB [64], 5BYU, 5KL9). Substrate-induced structural rearrangements have been described in other thioesterase families [17, 64], although the exact functional role for half-of-sites activity from prokaryotes through to eukaryotes remains to be established. A half-of-sites reactivity has also been described more broadly, with a large number of enzymes including aldehyde

dehydrogenase [65], thymidylate synthase [66], aspartate receptors [67] and bacterial adenylyltransferase [68], all displaying a half-of-sites activity.

That thioesterases from disparate ends of the evolutionary spectrum have retained a half-of-sites reactivity through different mechanisms implies an important role in regulation and/or function, despite a clear cellular role being determined fully. Common mechanisms were identified between the *N. meningitidis* acyl-CoA thioesterase (NmACT) and human ACOT12 [39]. The NmACT enzyme, comprised of a hexamer of single hotdog domains and was shown to possess a GDP binding pocket at the dimer interface, and in close proximity to a disulfide bond. Mutational analysis of the GDP binding residues established Arg^{93} as an important binding determinant for the GDP interaction, with an $R^{93}E$ mutation resulting in a marked decrease in activity, suggesting GDP binding is important for the thioesterase activity of NmACT. Structural superposition of NmACT with the human ACOT12 enzyme identified significant similarities between the structural arrangement of hotdog domains and nucleotide binding sites suggesting a conserved regulatory mechanism [39].

TE7 Family

TE7 enzymes include members such as ACOT9 (also known as MT-ACT48) and ACOT10 (MT-ACT48.2), and display substrate specificity against short to long chain acyl-CoA's. These thioesterases exhibit a double hotdog domain structure, however there are currently no structures or active site architectures available. Based on sequence similarities of ACOT9 and ACOT10 thioesterases with known TE structures, we have produced a representative model of ACOT9 (**Figure 8**) using PHYRE with a 100% confidence level in the overall fold [69, 70]. The modelling suggests that ACOT9 is likely to exhibit a hotdog fold that assembles into a hexamer, or "trimer of double hotdog domains", similar to ACOT7 [4] and ACOT12 [43]. A putative active site residue based on superposition with ACOT7 suggests that Asp^{150}, positioned in the middle of the central α-helix of ACOT9, is potentially involved in catalysis.

Expression studies have shown ACOT9 is expressed widely in both mouse and human tissues whilst ACOT10, specific to the mouse genome, is expressed at very low levels. ACOT9 is localised in the mitochondria, with highest activity observed in brown adipose tissue and kidney mitochondria. Thioesterase activity was noted against both short and long chain acyl-CoA's, with activity against C12-CoA enhanced in the presence of the short chain acyl-CoA isobutyryl-CoA, as well as intermediate substrates of amino acid metabolism. As a result of its activity against short chain acyl-CoA's, ACOT9 is thought to be a "multi-purpose" thioesterase regulating lipid and amino acid metabolism in mitochondria. Regulation of ACOT9 activity is mediated by NADH and CoA, both of which are potent inhibitors, however no structural basis for this regulation has been determined [71].

TE8 Family

The TE8 thioesterase family is typified by thioesterases such as ACOT13 (also known as thioesterase superfamily member 2 (Them2)), which exhibit activity against long chain acyl-CoA's. These thioesterases contain a single hotdog fold domain, as exhibited across a number of structures including human ACOT13 (PDB 2F0X, [72]; 2H4U; [73]), human undecan-2-one-CoA bound ACOT13 (PDB 3F5O; [74]), mouse apo-Acot13 (PDB 2CY9; [75]) and zebra fish apo-Acot13 (PDB 4ORD; [76]). The secondary structural elements within this family are

arranged as α1-β1-β2-α2-β3-β4-β5-β6, and the catalytic active site is comprised of residues at the interface of a hotdog dimer involving an Asp, positioned within the middle of the central α2-helix, a Ser residue located on β3-strand of one hotdog chain, and an Asn residue located on a loop connecting β2-α2 of the other chain [74, 76]. The structures of both the apo- and substrate-bound ACOT13 reveal a tetramer of hotdog domains arranged in a back-to-back configuration of double hotdog dimers (**Figure 9**).

ACOT13 exhibits thioesterase activity against long chain fatty acyl-CoA substrates. Its expression is enriched in oxidative tissues and is associated with mitochondria. Cellular roles of ACOT13 in regulating hepatic glucose [77] and lipid metabolism [6] have been demonstrated using Them2$^{-/-}$ mice. Zebra fish embryos deficient in Them2 demonstrated retarded cell division [76], and more recently, a direct regulatory role was demonstrated in heat production and thermogenesis with likely functions in brown adipose tissue to suppress adaptive increases in energy expenditure [78]. Regulation of ACOT13 and its binding partner STARD2 (phosphatidylcholine transfer protein (PC-PT)), a fatty acid metabolism regulator, is mediated by PPARα [78, 79].

TE9 Family

The TE9 thioesterases are represented by acyl-CoA thioester hydrolase YbgC, and exhibit activity across a broad range of short to long chain acyl-CoAs, and 4-hydroxybenzoyl-CoA. They contain a single hotdog fold domain, and structures have been determined from *E. coli* (PDB 1S5U; [80], 5KL9; [81], 5T06 and 5T07; [82]), *Thermus thermophilus* (PDB 1Z54; [83]), *Helicobacter pylori* (PDB 2PZH; [84]), *Bartonella henselae* (PDB 3HM0; [85]), *P. aeruginosa* (PDB 5V10; [86]) and *Aquifex aeolicus* (PDB 2EGR, 2EGJ; [87]). TE9 thioesterases exhibit a topology of β1-α1-α2-α3-β2-β3-β4-β5-β6-α4, and active site residues Tyr, Asp, His (**Figure 10**). The Tyr and Asp residues are positioned on a loop connecting β1-α1, and the His located on α1. All TE9 quaternary structures exist as homo-tetramers, with the central α-helices positioned in a "face-to-face" configuration.

Whilst the function of YbgC thioesterases remain to be characterised fully, their gene organisation within the Tol-Pal gene cluster is suggestive of putative roles in cell envelope integrity. The Tol-Pal system is found in the majority of gram-negative bacteria, and consists of five core proteins (TolQ, TolR, TolA, TolB and Pal) with the additional genes for YbgC and YbgF located in the operon. This Tol-Pal system spans across the cell envelope and functions to maintain structure and function of the cell envelope and cell division [88, 89]. Whilst not consistently part of the Tol-Pal operon loss of YbgC function results in poor cell envelope integrity, cell division [90], increased sensitivity to drugs and detergents, and a phenotype indicative of defects in cell separation [91]. A proteomics analysis of the YbgC protein in *Salmonella enterica* serovar Enteritidis identified that the *ybgC* gene is required for survivability in the presence of whole egg white. Moreover, there was decreased expression of *tolR* and *tolA* in the *ΔybgC* mutant strain providing evidence of a link between the Tol-Pal system and YbgC [92].

The thioesterase activity of YbgC have been characterised in *E. coli, H. influenzae, and H. pylori*, with suggested roles in phospholipid metabolism [84, 93]. YbgC protein from *H.*

influenza exhibits preference for short-chain substrates [94], while *H. pylori* YbgC exhibts specificity for stearoyl-CoA (C18:0), correlating with the unusual fatty-acid profile within this organism, but also suggesting that YbgC's have evolved different substrate preferences. YbgC interacts with ACP *in vivo*, also suggestive of putative roles in phospholipid metabolism [95].

TE10 Family

The TE10 family members are represented by 4-hydroxybenzoyl-CoA thioesterase-I (4HBT-I), and exhibit activity towards 4-hydroxybenzoyl-CoA. They contain a single hotdog domain as characterised by the structures from *Pseudomonas* sp. (PDB 1BVQ; [96], 1LO7, 1LO8 and 1LO9; [97]) . The topology of this family is arranged as β1-α1-α2-α3-β2-β3-β4-β5-β6-β7-β8-α4 (**Figure 11**). Only one active site residue has been reported to date, involving a nucleophilic Asp^{17} located on the loop connecting β1-α1 which proceeds via an anhydride intermediate [97, 98]. The structure supports a homo-tetramer of hotdog domains arranged in a face-to-face orientation similar to TE9 family members (**Figure 11**).

Functionally, 4HBTs catalyse the final step in the 4-chlorobenzoate degradation pathway which converts 4-chlorobenzoate to 4-hydroxybenzoate in soil dwelling bacteria. This enzymatic pathway has the potential to play an important role in environmental detoxification, by degradation of 4-chlorobenzoate which is prevalent in from herbicide and pesticide use [99, 100].

TE11 Family

TE11 family members comprise 4HBT-II, EntH (YbdB) and YdiI type thioesterases, and exhibit activity towards 4-hydroxybenzoyl-CoA, 2,4-dihydroxybenzoate-holo-EntB (for enterobactin biosynthesis) and 1,4-dihydroxynapthoyl-CoA (for menaquinone biosynthesis), respectively [101]. They possess a single hotdog fold and representative structures have been determined from *Arthrobacter sp.* (PDB 1Q4S, 1Q4T, 1Q4U; [102], 3R32, 3R34, 3R35, 3R36, 3R37, 3R3A, 3R3B, 3R3C, 3R3D, 3R3F and 3TEA; [103]) for 4HBT-II; *E. coli* (PDB 1VH9; [104], 4K4C and 4K4D; [105]), *H. influenzae* (PDB 2B6E; [106] and 1SC0; [107]) and *P. aeruginosa* (PDB 4QD9; [108]) for YbdB; and *E. coli* for YdiI (PDB 4K4A, 4K4B, 4K49; [105], 1VH5, 1VI8; [104] and 1SBK; [109]). The secondary structural elements of this family are organised as α1-α2-β1-β2-α3-α4-α5-β3-β4-β5-β6, and active site residues are comprised of a nucleophilic Glu^{73} located on the central α-helix while Gly^{65} located between β2 and α2 from the neighbouring protomer polarises the thioester C=O via a hydrogen bond to the backbone amide [102]. The reported quaternary structure of this family is a back-to-back tetramer of hotdog domains (**Figure 12**).

Functionally, 4HBT-II perform catalysis of 4-hydroxybenzoyl-CoA for the removal of 4-chlorobenzoate [102, 110], appearing to have evolved to fulfil the same role as members of TE10 and utilise the same active site mechanism, however containing a different active site architecture. Extensive mutational and biochemical studies of the *E. coli* YbdB and YdiI thioesterases identified that differences in substrate specificity are the result of subtle differences in the alkyl/aryl binding sites. For example, residue M^{68} in YbdB is equivalent to V^{68} in YdiI, and a $M^{68}V$ in YbdB increased the catalytic efficiency of YbdB towards 1,4-dihydroxynapthoyl-CoA by ~50-fold. This increase in efficiency is thought to be the result of either the increased size of the substrate binding site or that by reducing the hydrophobic packing of the side chains

within the binding site promotes an open conformation similar to that seen in the YdiI structure [105].

TE12 Family

Members of the TE12 family comprise thioesterases that hydrolyse 1,4-dihydroxy-2-naphthoyl-CoA (DHNA-CoA) releasing 1,4-dihydroxy-2-naphthoate (DHNA). They exhibit a single hotdog fold domain, and the structures from *A. thaliana* (PDB 4K02; [111]), and two bacteria, *Synechocystis* (PDB 4K00; [111]) and *Campylobacter* (PDB 2HX5; [112]), have been determined. The topology of TE12 family members are arranged as α1-β1-α2-α3-α4-β2-β3-β4-β5-β6-β7-α5 and contain either an Asp or Glu catalytic residue located on a flexible loop between α2 and α3. TE12 members form a tetramer in a face-to-face arrangement (**Figure 13**).

The release of DHNA is an essential step in the synthesis of phylloquinone (vitamin K_1) and menaquinone (vitamin K_2), catalysed by thioesterases of the TE12 family, in photosynthetic organisms. Consequently, these thioesterases are expressed frequently in cyanobacteria and plants [111]. This activity provides the naphthoquinone ring that is coupled subsequently to the polyisoprenol side chain of vitamin K and then methylated. The role of vitamin K differs amongst photosynthetic organisms and mammals: in bacteria vitamin K_2 is used as an electron transporter in the respiratory chain; plants use vitamin K_1 as the one-electron carrier in photosystem I; while mammals, which cannot synthesise their own vitamin K_1 require it for blood coagulation, bone and vascular metabolism, cell signalling and cell cycle regulation [113].

TE13 Family

The TE13 thioesterase family members are PaaI type thioesterases, named for their presence in the phenylacetic acid *paa* gene cluster, and exhibit activity against short and medium chain acyl-CoA, as well as several hydroxyphenylacetyl-CoA substrates. They exhibit a single hotdog fold, and representative structures have been solved from *E. coli* (PDB 1PSU and 2FS2; [114]), *P. aeruginosa* (PDB 1ZKI; [115]), *S. pneumoniae* (PDB 4I82, 4ZRF, 4ZRB, 4XY5 and 4XY6; [64]), *S. mutans* (PDB 3LBB and 3LBE; [116]), *S. aureus* (PDB 4M20, 5EP5; [117], 4YBV; [118]) and *T. thermophilus* (PDB 1J1Y, 1WLU, 1WLV, 1WM6, 1WN3; [119] and 2DSL; [120]). The topology of this family is arranged as α1-β1-β2-α2-α3-β3-β4-β5-β6 with residues important for catalysis including Asn, Asp and Thr (SpPaaI). The location of these active site residues is shown in Figure 14 [64, 115]. The quaternary structure is a tetramer of hotdog domains in a back-to-back arrangement (**Figure 14**).

The mechanism by which bacteria metabolise phenylacetate has been described previously [121, 122], and involves a large enzyme pathway encoded by the gene cluster *Paa*ABCDEFGHIJKXYZ. Phenylacetate is converted into phenylacetyl-CoA by phenylacetate-CoA ligase, and this product then undergoes a series of degradative steps through ring hydroxylation, ring opening and β-oxidation type degradation [123]. The PaaI thioesterases release CoA from phenylacetyl-CoA, as well as mono- and dihydroxylated compounds 4-hydroxyphenylacetyl-CoA, 3-hydroxyphenylacetyl-CoA, 3,4-dihydroxyphenylacetyl-CoA, and 3,5-dihydroxyphenylacetyl-CoA. These are early intermediates of the pathway and are thought to assist in avoiding CoA depletion in the bacterial cell as a result of dead-end products [114].

A structural basis for regulation of the PaaI thioesterases revealed an induced fit mechanism, involving a half-of-sites reactivity [119]. Binding of CoA at two of the four protomer sites in the *T. thermophilus* PaaI was shown to be mediated through a rigid-body rearrangement of the subunits, resulting in negative cooperativity by preventing further binding in the remaining two sites [119]. The induced fit mechanism was explored further in the *S. pneumoniae* PaaI thioesterase (SpPaaI) [64]. Interestingly, the SpPaaI thioesterase demonstrated higher activity towards medium chain-length fatty acyl-CoA substrates and when crystallised with CoA this was shown to bind at half the possible binding sites. Within the CoA bound subunits this induced a 34Å conformational change in the first 11 N-terminal residues changing β1 to an α-helix displacing Tyr38 and Tyr39 away from the substrate binding site allowing for the fatty acyl-CoA substrate to bind [64].

TE24 Family

Members of the TE24 family include fatty long-chain acyl-CoA thioesterase (Fcot) and type III thioesterases. They are found only in prokaryotes and contain a single hotdog fold. The Fcot thioesterase of *Mycobacterium* (Rv0098) is part of an operon with five other genes. The operon is conserved in pathogens *Mycobacterium leprae, M. bovis*, and *M. avium*, and the genes express a member of the PPE (Pro-Pro-Glu motif) family, an oxidoreductase, a fatty acid AMP ligase, an acyl carrier protein, and a nonribosomal peptide synthase. The genes are not essential for the growth of *Mycobacterium*, but are required for the survival of Mycobacterium in mice [124, 125].

The TE24 family members display activity against long-chain acyl-CoAs, with the greatest activity observed for palmitoyl-CoA [94]. The enzyme is proposed to be part of a lipopeptide-synthesis pathway, and in *M. bovis*, the operon was demonstrated to be essential in the synthesis of the virulence-enhancing lipids.

The only structure of a TE24 thioesterase available is from *M. tuberculosis* (PDB 2PFC; [94]). The topology of the structural elements is arranged as α1-β1-β2-α2-α3-β3-β4-β5-β6. The quaternary structure is distinctly different to other TE family members, displaying a hexamer with three dimers arranged 'head to tail' [126]. This was shown to be consistent with the elution profile during size exclusion chromatography. In the trimer of dimer configuration, each dimer is comprised of two identical protomers, with the dimers joining together in a head to tail arrangement, forming a triangle. Whilst a trimer of dimer arrangement of hotdog domains has been characterised in TE families TE6 and TE7, the arrangement of these dimers into a triangle is distinctly unique.

The structure was also solved with bound dodecenoate, assisting with the mutational analysis to describe active site molecules. Each dimer contains two putative symmetrically related active sites at the interface. Putative active site residues positioned near the thioester were considerably different to known active site residues of other thioesterases families. For example, neither Asp or Glu were in close proximity to the active site to act as a general base, and Thr or Ser, commonly associated with type II thioesterases, was also missing. From a total of seven structure-guided mutants, Tyr^{66}, Tyr^{33}, and Asn^{74} were shown to abolish activity of the enzyme [126]. Overall, these family members lack a nucleophile or a general base that is characteristic of other TE families, but rather, contain active site residues involving a Tyr located on the central α-helix, and Tyr and Asn residues located on a flexible loop (**Figure 15**).

TE25 Family

The most well characterised TE25 thioesterase is a flouroacetyl-CoA thioesterase (FlK). These enzymes harbour a single hotdog domain, and representative structures have been solved from *Streptomyces cattleya* (PDB 3KUV, 3KUW, 3KV7, 3KV8, 3KVI, 3KVU, 3KVZ, 3KW1, 3KX7, 3KX8; [127], 3P2Q, 3P2R, 3P2S, 3P3F and 3P3I; [128]) and *T. thermophilus* (PDB 2CWZ). The conserved secondary structural elements of this family are arranged as β1-α1-β2-β3-β4-β5-α2 and the active site is comprised of residues from two monomers, formed at the dimer interface of residues Thr and His located on the central α1-helix of one domain, and a flexible loop region between β2 and β3 [127]. These thioesterases form dimers with the active site located at a tight dimer interface (**Figure 16**).

The FlK from *S. cattleya* exhibits specificity for flouroacetyl-CoA, but not acetyl-CoA [127], conferring resistance to fluoroacetate, a surprisingly toxic organofluorine naturally produced by many plants [128]. This selectivity is important for ensuring acetyl-CoA is not cleaved and removed from the pool of metabolic intermediates. The catalytic mechanism has been resolved and involves the imidazole moiety within His^{76} acting as a base, and deprotonating the hydroxyl side chain of Thr^{42}. This activated nucleophile attacks the substrate and forms a transition intermediate. A water molecule is involved in stabilising the His^{76} residue. Interestingly, Glu, which is a catalytic residue in many type II thioesterases, does not contribute to the catalytic mechanism, but does maintain the active site configuration [127].

The main reported function of FlK thioesterases is linked directly to the hydrolysis of flouroacetyl-coenzyme A to produce fluoroacetate and CoA. This has important implications in the regulation of the tricarboxylic acid cycle since the substrate can be utilised by citrate synthase to produce 2-flourocitrate, which can be converted into 4-hydroxy-trans-aconitate, an inhibitor of aconitase, which catalyses the tricaboxylic acid [128, 129].

Proposed TE26 Family

This thioesterase family has not yet been formally assigned by the ThYme server, however we recommend that the thioesterases Them4 (Thioesterase superfamily member 4) and Them5/ACOT15 be assigned this family based on their unique quaternary structure and active site architecture. Structural characterization of these PaaI-like thioesterases revealed that the hot-dog domains form a dimer assembly [130]. This quaternary structure is unique given that PaaI-like thioesterases otherwise form "back-to-back" tetramers, and are represented in only two hotdog thioesterase families **(Figure 3; Table 1)**. Together with the assigned active site architecture described below, we believe these disparate dimeric and tetrameric assemblies provides a strong basis for their separation into a distinct family. Them4 and Them5 exhibit substrate specificity for long-chain acyl-CoAs, and possess a single hotdog fold domain in both Them4 (PDB 4AE8; [130]) and Them5/ACOT15 (PDB 4AE7; [130]). The conserved topological structural elements are arranged as α1-β1-β2-α2-β3-β4-β5-β6, and catalytic residues are located at the dimer interface consisting of a HGG motif located at the end of the central α-helix of one monomer, and conserved Asp and Thr residues from the other monomer in the central α-helix and loop region between α2 and β3, respectively **(Figure 17)** [130].

The cellular function of ACOT15 has only recently been determined through knockout mice studies by Zhuravleva *et al*,[130] demonstrating its activity against C18 polyunsaturated fatty acids, and its specific role in cardiolipin remodelling and lipid metabolism [130]. ACOT15$^{-/-}$ mice experienced a 2-fold increase in monolysocardiolipin, a specific metabolite of cardiolipin, and developed fatty liver as well as altered mitochondrial morphology and function. These physiological symptoms all correlate with a function of ACOT15 in cardiolipin remodeling and it was proposed that ACOT15 controls this process by regulating the pool of acyl groups with an emphasis on linoleyl, which reacylates stearoyl- and palmitoyl-containing monolysocardiolipin species in the cardiolipin cycle [130].

2.1.2. ACP Thioesterases

TE14 Family

The TE14 family exhibit substrate specificity for short to long chain acyl-molecules linked to ACP rather than CoA, and are found in both prokaryotes and eukaryotes. The main reported function of TE14 family members is to control the chain length and saturation state of fatty acids, with their specificity reflecting the profile of the major fatty acids in plants. The elongation of fatty acids in plants occurs in plastids and is mediated by fatty-acid synthase. Malonyl-ACP is condensed with either acyl-CoA or a previously synthesised acyl-ACP derivative to elongate the carbon chain by two units per cycle, with this process terminated by the activity of the TE14 acyl-ACP thioesterases FatA and FatB [131]. In essentially all plants the major products of fatty acid biosynthesis are oleate and palmitate, with FatA and FatB showing the greatest activity against oleoyl-ACP and palmitoyl-ACP respectively [132]. The FatB-type thioesterase from the California bay plant (*Umbellularia californica*), with specificity for medium chain fatty acid lauroyl-CoA [133], was first identified for its potential in the industrial production of detergent [134]. Medium chain-length fatty acids have a number of industrial uses [134-136] and, subsequently, the FatBs of a large range of plants have been extensively investigated for their chain-length specificities [137].

There are currently four TE14 structures available, from *Lactobacillus plantarum* (PDB 2OWN; [138]), *Bacteroides thetaiotaomicron* (PDB 2ESS; [139]), *Spirosima linguale* (PDB 4GAK; [140]) and *Umbellularia californica* (PDB 5X04; [141]). TE14 thioesterases consist of two tandem hot dog domains termed the N-terminal hotdog and the C-terminal hotdog domains. The structural topology of 5X04 is arranged α1-α2-β1-α3-α4-α5-β2-β3-β4-β5-α6-α7-α8-β6-α9-α10-α11-β7-β8-β9-β10, with helices α4and α10 forming the central α-helix of the N-terminal hotdog and C-terminal hotdog domains respectively. The crystal structures of TE14 members, in addition to non-crystallographic studies suggest that TE14 thioesterases form a dimer in solution (or essentially a tetramer of hotdog domains) [141-143].

The active site of TE14 thioesterases was previously predicted to be comprised of a Cys-His-Asn catalytic triad (**Figure 18)** [13]. However, structural alignment between the TE14 structures reveals a network of potentially catalytic residues, Asp^{281}, Asn^{283}, His^{285}, and Glu^{319}, located on the periphery of the C-terminal hotdog domain. Feng *et al.* [141] established that D^{281}N and H^{285}A mutations in *U. californica* FatB (UcFatB) abolished enzyme activity, while N^{283}A and E^{319}A mutants retained ~3% activity, thus confirming the importance of these residues. Mutation of the predicted Cys active site residue to Ala resulted in approximately 70% reduced activity compared to wild-type, thus it is possible that this Cys residue is important for substrate binding

but not catalytic activity, or that mutation of this residue perturbs the function of the conserved adjacent Glu^{319}. Furthermore, multiple sequence alignment of 1019 acyl-ACP TE sequences collected from the ThYme database revealed that Cys^{320} is only conserved among 22% of the 1019 sequences, and appears restricted to plant acyl-ACP TEs [144].

Docking and mutational studies suggest that the binding of acyl-ACP substrates to TE14 thioesterases results in a conformational change to an open conformation, whereby a β-strand is proposed to act as a lid domain, moves to accommodate the incoming acyl chain. The substrate binding pocket is formed by residues on the first hotdog domain, and dictates the length of acyl chain that can be accommodated. Binding of the substrate positions the thioester bond adjacent to the catalytic network. Two similar mechanisms have been proposed based on the structures of TE14 thioesterases, and while they differ in the exact role of the catalytic residues, in general, both mechanisms involve a nucleophile that attacks the thioester carbonyl carbon to form an acyl-anhydride intermediate, which is subsequently hydrolysed by water molecules to release non-esterified fatty acids [141, 144].

TE15 Family

Members of TE15 have only been identified in bacteria and exhibit substrate specificity for linear intermediates of the antitumor antibiotics calicheamicin and neocarzinostatin linked to ACP. TE15 family protomers contain a single hotdog domain, with the secondary structural elements arranged β1-α1-α2-α3-β2-β3-β4-β5-α4. Representative crystal structures have been determined from *Micromonospora echinospora* (CalE7; PDB 2W3X; [145]), *Micromonospora chersina* (DynE7; PDB 2XEM; [145]), and *Streptomyces globisporus* (SgcE10; PDB 4I4J; [146]). As evidenced by the crystal structures and size exclusion chromatography experiments, TE15 thioesterases form tetramers in solution, with two monomers forming a tandem hotdog domain arrangement in a dimer of dimers arrangement (**Figure 19**).

The structure of CalE7 revealed a novel active site which lacks the catalytic Glu or Asp residue conserved in other hotdog fold thioesterases. Rather, Arg^{37}, located on the central α-helix, catalyses the hydrolysis of the thioester bond, and Tyr^{29}, located on the adjacent hotdog central α-helix, in combination with a hydrogen bonded water network, decarboxylate the β-ketocarboxylic acid intermediate [145]. The crystal structures of DynE7 and SgcE10 reveal that these two residues are conserved amongst CalE7, DynE7, and SgcE10. Furthermore, all three enzymes display four possible active sites, two at each dimer interface. Despite containing the four possible active sites, Kotaka *et al.* [145] and Liew *et al.* [147] propose that dimerisation of two CalE7 or DynE7 protomers forms an L-shaped substrate binding channel, with an entrance in one subunit and an exit in the adjacent subunit. As such, there would only be two functional active sites in the tetrameric structure, which is consistent with the half-of-sites mechanism(s) observed in other hotdog fold thioesterase families.

The putative substrate binding channel is comprised of a short hydrophilic entrance (located at the outer channel) and a phosphopantetheinyl binding site, as well as a hydrophobic region (on the inner channel) that extends inside the other subunit. This hydrophobic region is enclosed by residues from helices α1, α2, and α3, with the β5-α3 loop acting as a flexible gate that controls access to the substrate binding channel. Residues Arg^{37}, Glu^{36}, and Thr^{60} from one monomer, and Asn^{19} and Tyr^{29} from the other monomer, form part of this substrate binding channel [145, 147].

In addition to tetrameric TE15 thioesterases displaying only two substrate binding channels, Liew *et al*. [147] suggest that upon ligand binding, the flexible β5-α3 loop, helices α1 and α2, and strand β2, undergo conformational changes that elongate and widen the substrate binding channel of one dimer, and appear to close the other substrate binding channel of the opposing dimer. This suggests that TE15 thioesterases undergo ligand induced negative cooperativity that reduces the tetramer to one functional active site at a time.

The recruitment of hotdog thioesterases for polyketide synthesis is quite unusual, with only a few examples of hotdog thioesterases having substrates not attached to CoA. The polyketide synthase CalE8, in conjunction with the thioesterase CalE7, catalyse the biosynthesis of the enediyne moiety of neocarzinostatin and calicheamicin [148-150]. While the exact function of CalE7 within this multi-enzyme system is not fully understood, it has been suggested to play a role in removing aberrant products from the polyketide synthase in a similar manner to polyketide synthase α/β hydrolases [145].

2.2. α/β Hydrolases

The α/β hydrolase fold, present in TE families 16-19, is highly conserved, with homologues present across prokaryotes and eukaryotes [151]. Initial studies describing thioesterase activity from α/β hydrolases were reported in rat liver in response to peroxisome proliferator activated receptor α [152]. The first mammalian α/β hydrolase thioesterase structure was determined from bovine palmitoyl protein thioesterase 1, with significant similarities to a eukaryotic myristoyl-ACP-specific α/β hydrolase thioesterase [153]. The active site mechanism of this family forms a catalytic triad, comprising a nucleophile, catalytic acid, and His [154]. The α/β hydrolase fold is comprised of a twisted 8-11 stranded β-sheet in which most of the strands are parallel, with α-helices flanking each side, and substrate selection often conferred through a flexible lid domain [155].

Many of the α/β hydrolase thioesterases are found as part of multi-domain assembly enzymes, including fatty acid synthase (FAS), polyketide synthase (PKS), or non-ribosomal peptide synthetase (NRPS) [156-158]. The thioesterase domains contained in each of these large protein complexes catalyse either cyclisation, termination, or the removal of aberrant products throughout synthesis. Most commonly, the thioesterase domain of these complexes provides an unloading mechanism, serving to release cargo from the phosphopantetheine arm of an ACP. The substrate specificity of the thioesterase domain can play a role in determining the synthesis of FAS, PKS, or NRPS products. For example, the thioesterase domain present in FAS enzymes regulates the synthesis of long chain fatty acids [159, 160], whereas the thioesterase domains present in PKS and NRPS enzymes regulate the production of secondary metabolites, a number of which possess therapeutic and antibiotic properties [1, 161-163].

2.2.1 Acyl-CoA Thioesterases

TE2 Family

Members of the TE2 family include ACOT1-6, and the bile acid-CoA amino acid N-acyltransferase (BAT) thioesterase. These enzymes exhibit activity for long-chain fatty acyl-CoAs (ACOT1 and 2), short and long-chain acyl-CoAs (ACOT3, 4 and 5), dicarboxylic acyl-CoA (particularly succinyl-CoA) esters (ACOT4) and methyl-branched acyl-CoA esters (ACOT6). Structures have been determined for two members, human ACOT4 (PDB 3K2I; [164]) and ACOT2 (also known as MTE-I and PTE2) (PDB 3HLK; [165]). The secondary

structural elements are arranged as β1-β2-β3-α1-β4-α2-β5-α3-β6-β7-α4-β8-α5, and unlike the hotdog fold hydrolases, the quaternary structures reported to date are all monomeric **(Figure 20)**. Active site residues, Ser^{294} located between β5 and α3, His^{422} located in the flexible loop region between β8 and α5, and Asp^{388} located in the flexible loop region between β7 and α4, are typical of α/β hydrolases.

ACOT1 and ACOT2 are expressed in the cytosol and mitochondria of the heart respectively and are regulated by PPARα in response to non-esterified fatty acid availability. The up-regulation of ACOT1 and ACOT2 within heart and contractile muscle of rats fed a high fat diet [166, 167] is thought to be an adaptive mechanism to prevent insulin resistance and maintain β-oxidation at a steady state during periods of fatty acid oversupply [5]. ACOT4 in humans has been speculated to have adapted the role of Acot3, Acot4 and Acot5 of other mammals. This is based on the broad spectrum activity of ACOT4 covering the combined activity profiles of Acot3-5, and humans encoding only ACOT4, whilst Acot3-5 are expressed in mouse tissues [168]. Additional functions of ACOT4 have stemmed from its activity against succinyl-CoA in conjunction with its peroxisomal location, and its over-expression in the kidneys where it can hydrolyse succinyl-CoA, a product of β-oxidation, to produce succinate, which is excreted in urine [18].

2.2.2 Acyl-ACP Thioesterases

TE16 Family

Thioesterases from the TE16 family are present in multienzyme complexes such as FAS, PKS, and NRPS. They typically exhibit substrate specificity for long chain acyl-ACP's, various polyketides, and non-ribosomal peptides, cleaving the bond between ACP or polypeptide carrier protein (PCP) and an acyl molecule. They exhibit a traditional α/β hydrolase domain, with a lid domain above the active site region containing a Ser-His-Asp catalytic triad. Representative structures have been solved for the human (PDB 1XKT; [159], 4Z49; [169], 2PX6; [170], 3TJM; [171]) and porcine (PDB 2VZ8 and 2VZ9; [160]) FAS thioesterase domain, the PKS thioesterase domain from *Aspergillus parasiticus* (PDB 3ILS; [161]) and *Bacillus subtilis* (PDB 4U3V; [172]), and the NRPS thioesterase domain from *B. subtilis* (PDB 2CB9; [163] and 1JMK; [1]) and *E. coli* (PDB 3TE7; [173]). The structure of fengycin thioesterase (FenTE; PDB 2CB9; [163]) suggests the role of the lid region is to control access to the active site and prevent binding of unwanted substrates more so than actively contributing to substrate binding [163]. The topological arrangement of PDB 2CB9 is β1-β2-α1-β3-α2-β4-α3-β5-α4-β6-α5-α6-β7-α7-α8 (**Figure 21**), with a monomeric quaternary structure, similar to other α/β hydrolases.

The TE16 family contains thioesterases from a number of multi-enzyme systems, the function of which is generally well characterised. Human FAS is upregulated in a number of cancers [174, 175], and as such, each of the domains presents an attractive target for anticancer drugs [8]. The FAS thioesterase domain (PDB 1XKT, 4Z49, 2VZ8) terminates the biosynthesis of palmitic acid by cleaving it from ACP in order to regulate the length of fatty acid released from FAS [159]. This protein forms the thioesterase domain in Claisen cyclase to produce aflatoxin, a common contaminant of nuts and grains [161].The NMR structure of the *E. coli* NRPS thioesterase domain (PDB 2ROQ) revealed the interaction between the *E. coli* enterobactin synthetase EntF NRPS subunit thiolation and thioesterase domains. Enterobactin is an iron acquisition siderophore which increases the virulence of a number of bacteria [176]. The NRPS thioesterase

domain of EntF catalyses the production of an oxoester bond between its own active site and the substrate (dihydroxybenzoate (DHB) or Ser), which is then recycled through the synthase twice to produce a tethered DHB-Ser trimer, followed by cyclisation before it is released by the thioesterase [162]. In a similar manner, fengycin thioesterase from *B. subtilis* (FenTE; PDB 2CB9) catalyses the cyclisation of fengycin to produce a lactone bond and initiate product release [163], the surfactin thioesterase from *B. subtilis* (SrfTE; PDB 1JMK) catalyses a cyclisation and product termination to produce the cyclic macrolactone surfactin [1], and the terminal thioesterase domain of valinomycin synthetase (VLM2; PDB 6ECB, 6ECC) catalyses the oligomerisation and cyclisation of tetradepsipeptidyl intermediates to produce valinomycin [177].

Typical of TE16 thioesterases, a helical lid region covers the catalytic triad and appears to play a role in regulating catalysis, with the lid region not only interacting with the carrier protein to which substrates are tethered, but also playing a role in substrate orientation [162, 177]. In the case of VLM2, comparison of apo (PDB 6ECB, 6ECC) and ligand-bound structures (PDB 6ECD, 6ECE, 6ECF) reveals that the lid region adopts multiple conformations depending upon the extent of oligomerisation, and ultimately controls cyclisation [177]. As such, the lid region of TE16 thioesterases likely plays a key role in determining the oligomerisation and cyclisation of the TE16 products.

TE17 Family

The members of TE17 harbour a PKS type α/β hydrolase domain, which exhibits activity towards polyketides. Currently, structures have been solved from three representative members of this family, including *Saccharopolyspora erythraea* (PDB 1KEZ; [178], 1MO2; [179], 5D3K, 5D3Z; [180], 6MLK; [181]), *Streptomyces sp. CK4412* (PDB 3LCR; [182]), and *Streptomyces venezuelae* (PDB 1MN6, 1MNA, 1MNO; [179], 2H7X, 2H7Y; [183], 2HFJ and 2HFK; [184]). Like TE16, TE18, and TE19 family thioesterases, TE17 family members typically harbour a Ser-His-Asp catalytic triad positioned along a substrate binding pocket [178, 179, 183, 184]. The topology of TE17 family members is arranged α1-β1-β2-β3-α2-α3-β4-β5-α4-β6-α5-β7-α6-α7-β8-β9-α8 (**Figure 22**), with a dimeric quaternary structure, differentiating this family from TE2 and TE16.

The biosynthesis of polyketides, complex organic compounds that often form the basis of human and veterinary drugs, utilises a complex of multifunctional enzymes assembled to form the PKS. The PKS thioesterase structures from 6-deoxyerythronolide synthase (DEBS TE; PDB 1KEZ, 1MO2, 5D3K, 5D3Z, 6MLK) and pikromycin synthase (PICS TE; PDB 1MN6) revealed insights into the substrate channel architecture and substrate specificity. Each of these PKS thioesterases catalyses the cyclisation and release of a heptaketide chain via lactonisation. The Ser^{142}, Asp^{169}, and His^{259} catalytic triad of DEBS TE, situated at the centre of a substrate channel that runs ~20Å across the length of the protein, is also observed in PICS TE. The catalytic Ser residue is positioned at the nucleophilic elbow between β6 and α5, a characteristic feature of α/β hydrolases. Regulation of substrate binding is thought to occur through a flexible loop acting as a lid located between residues 175-200, helix α6 in DEBS TE, and helices α6 and α7 in PICS TE. The structures of DEBS TE and PICS TE crystallised at differing pH values demonstrate pH induced conformational changes, with the lid region closing to form a long substrate channel in DEBS TE structures crystallised at a pH ≤7.5 (PDB 1KEZ, 5D3K, 5D3Z), whereas the crystal

structure of DEBS TE at pH 8.5 displays an open conformation. A similar widening of the substrate binding channel is observed in PICS TE structures at pH 7.6, 8.0, and 8.4.

Additional pH induced conformational changes are observed in the loop region between strands β8 and β9 (residues 230-250), and the short loop between the C-terminal of strand β9 and N-terminal of helix α9 (residues 255-260). Tsai *et al.* [144] suggest that at pH 8.5, the DEBS TE structure represents an inactive conformation. At this pH, the conformational change in the flexible lid region alters the loop between strands β8 and β9, which appears to partially unravel helix α9 and displace residues 255-260. As a result of these structural changes, the active site His^{256}, which resides on the short loop between the C-terminal of strand β9 and N-terminal of helix α9, is flipped ~180º and moved ~20Å away from the active site. However, both the DEBS and PICS thioesterase domains display catalytic active at pH 8 and pH 9, thus the pH 8.5 DEBS TE structure may represent an open conformation rather than an inactive one.

In both the DEBS and PICS TE structures, two hydrophobic α-helices (α1 and α2) at the N-terminus of each molecule mediate the dimer interface, forming a dimer along a two-fold axis [179]. Although the dimer interfaces are similarly maintained by hydrophobic interactions, composition of the interfaces differs, with the DEBS TE interface being Leu-rich, while the PICS TE interface is largely comprised of Phe residues [178]

The recent structure of the tautomycetin thioesterase (PDB 3LCR) revealed a PKS type thioesterase domain, which is not involved in the cyclisation of the hexaketide product, but rather is involved in hydrolysis of the substrate. Notably, it also contains an extra α-helix (α4) which is not present in either the DEBS or PICS thioesterases [182].

TE18 Family

In contrast to the many α/β hydrolases that are part of large FAS, PKS, or NRPS complexes, members of the TE18 family form independent enzymes that work in conjunction with other modular enzymes. They typically exhibit activity for medium chain acyl-ACP, various polyketides, and non-ribosomal peptides, and display a traditional α/β hydrolase topology with a Ser-His-Asp catalytic triad and a lid domain, as represented by the structures of RedJ from *S. coelicolor* (PDB 3QMV, 3QMW; [185]), RifR from *Amycolatopsis mediterranei* (PDB 3FLA, 3FLB; [186]), and SrfD (also known as SrfTEII) from *B. subtilis* (PDB 2RON; [187]). The secondary structure elements of TE18 thioesterases are arranged α1-β1-α2-α3-β2-α4-α5-β3-α6-β4-α7-α8-α9-α10-β5-α11-β6-α12-α13 (**Figure 23**), similar to members of the TE17 family, and also exist as dimers.

The rifamycin and prodiginine synthesis hybrid NRPS/PKS systems are composed of a number of NRPS and PKS modules, with a thioesterase (such as those from TE16 and TE17) releasing the substrate at the end of this pathway, and a TE18 thioesterase, RifR and RedJ, performing an editing function to prevent the accumulation of aberrant acyl-units from carrier domains [186]. TE18 thioesterases appear to predominantly carry out such editing functions, effectively regenerating the reactive thiol group of misacylated carrier proteins or thiolation domains (analogous to carrier proteins of multi-domain complexes) by catalysing the removal of CoA-derivatives and aberrant synthesis intermediates from the thiol group of the carrier protein or thiolation domain phosphopantetheine arm. The RifR thioesterase was shown to have greater

activity towards propionyl-ACP over methylmalonyl-ACP, enabling removal of the aberrant decarboxylated form, propionyl-CoA, and favoring the production of rifamycin from methylmalonyl-ACP [186]. Similarly, the production of prodiginine in *S. coelicolor* is edited by the thioesterase, RedJ (PDB 3QMV; [185]), which transfers dodecanoyl-CoA tethered to RedQ to RedL, which in turn elongates the substrate to proceed through the pathway [185, 188]. The thioesterase SrfD, from *B. subtilis*, fulfils this editing role in surfactin NRPS systems. The NMR structures of SrfD in an unligand bound form (PDB 2RON) as well as in complex with the thiolation domain of TycC3 (the third subunit of the tyrocidine C module from *Brevibacillus parabrevis*) (PDB 2K2Q) reveal the flexible lid loop binds with the thiolation domain to orient the substrate so that the thiol-group is in close proximity to the active site residues [187], suggesting that interactions with the subunits of the NRPS or PKS domain influence substrate specificity within TE18.

YbtT is a thioesterase encoded within the yersiniabactin biosynthetic operon of *Yersinia* spp. and uropathogenic *E. coli*, and is thought to remove aberrant yersiniabactin precursors from carrier proteins, that would otherwise stall or inhibit yersiniabactin synthesis [189]. YbtT and RifR have been suggested to behave as low-specificity editing thioesterases, meaning they would display greater substrate promiscuity in regards to acyl chain length than others thioesterases, such as RedJ. This appears to be at least partly due to the composition of residues within the flexible lid region of these enzymes, with RedJ having a greater composition of hydrophobic residues in the lid region compared to RifR and YbtT, in which the hydrophobic residues are largely replaced by polar residues [185, 189].

Unusually, the *E. coli* colibactin hybrid NRPS/PKS pathway does not contain both editing and terminal releasing thioesterases, instead, the thioesterase ClbQ appears to release both correct and aberrant linear colibactin intermediates attached to NRPS/PKS carrier proteins, with cyclisation of colibactins thought to occur through additional pathways. ClbQ is structurally similar to both RedJ and RifR, with an RMSD of 1.7Å over 227 aligned αC atoms with the N-terminal domain of RedJ, and an RMSD of 2.3Å over 223 aligned αC atoms with RifR [190]. However, sequence and structural differences within the lid region compared to RedJ and RifR, presumably accommodate different colibactin intermediates, and highlights the flexibility of the lid region and its importance in determining the substrate selectivity.

TE19 Family

The TE19 thioesterases are found in the fatty aldehyde synthesis pathway of bioluminescent bacteria, with specific activity for myristoyl-ACP. TE19 thioesterases remain poorly characterised, both in terms of structure and function, with the only structural data to date arising from the single crystal structure of LuxD from *Vibrio harveyi* (PDB 1THT; [153]). TE19 thioesterases appear to exhibit a classic α/β hydrolase fold with a pronounced cap domain or lid [153], and β1-β2-β3-α1-α2-β4-α3-β5-α4-β6-α5-β7-β8-α6-α7-β9-α8-β10-α9-α10-β11 topology **(Figure 24)**. LuxD thioesterases are responsible for cleaving myristoic acid from the ACP of FAS to divert it into the bioluminescence pathway. This produces an aliphatic aldehyde which serves as a substrate for the heterodimeric bacterial luciferase (LuxAB). LuxD can function both as a thioesterase and as an acyl-transferase. LuxD from *Photobacterium phosphoreum*, and presumably other organisms, along with the acyl-protein synthetase LuxE and acyl-CoA reductase LuxC, forms the fatty acid reductase complex (LuxCDE) at a 4:4:2-4

stoichiometry, with 4 LuxD subunits required for optimal catalytic activity [191-193]. The LuxCDE reaction is initiated by LuxD, which catalyses the cleavage of myristoyl groups from myristoyl-ACP and facilitates transfer of the acyl moiety to the acyl-protein synthetase LuxE. LuxE converts the acyl moiety to acyl-AMP, and then covalently attaches the acyl molecule to a C-terminally located cysteine residue of LuxE (Cys^{362}) that funnels the acyl group to the active site of the reductase LuxC, where it is transferred from LuxE to LuxC before being reduced with NADPH to form myristyl aldehyde (tetradecanal). LuxD is highly specific for C14 acyl chains, particularly myristoyl-ACP, however, myristoyl-CoA, and other derivatives have also been utilised as substrates *in vitro* [153, 194, 195]. The specificity of LuxD is in agreement with reports that tetradecanal is the main substrate in the luminescence reaction catalysed by LuxAB [196].

Whilst displaying a traditional α/β hydrolase fold and Ser-His-Asp catalytic triad typical of other thioesterase families such as TE16-18, structurally LuxD more closely resembles cinnamoyl/feruloyl esterases and lipases than that of other determined thioesterase structures. In particular, LuxD shows greatest structural similarity to the cinnamoyl esterase Est1E from *Butyrivibrio proteoclasticus* (PDB 2WTM), with an RMSD of 2.8Å over 229 aligned Cα atoms, the cinnamoyl esterase LJ0536 from *Lactobacillus johnsonii* (PDB 3PF8, 3PF9), with an RMSD of 2.8Å over 227 Cα atoms, and human monoglyceride lipase (PDB 3PE6, 5ZUN), with an RMSD of 2.8Å over 235 Cα atoms. In contrast to many TE16-18 thioesterases which contain a Gly-X-Ser-X-Gly nucleophilic elbow, LuxD displays an Ala-X-Ser-X-Ser motif in the nucleophilic elbow, that is reportedly conserved amongst marine and terrestrial luminescent bacteria [153, 195]. Mutation of this motif to Ala-X-Ser-X-Gly or Gly-X-Ser-X-Gly in *V. harveyi* LuxD has been shown to cause an ~3 fold increase in deacylation. One potential reason for the reduced rate of catalytic activity shown in LuxD thioesterases is that higher activity may result in unwanted release of non-esterified fatty acids, while reducing the catalytic rate causes LuxD to act as an ACP, retaining myristoyl intermediates and allowing sustained release of tetradecanal [195]. Similarly to other α/β hydrolases, a flexible lid or cap subdomain adjacent to the active site of LuxD has been proposed [153], with the putative lid domain appearing to create a substrate binding pocket predominantly lined with hydrophobic residues, which is consistent with binding of acyl chain substrates. However, the role of the lid region and its implications in substrate binding or regulation are yet to be identified.

2.2.3 Protein Acyl/palmitoyl Thioesterases

TE20 Family

Members of TE20 are palmitoyl-protein thioesterases (PPT) exhibiting an α/β hydrolase domain, a cap domain, and an accessory domain of unknown function. The structures of two TE20 members have been solved, PPT1 (PDB 3GRO, 1EH5; [197]) and PPT2 (PDB 1PJA; [198]). The topology of 1PJA is arranged β1-α1-β2-α2-β3-α3-β4-α4-α5-α6-α7-α8-α9-α10-β5-α11-β6-β7-α12-α13-α14-β8-α15-α16, which form monomers (**Figure 25**).

The hydrolase domains contained with the PPT enzymes have been shown to remove thioester-linked palmitate groups from modified cysteines. This process regulates cellular localisation and failures of this system result in severe pathologies including neuronal ceroid lipofuscinosis (NCL) [199], shown to be caused by a single mutation in the PPT1 [200]. The depalmitoylation reaction of PPT1 is governed by a positive feedback loop, where palmitoylation of the enzyme decreases activity, exasperating the effects of disease-causing mutants [201]. Deletion of either

PPT1 or PPT2 results in a similar phenotype in mice with a mortality rate of 100% in PPT1 knockouts and 20% in PPT2 knockouts by 10 months of age [200]. This has been attributed to differences in the activity with PPT1 able to accommodate and catalyse palmitoylated proteins; however, PPT2 has a smaller substrate entrance tunnel so that the "branched" or bulky heads of these substrates cannot be accommodated in the active site [198]. PPT1 has also recently been found to be overexpressed in multiple cancer types [202]. The role of overexpression of PPT1, and the inhibition of PPT1 as a treatment are still being investigated.

TE21 Family

The TE21 thioesterases, also known as acyl-protein thioesterases (APT), lysophospholipase and carboxylesterase, hydrolyse thioester bonds between Cys residues on proteins and acyl chains. They exhibit a classic α/β hydrolase domain, and the structures of both eukaryotic lysophospholipase-like 1 (LYPLAL1; PDB 3U0V; [203]) and APT1 (PDB 1FJ2; [204]) as well as a number of bacterial carboxylesterase/phospholipase family proteins, *P. aeruginosa* (PDB 3CN7; [205]), *P. fluorescens* (PDB 1AUO and 1AUR; [206]) and *Rhodobacter sphaeroides* (PDB 4FHZ; [207]) have been solved. The topology present within this family is arranged β1-β2-α1-β3-β4-α2-β5-α3-α4-β6-α5-β7-α6-β8-α7-β9-α8 (**Figure 26**). These structures revealed differences in quaternary structure amongst these related thioesterases with 4F21 (*Francisella tularensis*) [208], 3CN7 and 3U0V forming monomers and the other members of this family 1FJ2, 1AUO and 4FHZ forming dimers. Dimerisation of APT1 has been shown to reduce activity. However, phosphorylation of $Ser^{209/210}$ blocks dimerisation, maintaining the active monomeric form [209]. Human acyl-protein thioesterases 1 and 2 (APT1 and APT2) are the best characterised TE21 family members and work in conjunction with palmitoyl transferases to regulate the cell surface expression of palmitoylated proteins, H-Ras and growth-associated protein-43 (GAP43), in calcium-activated potassium channels. Whilst APT1 and APT2 normally reside in the Golgi, Kong *et al.* [210] described the mechanism regulating membrane localisation and function of APT1 and APT2. APT1 and APT2 are palmitoylated in the Golgi to facilitate membrane relocation, where APT1 depalmitoylates H-Ras and APT2 depalmitoylates GAP43 promoting their return to the Golgi where they are repalmitoylated to begin the cycle again. Importantly, APT1 has demonstrated activity against palmitoylated APT2, translocating it into the Golgi, prior to depalmitoylating itself to return to the Golgi. In a similar mechanism APT1 and APT2 regulate palmitoylation of the calcium and voltage-activated potassium channels altering cell surface expression of the channel [211].

2.2.4 Glutathione thioesterases

TE22 Family

Members of TE22 are S-formylglutathione hydrolases, acetyl esterases (Esterase A, EstA) or carboxylesterases (Esterase D, EstD) and exhibit activity towards S-formylglutathione. They exhibit a classic α/β hydrolase fold and a conserved cap region above the active site. Structures have been determined for both the *S. pneumoniae* esterase A (PDB 2UZ0; [212]), *Agrobacterium tumefaciens* S-formylglutathione hydrolase (3E4D; [213]) *Neisseria meningitidis* esterase D (PDB 4B6G; [214]), *Oleispira Antarctica* esterase (PDB 3I6Y, 3S8Y; [215]), *Pseudoalteromonas haloplanktis* S-formylglutathione hydrolase (PDB 3LS2; [216]), *Saccharomyces cerevisiae* esterase D (PDB 1VP1, 3C6B; [217], 4FLM, 4FOL; [218]) and the human esterase D (PDB 3FCX; [219]). The topology of this family is arranged as β1-β2-β3-α1-

α2-β4-α3-α4-α5-β5-α6-β6-α7-α8-α9-α10-β7-α11-β8-α12 (**Figure 27**). Esterase A from *S. pneumoniae* forms a dimer in solution, as demonstrated through a combination of size exclusion chromatography and X-ray crystallography. The latter of which identified a calcium ion at the dimer interface, shown to be essential for activity [212].

The function of TE22 members, for example EstD, include the participation within pathways to detoxify formaldehyde, produced during the oxidation of methanol, methylamine and choline [214, 219, 220]. Here, formaldehyde reacts with glutathione to produce S-hydroxymethylglutathione, which following oxidisation by alcohol dehydrogenase into S-formylglutathione, is hydrolysed by EstD, regenerating glutathione [214, 219, 220].
Human EstD is located on chromosome 13 in a similar locus to mutations, which cause retinoblastoma, a cancer of the eye, and has been used as a marker to detect retinoblastoma [221, 222].

2.3. Other Thioesterase Folds

2.3.1 Acyl-CoA Thioesterases

TE1 Family

Members of the TE1 thioesterase family, also known as acetyl-CoA hydrolase 1 (Ach1), exhibit specificity for acetyl-CoA. TE1 thioesterases are comprised of two NagB domains which display an α/β fold. These two domains are linked through a rigid loop and a flexible linker domain, and this flexible linker (residues 224−235) is positioned close to a deep, funnel-shaped cleft containing the active-site glutamate (Glu224) [223]. Representative structures have been determined from *Acetobacter aceti* (PDB 4EUD; [223]), *Porphyromonas gingivalis* (PDB 2NVV; [224]) and *P. aeruginosa* (PDB 2G30; [225]). Two of the three TE1 thioesterases have been deposited to the PDB but remain unpublished, and here we provide an initial characterisation. There is a conserved and extensive interface buried at the dimer interface for each of the three structures. This surface area is 3,476 Å^2 in PDB 4EUD, 3,178 Å^2 in PDB 2NVV, and 3,361 Å^2 in PDB 2G29. Overall, this strongly implies that the TE1 thioesterases are dimers. The secondary structural elements of this family are arranged as α1-α2-β1-α3-β2-α4-β3-α5-β4-α6-α7-β5-β6-β7-α8-β8-α9-β9-α10-β10-α11-β11-α12-β12-β13-α13-β14-β15-α14-α15-β16-α16-α17-β17-β18-β19-β20-α18-β21-α19-β22-β23-α20-β24-β25-α21-β26-β27-α22-α23-α24. The active site residues are comprised of Asn, Glu and Gly residues (Glu^{294} between β12 and β13, Asn^{347} on α17, and Gly^{388} on α19 for *A. aceti*) [223] **(Figure 28)**.

The NagB fold for thioesterases of TE1 exhibit both hydrolase and CoA transferase activity, transferring the CoA S-anion from a CoA-thioester to a free acid receptor. The function of AarC has been well established as an acetic acid resistance factor in acetic acid bacteria (AAB), by catalysing the oxidative decarboxylation of acetate utilising the citric acid cycle dehydrogenases to reduce acetate to CO_2. This is performed using the *aarABC* genes, where AarA is a citrate synthase and AarC acts as a succinyl-CoA:acetate-CoA transferase, in conjunction with malate:quinone oxidoreductase [226].The crystal structure of the *A. aceti* (PDB 4EUD) [223] succinyl-CoA:acetate-CoA transferase, AarC, confirmed the active site mechanism predicted by White and Jencks [227]. Energy held within the acyl-CoA bond is used to increase rate-limiting acyl transfers utilising conformational changes to hold the CoA group tightly against the catalytic glutamate, and this activity has been conserved throughout other CoA transferases. This is mediated through a conserved loop G(V/I)G adjacent to the active site involving electrostatic

and hydrophobic interactions with the panteteine moiety of CoA, with a positively charged active site region surrounded by a negatively charged zone to attract the CoA moiety into the binding cleft [228]. The active site also inhibits further processing of CoA. This is done through an interaction of the CoA thiol with Glu^{294}, which prevents the active site from fully closing [229].

TE3 Family

Members of the TE3 thioesterase family, also known as thioesterase I/protease I/lysophospholipase L_1 (TesA/ApeA/PldC (TAP)), exhibit acyl-CoA thioesterase activity against medium to long chain acyl-CoA substrates. They exhibit a flavodoxin-like fold, and structures have been solved for three members; *E. coli* (PDB 1IVN; [230]), *Pseudoalteromonas sp. 634A* (PDB 3HP4; [231]) and *P. aeruginosa* (PDB 4JGG; [232]). The topology structural elements within this family are arranged as β1-α1-α2-β2-α3-β3-α4-β4-α5-β5-α6-α7 **(Figure 29)**. The TE3 thioesterases are from the SGNH-hydrolase family, characterised by four conserved blocks of residues each containing a completely conserved residue playing a role in catalytic function: Ser, Gly, Asn, His. In similar fashion to the α/β hydrolase fold, the active site residues of SGNH-hydrolases contain a catalytic Ser, Asp, His triad [230]. These domains form monomers, and contain a switch loop mechanism stabilising substrate intermediates throughout catalysis rather than a lid domain present in many other α/β hydrolase folds [230].

Members of this family have acyl-CoA hydrolase activity and the best studied family member is TAP. The physiological role of TAP remains to be fully established, but multiple studies have shown the enzyme localised in the periplasm [233, 234]. However, when overexpressed within the cytosol, it increases the concentration of intracellular fatty acids by hydrolysing acyl-ACP intermediates [235] [236]. Deletion of the signal sequence of TAP (leaderless TesA; 'TesA) will cause accumulation of the enzyme in the cytosol, where a range of fatty acid substrates may be targeted [237-239]. The mutated TesA has been of interest for industrial purposes, aiding the production of biofuels and pharmaceuticals.

2.3.2 Glutathione Thioesterases

TE23 Family

Members of the TE23 thioesterase family, also known as glyoxalase II (EC 3.1.2.6), are found in both prokaryotes and eukaryotes. They have catalytic activity against S-D-lactoylglutathione, and form part of the glyoxalase system, mediating the detoxification of methylglyoxal produced during metabolism and cell stress [240-242]. All TE23 members studied to date are monomers, and contain two structural domains: an N-terminal metallo-lactamase domain and a C-terminal hydroxyacylglutathione hydrolase domain. The N-terminal domain contains two mixed β-sheets flanked by α-helices, while the C-terminus is an all α-helical domain. The topology, depicted in **Figure 30**, is comprised of β1-β2-β3-α1-β4-α2-α3-β5-β6-β7-β8-β9-β10-β11-β12-α4-β13-α5-α6-β14-α7-α8-α9. Two repeating units make a β-sheet sandwich from β1-β2-β3-α1-β4-α2-α3-β5-β6 and β7-β8-β9-β10-β11-β12-α4-β13, and this arrangement is conserved in structures from *A. acidocaldarius* (PDB 3TP9; [243]), *S. enterica* (PDB 2XF4; [244]), *S. typhimurium* (PDB 2QED; [245]), *A. thaliana* (PDB 1XM8; [246], 2Q42; [247] and 2GCU; [248]), *L. infantum* (PDB 2P18; [249]), and *H. sapiens* (PDB 1QH3 and 1QH5; [250]). TE23 thioesterases require divalent cations for their activity, harbouring a binuclear metal binding center (iron and/or zinc) and a conserved metal binding motif "THXHXDH" [246, 251, 252]. The active site residues are comprised of His and Asp residues in conjunction with a bound Zn and/or Fe ion located at the

interface of the sandwich and α-helical domains. TE23 enzymes have shown to be inhibited by the reaction products, glutathione [245, 253] and D-lactate, which is proposed to regulate cellular glutathione levels and redox balance in the cell [253].

Methylglyoxal, produced during glycolysis and other metabolic pathways, plays a role in cell signalling at low concentrations, but is toxic at high concentrations due to its reactivity with protein and nucleotides [254]. The role of the glyoxylase system has been well documented in chronic kidney disease [255], environmental stress tolerance in plants [256, 257] and prokaryotic stress response [258]. In the glyoxalase pathway, glyoxalase I condenses methylglyoxalase and glutathione to produce S-D-lactoylglutathione, which is then hydrolysed by glyoxalase II to produce lactic acid and regeneration of glutathione. The lactic acid can then be converted into pyruvate and metabolised through the citric acid cycle, whilst the reduced glutathione is recycled and used in glyoxalase detoxification pathways.

3. Conclusions

Significant insights into thioesterase structure, function, and regulation have been achieved in recent years. This has led to an effective system of classification based on sequence, structure, and active site similarity. Most families now contain representative structures, complemented with detailed mutagenesis and enzyme characterisation, and cellular and/or system wide function analysis. The 25 TE families and proposed 26th, contain five highly conserved structural domains, however, the organisation of these domains vary significantly. Some thioesterase families are able function as discrete monomers, while others form assemblies ranging from dimers, trimers, tetramers, and hexamers. There are also different types of arrangements within these assemblies, including face-to-face, back-to-back, and head-to-tail configurations. The domain organisation at the primary level is also be markedly different, with some families exhibiting only single domains in prokaryotes, but fused domains in eukaryotes. Remarkably, members within the same family can form the same quaternary assembly from these markedly different sequences. There is also considerable variation in active site configurations, with some sites located solely on a single domain, others mediated at the interface of dimers, and some containing asymmetric sites, with only half catalytically active. This variation may accommodate the vast range of substrates that thioesterases act upon. These range from very short chain acyl-CoA metabolites including acetyl-CoA, medium to long chain fatty acids, highly complex branched chain fatty acids, a vast array of small molecules bound to CoA, and moieties linked to carrier proteins. Finally, many of the TE families exhibit different modes of regulation, ranging from a half of sites reactivity, achieved through substrate induced mechanisms or half active sites, ATP and ADP modulation of regulatory domains, negative feedback of reaction end-products, and regulation at the gene expression level. Here in this review we provide a snapshot of the current understanding of the structure, function, and regulation of the thioesterases families.

Table 1- Features of each thioesterase family

Family	Fold	PDB ID (Ref)	Quaternary Structure	Active Site Residues	Secondary Structural Elements
TE1	NagB	4EUD; [223] 2NVV; [224] 2G39; [225]	Dimer	Asn^{347}, Glu^{294} and Gly^{388} [223]	α1-α2-β1-α3-β2-α4-β3-α5-β4-α6-α7-β5-β6-β7-α8-β8-α9-β9-α10-β10-α11-β11-α12-β12-β13-α13-β14-β15-α14-α15-β16-α16-α17-β17-β18-β19-β20-α18-β21-α19-β22-β23-α20-β24-β25-α21-β26-β27-α22-α23-α24
TE2	α/β Hydrolase	3K2I; [164] 3HLK; [165]	Monomer	Ser^{294}, His^{422} and Asp^{388} [165]	β1-β2-β3-α1-β4-α2-β5-α3-β6-β7-α4-β8-α5
TE3	Flavodoxin-Like	1IVN; [230] 3HP4; [231] 4JGG; [232]	Monomer	Ser^{10}, Asp^{154} and His^{157} [230]	β1-α1-α2-β2-α3-β3-α4-β4-α5-β5-α6-α7
TE4	Hotdog	1C8U; [20] 4QFW; [17] 3RD7; [21] 3U0A; [21] 4R9Z; [22] 1TBU; [23]	Octamer	Asp^{204}, Thr^{28} and Gln^{278} [17, 20]	α1-β1-β2-α2-β3-β4-β5-β6-*α3-β7-β8-α4-β9-β10-β11-β12*
TE5	Hotdog	1NJK; [33]	Face-to-face tetramer	Asp^{13} [13]	β1-α1-α2-α3-β2-β3-β4-β5-α4
TE6	Hotdog	3D6L; [40] 1YLI [63] 5V3A, 5SZZ, 5SZY, 5TO2 and 5SZU; [39] 4ZV3; [42] 2Q2B, 2V1O; [4] 2QQ2; [41]	Hexamer	Asp^{44} [63] Asn24 and Asp39 [39] Asp^{213} and Asn^{24} [4]	Prokaryotes: β1-α1-β2-β3-β4-β5 Eukaryotes: β1-α1-β2-β3-β4-β5-α2-*β6-α3-β7-β8-β9-β10-α4*

		4MOB, 4MOC, 3B7K; [43]		Asp^{36} and Asn^{195} [43]	
TE7	Hotdog	-	Hexamer	-	β1-α1-β2-β3-β4-β5-α2-*β6-α3-β3-β7-β8-β9-β10-α4*
TE8	Hotdog	2F0X, [72]; 3F5O; [74] 2H4U; [73] 2CY9; [75] 4ORD; [76]	Back-to-back tetramer	Asn^{50}, Asp^{65} and Ser^{83} [72, 74] Asn^{50}, Gly^{57}, Asp^{65} and Ser^{83} [13] Asn^{51}, Gly^{58}, Asp^{66} and Ser^{84} [76]	α1-β1-β2-α2-β3-β4-β5-β6
TE9	Hotdog	1S5U; [80], 5KL9; [81], 5T06 and 5T07; [82] 1Z54; [83] 2PZH; [84] 3HM0; [85] 5V10; [86] 2EGR, 2EGJ; [87]	Face-to-face tetramer	Tyr^{14}, Asp^{18} and His^{35} [13, 84] Tyr^{23}, Asp^{28} and His^{35} [13]	β1-α1-α2-α3-β2-β3-β4-β5-β6-α4
TE10	Hotdog	1BVQ; [96] 1LO7, 1LO8 and 1LO9; [97]	Face-to-face tetramer	Asp^{17} [97, 98]	β1-α1-α2-α3-β2-β3-β4-β5-β6-β7-β8-α4
TE11	Hotdog	1Q4S, 1Q4T, 1Q4U; [102] 3R32, 3R34, 3R35, 3R36, 3R37, 3R3A,	Back-to-back tetramer	Gly^{65} and Glu^{73} [102] Gln^{58}, Gly^{65} and Glu^{73} [103]	α1-α2-β1-β2-α3-α4-α5-β3-β4-β5-β6

		3R3B, 3R3C, 3R3D, 3R3F and 3TEA; [103] 2B6E; [106] 1SC0; [107] 4QD9; [108] 4K4A, 4K4B, 4K4C, 4K4D, 4K49; [105] 1VH5, 1VH9, 1VI8; [104] 1SBK; [109]		Gly[55] and Glu[63] [13, 104, 105]	
TE12	Hotdog	4K02; [111] 4K00; [111] 2HX5; [112]	Face-to-face tetramer	Glu[57] [111] Asp[16] [111] Asp[49] [113]	α1-β1-α2-α3-α4-β2-β3-β4-β5-β6-β7-α5
TE13	Hotdog	1PSU and 2FS2; [114] 1ZKI; [115] 4I82, 4ZRF, 4ZRB, 4XY5 and 4XY6; [64] 3LBB and 3LBE; [116] 4M20, 5EP5; [117] 4YBV; [118] 1J1Y, 1WLU, 1WLV, 1WM6, 1WN3; [119] 2DSL; [120]	Back-to-back tetramer	Gly[53] and Asp[61] [114] Asp[16], Asn[46], Asp[61] and Thr[62] [64, 115] Gly[40] and Asp[48] [13, 119]	α1-β1-β2-α2-α3-β3-β4-β5-β6

TE14	Hotdog	2OWN; [138] 2ESS; [139] 4GAK; [140] 5X04; [141]	Dimer	Asp^{281}, Asn^{283}, His^{285}, and Glu^{319} [141]	α1-α2-β1-α3-α4-α5-β2-β3-β4-β5-α6-α7-α8-β6-α9-α10-α11-β7-β8-β9-β10
TE15	Hotdog	2W3X; [145] 2XEM; [145] 4I4J; [146]	Dimer	Arg^{37} and Tyr^{29} [145]	β1-α1-α2-α3-β2-β3-β4-β5-α4
TE16	α/β Hydrolase	1XKT; [159] 2PX6; [170] 3TJM; [171] 4Z49; [169] 2VZ8 and 2VZ9; [160] 3ILS; [161] 2CB9; [163] 1JMK; [1] 3TEJ; [173]	Monomer	Ser^{2308}, Asp^{2338} and His^{2481} [159, 170, 171] Ser^{1937}, Asp^{1964} and His^{2088} [161] Ser^{84}, Asp^{111} and His^{201} [163] Ser80, Asp107 and His207 [1]	β1-β2-α1-β3-β2-β4-α3-β5-α4-β6-α5-α6-β7-α7-α8
TE17	α/β Hydrolase	1KEZ; [173] 1MO2; [179] 5D3K, 5D3Z; [180] 6MLK; [181] 3LCR; [182] 1MN6, 1MNA, 1MNQ; [179] 2H7X, 2H7Y; [183]	Dimer	Ser^{142}, Asp^{169}, and His^{259} [178, 179] Ser^{148}, Asp^{176} and His^{268} [183, 184]	α1-β1-β2-β3-α2-α3-β4-β5-α4-β6-α5-β7-α6-α7-β8-β9-α8

		2HFJ and 2HFK; [184]		Ser^{148}, Asp^{176} and His^{268} [184]	
TE18	α/β Hydrolase	3FLA, 3FLB; [186] 3QMV, 3QMW; [185] 2RON; [187]	Dimer	Ser94, Asp200 and His228 [186] Ser^{107}, Asp^{213} and His^{241} [185, 187]	α1-β1-α2-α3-β2-α4-α5-β3-α6-β4-α7-α8-α9-α10-β5-α11-β6-α12-α13
TE19	α/β Hydrolase	1THT; [153]	Monomer	Ser^{114}, Asp^{211} and His^{241} [153]	β1-β2-β3-α1-α2-β4-α3-β5-α4-β6-α5-β7-β8-α6-α7-β9-α8-β10-α9-α10-β11
TE20	α/β Hydrolase	3GRO, 1EH5; [197] 1PJA; [198]	Monomer	Ser^{115}, Asp^{2} and His^{89} [197] Ser^{1}, Asp^{228} and His^{283} [198]	1-α1-β2-α2-β3-α3-β4-α4-α5-α6-α7-α8-α9-α10-β5-α11-β6-β7-α12-α13-α14-β8-α15-α16
TE21	α/β Hydrolase	3U0V; [203] 3CN7; [205] 1FJ2; [204] 1AUO, 1AUR; [206] 4FHZ; [207]	Monomer Dimer	Ser^{113}, Asp^{166} and His^{197} [13] Ser^{114}, Asp^{169} and His^{203} [204] Ser^{114}, Asp^{168} and His^{199} [206]	β1-β2-α1-β3-β4-α2-β5-α3-α4-β6-α5-β7-α6-β8-α7-β9-α8
TE22	α/β Hydrolase	2UZ0; [212] 3E4D; [213] 4B6G; [214] 3I6Y, 3S8Y; [215] 3LS2; [216]	Dimer	Ser^{120}, Asp^{202} and His^{231} [212] Ser^{147}, Asp^{223} and His^{256} [213] Ser^{145}, Asp^{221} and His^{254} [214]	β1-β2-β3-α1-α2-β4-α3-α4-α5-β5-α6-β6-α7-α8-α9-α10-β7-α11-β8-α12

		3FCX; [219] 1PV1, 3C6B; [217], 4FLM, 4FOL; [218]		Ser^{148}, Asp^{224} and His^{257} [215] Ser^{147}, Asp^{225} and His^{258} [216] Ser^{149}, Asp^{226} and His^{260} [219] Ser^{161}, Asp^{241} and His^{276} [217, 218]	
TE23	Lactamase	3TP9; [243] 2XF4; [244] 2QED; [245] 1XM8; [246] 2Q42; [247] 2GCU; [248] 2P18; [249] 1QH3 and 1QH5; [250]	Monomer	 His^{53}, His^{55}, Asp^{57}, His^{58} His^{110}, $Asp^{1..}$ and $His^{..65}$ [245] $His^{5..}$, His^{56}, Asp^{58}, His^{59}, His^{112}, Asp^{131} and His^{169} [246] His^{110}, Asp^{134} and His^{173} [250]	β1-β2-β3-α1-β4-α2-α3-β5-β6-β7-β8-β9-β10-β11-β12-α4-β13-α5-α6-β14-α7-α8-α9
TE24	Hotdog	2PFC; [94]	Head to tail hexamer	Y^{66}, Y^{33} and N^{74} [126]	α1-β1-β2-α2-α3-β3-β4-β5-β6
TE25	Hotdog	3KUV, 3KUW, 3KV7, 3KV8, 3KVI, 3KVU, 3KVZ, 3KW1, 3KX7,	Dimer	Thr^{42}, Glu^{50} and His^{76} [127]	β1-α1-β2-β3-β4-β5-α2

		3KX8; [127] 3P2Q, 3P2R, 3P2S, 3P3F and 3P3I; [128] 2CWZ			
TE26	Hotdog	4AE7 and 4AE8; [130]	Dimer	His^{158}, Gly^{159}, Gly^{160}, Asp^{167} and Thr^{183} [130]	α1-β1-β2-α2-ß3-β4-β5-β6

4. REFERENCES

[1.] Bruner, S.D., T. Weber, R.M. Kohli, D. Schwarzer, M.A. Marahiel, C.T. Walsh, et al., *Structural basis for the cyclization of the lipopeptide antibiotic surfactin by the thioesterase domain srfte.* Structure, 2002. **10**(3): p. 301-10.

[2.] Ellis, J.M., C.E. Bowman, and M.J. Wolfgang, *Metabolic and tissue-specific regulation of acyl-coa metabolism.* PLoS One, 2015. **10**(3): p. e0116587.

[3.] Feng, Y. and J.E. Cronan, *A new member of the escherichia coli fad regulon: Transcriptional regulation of fadm (ybaw).* J. Bacteriol., 2009. **191**(20): p. 6320-8.

[4.] Forwood, J.K., A.S. Thakur, G. Guncar, M. Marfori, D. Mouradov, W. Meng, et al., *Structural basis for recruitment of tandem hotdog domains in acyl-coa thioesterase 7 and its role in inflammation.* Proc. Natl. Acad. Sci. USA, 2007. **104**(25): p. 10384-7.

[5.] Fujita, M., A. Momose, T. Ohtomo, A. Nishinosono, K. Tanonaka, H. Toyoda, et al., *Upregulation of fatty acyl-coa thioesterases in the heart and skeletal muscle of rats fed a high-fat diet.* Biol. Pharm. Bull., 2011. **34**(1): p. 87-91.

[6.] Kang, H.W., C. Ozdemir, Y. Kawano, K.B. LeClair, C. Vernochet, C.R. Kahn, et al., *Thioesterase superfamily member 2/acyl-coa thioesterase 13 (them2/acot13) regulates adaptive thermogenesis in mice.* J. Biol. Chem., 2013. **288**(46): p. 33376-86.

[7.] Koglin, A., M.R. Mofid, F. Löhr, B. Schäfer, V.V. Rogov, M.-M. Blum, et al., *Conformational switches modulate protein interactions in peptide antibiotic synthetases.* Science, 2006. **312**(5771): p. 273-6.

[8.] Pandey, P., W. Liu, F. Xing, K. Fukuda, and K. Watabe, *Anti-cancer drugs targeting fatty acid synthase (fas).* Recent Pat. Anticancer Drug Discov., 2012. **7**(2): p. 185-97.

[9.] Grevengoed, T.J., E.L. Klett, and R.A. Coleman, *Acyl-coa metabolism and partitioning.* Annu. Rev. Nutr., 2014. **34**: p. 1-30.

[10.] Tillander, V., S.E.H. Alexson, and D.E. Cohen, *Deactivating fatty acids: Acyl-coa thioesterase-mediated control of lipid metabolism.* Trends Endocrinol Metab, 2017. **28**(7): p. 473-84.

[11.] Gergely, J., P. Hele, and C. Ramakrishnan, *Succinyl and acetyl coenzyme a deacylases.* J. Biol. Chem., 1952. **198**(1): p. 323-34.

[12.] Alexson, S., H. Osmundsen, and R.K. Berge, *The presence of acyl-coa hydrolase in rat brown-adipose-tissue peroxisomes.* Biochem. J, 1989. **262**: p. 41-6.

[13.] Cantu, D.C., Y. Chen, and P.J. Reilly, *Thioesterases: A new perspective based on their primary and tertiary structures.* Protein Sci., 2010. **19**(7): p. 1281-95.

[14.] Brocker, C., C. Carpenter, D.W. Nebert, and V. Vasiliou, *Evolutionary divergence and functions of the human acyl-coa thioesterase gene (acot) family.* Human genomics, 2010. **4**(6): p. 411.

[15.] Dillon, S.C. and A. Bateman, *The hotdog fold: Wrapping up a superfamily of thioesterases and dehydratases.* BMC Bioinformatics, 2004. **5**(1): p. 109.

[16.] Leesong, M., B.S. Henderson, J.R. Gillig, J.M. Schwab, and J.L. Smith, *Structure of a dehydratase–isomerase from the bacterial pathway for biosynthesis of unsaturated fatty acids: Two catalytic activities in one active site.* Structure, 1996. **4**(3): p. 253-64.

[17.] Swarbrick, C., M. Perugini, N. Cowieson, and J. Forwood, *Structural and functional characterization of tesb from yersinia pestis reveals a unique octameric arrangement of hotdog domains.* Acta Crystallogr. Sect. D. Biol. Crystallogr., 2015. **71**(4).

[18.] Westin, M.A., M.C. Hunt, and S.E. Alexson, *The identification of a succinyl-coa thioesterase suggests a novel pathway for succinate production in peroxisomes*. J. Biol. Chem., 2005. **280**(46): p. 38125-32.

[19.] Ofman, R., L. el Mrabet, G. Dacremont, D. Spijer, and R.J. Wanders, *Demonstration of dimethylnonanoyl-coa thioesterase activity in rat liver peroxisomes followed by purification and molecular cloning of the thioesterase involved.* Biochem. Biophys. Res. Commun., 2002. **290**(2): p. 629-34.

[20.] Li, J., U. Derewenda, Z. Dauter, S. Smith, and Z.S. Derewenda, *Crystal structure of the escherichia coli thioesterase ii, a homolog of the human nef binding enzyme.* Nat. Struct. Biol., 2000. **7**(7): p. 555-9.

[21.] Baugh, L., I. Phan, D.W. Begley, M.C. Clifton, B. Armour, D.M. Dranow, et al., *Increasing the structural coverage of tuberculosis drug targets.* Tuberculosis (Edinb), 2015. **95**(2): p. 142-8.

[22.] Swarbrick, C.M.D., G.V. Bythrow, D. Aragao, G.A. Germain, L.E.N. Quadri, and J.K. Forwood, *Mycobacteria encode active and inactive classes of tesb fatty-acyl coa thioesterases revealed through structural and functional analysis.* Biochem., 2017. **56**(10): p. 1460-72.

[23.] Devedjiev, Y.D., J. Li, U. Derewenda, and Z.S. Derewenda, *Crystal structure of n-terminal domain of yeast peroxisomal thioesterase-1 doi: 10.2210/pdb1tbu/pdb.* 2003.

[24.] Hung, Y.-H., Y.-S. Chan, Y.-S. Chang, K.-T. Lee, H.-P. Hsu, M.-C. Yen, et al., *Fatty acid metabolic enzyme acyl-coa thioesterase 8 promotes the development of hepatocellular carcinoma.* Oncol. Rep., 2014. **31**(6): p. 2797-803.

[25.] Jung, W.Y., Y.H. Kim, Y.J. Ryu, B.-H. Kim, B.K. Shin, A. Kim, et al., *Acyl-coa thioesterase 8 is a specific protein related to nodal metastasis and prognosis of lung adenocarcinoma.* Pathol. Res. Pract., 2013. **209**(5): p. 276-83.

[26.] Hunt, M.C., K. Solaas, B.F. Kase, and S.E. Alexson, *Characterization of an acyl-coa thioesterase that functions as a major regulator of peroxisomal lipid metabolism.* J. Biol. Chem., 2002. **277**(2): p. 1128-38.

[27.] Jump, D.B., D. Botolin, Y. Wang, J. Xu, B. Christian, and O. Demeure, *Fatty acid regulation of hepatic gene transcription.* J. Nutr., 2005. **135**(11): p. 2503-6.

[28.] Chinetti, G., J.-C. Fruchart, and B. Staels, *Peroxisome proliferator-activated receptors (ppars): Nuclear receptors at the crossroads between lipid metabolism and inflammation.* Inflamm. Res., 2000. **49**(10): p. 497-505.

[29.] Ziouzenkova, O., S. Perrey, N. Marx, D. Bacqueville, and J. Plutzky, *Peroxisome proliferator-activated receptors.* Curr. Atheroscler. Rep., 2002. **4**(1): p. 59-64.

[30.] Liu, L.X., F. Margottin, S. Le Gall, O. Schwartz, L. Selig, R. Benarous, et al., *Binding of hiv-1 nef to a novel thioesterase enzyme correlates with nef-mediated cd4 down-regulation.* J. Biol. Chem., 1997. **272**(21): p. 13779-85.

[31.] Serena, M., A. Giorgetti, M. Busato, F. Gasparini, E. Diani, M.G. Romanelli, et al., *Molecular characterization of hiv-1 nef and acot8 interaction: Insights from in silico structural predictions and in vitro functional assays.* Sci. Rep., 2016. **6**: p. 22319.

[32.] Nie, L., Y. Ren, and H. Schulz, *Identification and characterization of escherichia coli thioesterase iii that functions in fatty acid β-oxidation†.* Biochem., 2008. **47**(29): p. 7744-51.

[33.] Kim, Y., Joachimiak, A., Edwards, A., Xu, X., Savchenko, A., Midwest Center for Structural Genomics (MCSG), *Crystal structure of escherichia coli hypothetical protein ybaw doi: 10.2210/pdb1njk/pdb.* 2003.

[34.] Xu, Q., A.A. Canutescu, G. Wang, M. Shapovalov, Z. Obradovic, and R.L. Dunbrack, Jr., *Statistical analysis of interface similarity in crystals of homologous proteins.* J. Mol. Biol., 2008. **381**(2): p. 487-507.

[35.] Ren, Y., J. Aguirre, A.G. Ntamack, C. Chu, and H. Schulz, *An alternative pathway of oleate beta-oxidation in escherichia coli involving the hydrolysis of a dead end intermediate by a thioesterase.* J. Biol. Chem., 2004. **279**(12): p. 11042-50.

[36.] Van Aalten, D.M., C.C. DiRusso, and J. Knudsen, *The structural basis of acyl coenzyme a-dependent regulation of the transcription factor fadr.* EMBO J., 2001. **20**(8): p. 2041-50.

[37.] Dellomonaco, C., J.M. Clomburg, E.N. Miller, and R. Gonzalez, *Engineered reversal of the [bgr]-oxidation cycle for the synthesis of fuels and chemicals.* Nature, 2011. **476**(7360): p. 355-9.

[38.] My, L., B. Rekoske, J.J. Lemke, J.P. Viala, R.L. Gourse, and E. Bouveret, *Transcription of the escherichia coli fatty acid synthesis operon fabhdg is directly activated by fadr and inhibited by ppgpp.* J. Bacteriol., 2013. **195**(16): p. 3784-95.

[39.] Khandokar, Y.B., P. Srivastava, N. Cowieson, S. Sarker, D. Aragao, S. Das, et al., *Structural insights into gdp-mediated regulation of a bacterial acyl-coa thioesterase.* J. Biol. Chem., 2017. **292**(50): p. 20461-71.

[40.] Yokoyama, T., K.J. Choi, A.M. Bosch, and H.J. Yeo, *Structure and function of a campylobacter jejuni thioesterase cj0915, a hexameric hot dog fold enzyme.* Biochim Biophys Acta, 2009. **1794**(7): p. 1073-81.

[41.] Busam, R., Lehtio, L., Arrowsmith, C.H., Berglund, H., Collins, R., Dahlgren, L.G., Herman, M.D., Edwards, A., Flodin, S., Flores, A., Graslund, S., Hammarstrom, M., Hallberg, B.M., Holmberg-Schiavone, L., Johansson, I., Kallas, A., Karlberg, T., Kotenyova, T., Moche, M., Nordlund, P., Nyman, T., Sagemark, J., Stenmark, P., Sundstrom, M., Thorsell, A.G., Tresaugues, L., van den Berg, S., Weigelt, J., Welin, M., Persson, C., Structural Genomics Consortium (SGC), *Crystal structure of c-terminal domain of human acyl-coa thioesterase 7 doi: 10.2210/pdb2qq2/pdb.* 2007.

[42.] Swarbrick, C.M.D., Forwood, J.K., *Crystal structure of the n- and c-terminal domains of mouse acyl-coa thioesterase 7 doi: 10.2210/pdb4zw3/pdb.* 2015.

[43.] Swarbrick, C.M., N. Roman, N. Cowieson, S.I. Patterson, J. Nanson, M.I. Siponen, et al., *Structural basis for regulation of the human acetyl-coa thioesterase 12 and interactions with the steroidogenic acute regulatory protein-related lipid transfer (start) domain.* J. Biol. Chem., 2014. **289**(35): p. 24263-74.

[44.] Kuramochi, Y., M. Takagi-Sakuma, M. Kitahara, R. Emori, Y. Asaba, R. Sakaguchi, et al., *Characterization of mouse homolog of brain acyl-coa hydrolase: Molecular cloning and neuronal localization.* Mol. Brain Res., 2002. **98**(1): p. 81-92.

[45.] Ellis, J.M., G.W. Wong, and M.J. Wolfgang, *Acyl coenzyme a thioesterase 7 regulates neuronal fatty acid metabolism to prevent neurotoxicity.* Mol. Cell. Biol., 2013. **33**(9): p. 1869-82.

[46.] Swarbrick, C., N. Roman, and J.K. Forwood, *Role of acot7 in arachidonic acid production and inflammation*, in *Inflammatory diseases*, A. Nagal, Editor. 2011, InTech. p. 201-18.

[47.] Ohtomo, T., C. Nakao, M. Sumiya, O. Kaminuma, A. Abe, A. Mori, et al., *Identification of acyl-coa thioesterase in mouse mesenteric lymph nodes.* Biol. Pharm. Bull., 2013. **36**(5): p. 866-71.

[48.] Westin, M., M. Hunt, and S. Alexson, *Short-and medium-chain carnitine acyltransferases and acyl-coa thioesterases in mouse provide complementary systems for transport of β-oxidation products out of peroxisomes.* Cell. Mol. Life Sci., 2008. **65**(6): p. 982-90.

[49.] Bauer, D.E., G. Hatzivassiliou, F. Zhao, C. Andreadis, and C.B. Thompson, *Atp citrate lyase is an important component of cell growth and transformation.* Oncogene, 2005. **24**(41): p. 6314-22.

[50.] Fujino, T., J. Kondo, M. Ishikawa, K. Morikawa, and T.T. Yamamoto, *Acetyl-coa synthetase 2, a mitochondrial matrix enzyme involved in the oxidation of acetate.* J. Biol. Chem., 2001. **276**(14): p. 11420-6.

[51.] Suematsu, N., K. Okamoto, and F. Isohashi, *Mouse cytosolic acetyl-coa hydrolase, a novel candidate for a key enzyme involved in fat metabolism: Cdna cloning, sequencing and functional expression.* Acta Biochim. Pol, 2002. **49**: p. 937-45.

[52.] Suematsu, N., K. Okamoto, K. Shibata, Y. Nakanishi, and F. Isohashi, *Molecular cloning and functional expression of rat liver cytosolic acetyl-coa hydrolase.* Eur. J. Biochem., 2001. **268**(9): p. 2700-9.

[53.] Suematsu, N. and F. Isohashi, *Molecular cloning and functional expression of human cytosolic acetyl-coa hydrolase.* Acta Biochim. Pol., 2006. **53**(3): p. 553.

[54.] Hallows, W.C., S. Lee, and J.M. Denu, *Sirtuins deacetylate and activate mammalian acetyl-coa synthetases.* Proc. Natl. Acad. Sci. USA, 2006. **103**(27): p. 10230-5.

[55.] Martin, B. and R. Denton, *Intracellular localization of enzymes in white-adipose-tissue fat-cells and permeability properties of fat-cell mitochondria. Transfer of acetyl units and reducing power between mitochondria and cytoplasm.* Biochem. J, 1970. **117**: p. 861-77.

[56.] Cai, L., B.M. Sutter, B. Li, and B.P. Tu, *Acetyl-coa induces cell growth and proliferation by promoting the acetylation of histones at growth genes.* Mol. Cell, 2011. **42**(4): p. 426-37.

[57.] Lee, J.V., C.T. Berry, K. Kim, P. Sen, T. Kim, A. Carrer, et al., *Acetyl-coa promotes glioblastoma cell adhesion and migration through ca2+–nfat signaling.* Genes Dev., 2018. **32**(7-8): p. 497-511.

[58.] Horibata, Y., H. Ando, M. Itoh, and H. Sugimoto, *Enzymatic and transcriptional regulation of the cytoplasmic acetyl-coa hydrolase acot12.* J. Lipid Res., 2013. **54**(8): p. 2049-59.

[59.] Isohashi, F., Y. Nakanishi, and Y. Sakamoto, *Effects of nucleotides on a cold labile acetyl-coenzyme a hydrolase from the supernatant fraction of rat liver.* Biochem., 1983. **22**(3): p. 584-90.

[60.] Han, S. and D.E. Cohen, *Functional characterization of thioesterase superfamily member 1/acyl-coa thioesterase 11: Implications for metabolic regulation.* J. Lipid Res., 2012. **53**(12): p. 2620-31.

[61.] Zhang, Y., Y. Li, M.W. Niepel, Y. Kawano, S. Han, S. Liu, et al., *Targeted deletion of thioesterase superfamily member 1 promotes energy expenditure and protects against obesity and insulin resistance.* Proc. Natl. Acad. Sci. USA, 2012. **109**(14): p. 5417-22.

[62.] Zhuang, Z., F. Song, H. Zhao, L. Li, J. Cao, E. Eisenstein, et al., *Divergence of function in the hot dog fold enzyme superfamily: The bacterial thioesterase ycia†.* Biochem., 2008. **47**(9): p. 2789-96.

[63.] Willis, M.A., Z. Zhuang, F. Song, A. Howard, D. Dunaway-Mariano, and O. Herzberg, *Structure of ycia from haemophilus influenzae (hi0827), a hexameric broad specificity acyl-coenzyme a thioesterase†,‡.* Biochem., 2008. **47**(9): p. 2797-805.

[64.] Khandokar, Y.B., P. Srivastava, S. Sarker, C.M. Swarbrick, D. Aragao, N. Cowieson, et al., *Structural and functional characterization of the paai thioesterase from streptococcus pneumoniae reveals a dual specificity for phenylacetyl-coa and medium-chain fatty acyl-coas and a novel coa-induced fit mechanism.* J. Biol. Chem., 2016. **291**(4): p. 1866-76.

[65.] Takahashi, K. and H. Weiner, *Magnesium stimulation of catalytic activity of horse liver aldehyde dehydrogenase. Changes in molecular weight and catalytic sites.* J. Biol. Chem., 1980. **255**(17): p. 8206-9.

[66.] Anderson, A.C., R.H. O'Neil, W.L. DeLano, and R.M. Stroud, *The structural mechanism for half-the-sites reactivity in an enzyme, thymidylate synthase, involves a relay of changes between subunits.* Biochem., 1999. **38**(42): p. 13829-36.

[67.] Biemann, H.P. and D.E. Koshland Jr, *Aspartate receptors of escherichia coli and salmonella typhimurium bind ligand with negative and half-of-the-sites cooperativity.* Biochem., 1994. **33**(3): p. 629-34.

[68.] Izard, T. and A. Geerlof, *The crystal structure of a novel bacterial adenylyltransferase reveals half of sites reactivity.* EMBO J., 1999. **18**(8): p. 2021-30.

[69.] Jefferys, B.R., L.A. Kelley, and M.J. Sternberg, *Protein folding requires crowd control in a simulated cell.* J. Mol. Biol., 2010. **397**(5): p. 1329-38.

[70.] Kelley, L.A., S. Mezulis, C.M. Yates, M.N. Wass, and M.J. Sternberg, *The phyre2 web portal for protein modeling, prediction and analysis.* Nat. Protoc., 2015. **10**(6): p. 845.

[71.] Tillander, V., E.A. Nordström, J. Reilly, M. Strozyk, P.P. Van Veldhoven, M.C. Hunt, et al., *Acyl-coa thioesterase 9 (acot9) in mouse may provide a novel link between fatty acid and amino acid metabolism in mitochondria.* Cell. Mol. Life Sci., 2014. **71**(5): p. 933-48.

[72.] Cheng, Z., F. Song, X. Shan, Z. Wei, Y. Wang, D. Dunaway-Mariano, et al., *Crystal structure of human thioesterase superfamily member 2.* Biochem. Biophys. Res. Commun., 2006. **349**(1): p. 172-7.

[73.] Ogg, D.J., Uppenberg, J., Arrowsmith, C., Berglund, H., Edwards, A., Ehn, M., Grasslund, S., Flodin, S., Hammerstrom, M., Hogbom, M., Holmberg-Schiavone, L., Kotenyova, T., Nilsson-Ehle, P., Nordlund, P., Nyman, T., Persson, C., Sagemark, J., Sundstrom, M., Thorsell, A.-G., Weigelt, J., Hallberg, M., Structural Genomics Consortium (SGC), *Crystal structure of human thioesterase superfamily member 2 (casp target) doi: 10.2210/pdb2h4u/pdb.* 2006.

[74.] Cao, J., H. Xu, H. Zhao, W. Gong, and D. Dunaway-Mariano, *The mechanisms of human hotdog-fold thioesterase 2 (hthem2) substrate recognition and catalysis illuminated by a structure and function based analysis†,‡.* Biochem., 2009. **48**(6): p. 1293-304.

[75.] Hosaka, T., Murayama, K., Kishishita, S., Shirouzu, M., Yokoyama, S., RIKEN Structural Genomics/Proteomics Initiative (RSGI), *Crystal structure of thioesterase superfamily member2 from mus musculus doi: 10.2210/pdb2cy9/pdb.* 2006.

[76.] Yu, S., H. Li, F. Gao, and Y. Zhou, *Crystal structure and potential physiological role of zebra fish thioesterase superfamily member 2 (fthem2).* Biochem. Biophys. Res. Commun., 2015. **463**(4): p. 912-6.

[77.] Kang, H.W., M.W. Niepel, S. Han, Y. Kawano, and D.E. Cohen, *Thioesterase superfamily member 2/acyl-coa thioesterase 13 (them2/acot13) regulates hepatic lipid and glucose metabolism.* FASEB J., 2012. **26**(5): p. 2209-21.

[78.] Kawano, Y., B.A. Ersoy, Y. Li, S. Nishiumi, M. Yoshida, and D.E. Cohen, *Thioesterase superfamily member 2 (them2) and phosphatidylcholine transfer protein (pc-tp) interact to promote fatty acid oxidation and control glucose utilization.* Mol. Cell. Biol., 2014. **34**(13): p. 2396-408.

[79.] Wei, J., H. Kang, and D. Cohen, *Thioesterase superfamily member 2 (them2)/acyl-coa thioesterase 13 (acot13): A homotetrameric hotdog fold thioesterase with selectivity for long-chain fatty acyl-coas.* Biochem. J, 2009. **421**: p. 311-22.

[80.] Kim, Y., Joachimiak, A., Skarina, T., Savchenko, A., Edwards, A., Midwest Center for Structural Genomics (MCSG), *Crystal structure of hypothetical protein ec709 from escherichia coli doi: 10.2210/pdb1s5u/pdb.* 2004.

[81.] Stogios, P.J., Skarina, T., Di Leo, R., Savchenko, A., Anderson, W.F., Center for Structural Genomics of Infectious Diseases (CSGID), *Crystal structure of a putative acyl-coa thioesterase ec709/eck0725 from escherichia coli in complex with coa doi: 10.2210/pdb5kl9/pdb.* 2016.

[82.] Watanabe, N., Stogios, P.J., Skarina, T., Di Leo, R., Savchenko, A., Anderson, W.F., Center for Structural Genomics of Infectious Diseases (CSGID), *Crystal structure of a putative acyl-coa thioesterase ec709/eck0725 from escherichia coli in complex with hexanoyl-coa doi: 10.2210/pdb5t06/pdb.* 2016.

[83.] Ihsanawati, K., T., Murayama, K., Terada, T., Shirouzu, M., Yokoyama, S., RIKEN Structural Genomics/Proteomics Initiative (RSGI), *Crystal structure of a hypothetical protein tt1821 from thermus thermophilus doi: 10.2210/pdb1z54/pdb.* 2005.

[84.] Angelini, A., L. Cendron, S. Goncalves, G. Zanotti, and L. Terradot, *Structural and enzymatic characterization of hp0496, a ybgc thioesterase from helicobacter pylori.* Proteins, 2008. **72**(4): p. 1212-21.

[85.] Edwards, T.E., Staker, B.L., Seattle Structural Genomics Center for Infectious Disease, *Crystal structure of probable thioesterase from bartonella henselae doi: 10.2210/pdb3hm0/pdb.* 2009.

[86.] Borek, D., Wawrzak, Z., Grimshaw, S., Sandoval, J., Evdokimova, E., Savchenko, A., Anderson, W.F., Center for Structural Genomics of Infectious Diseases (CSGID), *Crystal structure of the putative tol-pal system-associated acyl-coa thioesterase from pseudomonas aeruginosa pao1 doi: 10.2210/pdb5v10/pdb.* 2017.

[87.] Kumarevel, T.S., Niwa, H., Kuramitsu, S., Yokoyama, S., RIKEN Structural Genomics/Proteomics Initiative (RSGI), *Crystal structure of hypothetical protein(aq1494) from aquifex aeolicus doi: 10.2210/pdb2egr/pdb.* 2007.

[88.] Godlewska, R., K. Wiśniewska, Z. Pietras, and E.K. Jagusztyn-Krynicka, *Peptidoglycan-associated lipoprotein (pal) of gram-negative bacteria: Function, structure, role in pathogenesis and potential application in immunoprophylaxis.* FEMS Microbiology Letters, 2009. **298**(1): p. 1-11.

[89.] Egan, A.J., *Bacterial outer membrane constriction.* Molecular microbiology, 2018. **107**(6): p. 676-87.

[90.] Gao, T., Q. Meng, and H. Gao, *Thioesterase ybgc affects motility by modulating c-di-gmp levels in shewanella oneidensis.* Sci. Rep., 2017. **7**(1): p. 3932.

[91.] Gerding, M.A., Y. Ogata, N.D. Pecora, H. Niki, and P.A. De Boer, *The trans-envelope tol–pal complex is part of the cell division machinery and required for proper outer-membrane invagination during cell constriction in e. Coli.* Mol. Microbiol., 2007. **63**(4): p. 1008-25.

[92.] Qin, X., S. He, X. Zhou, X. Cheng, X. Huang, Y. Wang, et al., *Quantitative proteomics reveals the crucial role of ybgc for salmonella enterica serovar enteritidis survival in egg white.* International Journal of Food Microbiology, 2019. **289**: p. 115-20.

[93.] Zhuang, Z., F. Song, B.M. Martin, and D. Dunaway-Mariano, *The ybgc protein encoded by the ybgc gene of the tol-pal gene cluster of haemophilus influenzae catalyzes acyl-coenzyme a thioester hydrolysis.* FEBS Lett., 2002. **516**(1-3): p. 161-3.

[94.] Wang, F., R. Langley, G. Gulten, L. Wang, and J.C. Sacchettini, *Identification of a type iii thioesterase reveals the function of an operon crucial for mtb virulence.* Chem. Biol., 2007. **14**(5): p. 543-51.

[95.] Gully, D. and E. Bouveret, *A protein network for phospholipid synthesis uncovered by a variant of the tandem affinity purification method in escherichia coli.* Proteomics, 2006. **6**(1): p. 282-93.

[96.] Benning, M.M., G. Wesenberg, R. Liu, K.L. Taylor, D. Dunaway-Mariano, and H.M. Holden, *The three-dimensional structure of 4-hydroxybenzoyl-coa thioesterase from pseudomonas sp. Strain cbs-3.* J. Biol. Chem., 1998. **273**(50): p. 33572-9.

[97.] Thoden, J.B., H.M. Holden, Z. Zhuang, and D. Dunaway-Mariano, *X-ray crystallographic analyses of inhibitor and substrate complexes of wild-type and mutant 4-hydroxybenzoyl-coa thioesterase.* J Biol Chem, 2002. **277**(30): p. 27468-76.

[98.] Zhuang, Z., J. Latham, F. Song, W. Zhang, M. Trujillo, and D. Dunaway-Mariano, *Investigation of the catalytic mechanism of the hotdog-fold enzyme superfamily pseudomonas sp. Strain cbs3 4-hydroxybenzoyl-coa thioesterase.* Biochem., 2012. **51**(3): p. 786-94.

[99.] Cork, D.J. and J.P. Krueger, *Microbial transformations of herbicides and pesticides.* Adv. Appl. Microbiol., 1991. **36**: p. 1-66.

[100.] Furukawa, K., *Molecular genetics and evolutionary relationship of pcb-degrading bacteria.* Biodegradation, 1994. **5**(3-4): p. 289-300.

[101.] Latham, J.A., D. Chen, K.N. Allen, and D. Dunaway-Mariano, *Divergence of substrate specificity and function in the escherichia coli hotdog-fold thioesterase paralogs ydii and ybdb.* Biochem., 2014. **53**(29): p. 4775-87.

[102.] Thoden, J.B., Z. Zhuang, D. Dunaway-Mariano, and H.M. Holden, *The structure of 4-hydroxybenzoyl-coa thioesterase from arthrobacter sp. Strain su.* J. Biol. Chem., 2003. **278**(44): p. 43709-16.

[103.] Song, F., J.B. Thoden, Z. Zhuang, J. Latham, M. Trujillo, H.M. Holden, et al., *The catalytic mechanism of the hotdog-fold enzyme superfamily 4-hydroxybenzoyl-coa thioesterase from arthrobacter sp. Strain su.* Biochem., 2012. **51**(35): p. 7000-16.

[104.] Badger, J., J.M. Sauder, J.M. Adams, S. Antonysamy, K. Bain, M.G. Bergseid, et al., *Structural analysis of a set of proteins resulting from a bacterial genomics project.* Proteins, 2005. **60**(4): p. 787-96.

[105.] Wu, R., J.A. Latham, D. Chen, J. Farelli, H. Zhao, K. Matthews, et al., *Structure and catalysis in the escherichia coli hotdog-fold thioesterase paralogs ydii and ybdb.* Biochem., 2014. **53**(29): p. 4788-805.

[106.] Kuzin, A.P., Benach, J., Chen, Y., Acton, T., Xiao, R., Conover, K., Ma, L.-C., Kellie, R., Cunningham, K.E., Montelione, G., Hunt, J.F., Tong, L., Northeast Structural Genomics Consortium (NESG), *X-ray crystal structure of protein hi1161 from haemophilus influenzae. Northeast structural genomics consortium target ir63. Doi: 10.2210/pdb2b6e/pdb.* 2005.

[107.] Kuzin, A.P., Lee, I., Chiang, Y., Acton, T.B., Montelione, G.T., Hunt, J.F., Tong, L., Northeast Structural Genomics Consortium (NESG), *X-ray structure of yb61_haein northeast structural genomics consortium target ir63 doi: 10.2210/pdb1s40/pdb.* 2004.

[108.] Ji, T., Allen, K.N., Dunaway-Mariano, D., *Crystal structure of thioesterase pa1618 from pseudomonas aeruginosa in complex with benzoyl-do-coa doi: 10.2210/pdb4qd9/pdb.* 2015.

[109.] Kuzin, A.P., Edstrom, W., Vorobiev, S.M., Lee, I., Forouhar, F., Ma, L., Chiang, Y., Rong, X., Acton, T.B., Montelione, G.T., Hunt, J.F., Tong, L., Northeast Structural Genomics Consortium (NESG), *X-ray structure of ydii_ecoli northeast structural genomics consortium target er29. Doi: 10.2210/pdb1sbk/pdb.* 2004.

[110.] Claudio, F.G., T. Anatoli, B. Greg, F. Robert, E. Elena, X. Xiaohui, et al., *Structure and activity of the pseudomonas aeruginosa hotdog-fold thioesterases pa5202 and pa2801.* Biochem. J, 2012. **444**(3): p. 445-55.

[111.] Furt, F., W.J. Allen, J.R. Widhalm, P. Madzelan, R.C. Rizzo, G. Basset, et al., *Functional convergence of structurally distinct thioesterases from cyanobacteria and plants involved in phylloquinone biosynthesis.* Acta Crystallogr. Sect. D. Biol. Crystallogr., 2013. **69**(10): p. 1876-88.

[112.] (JCSG), J.C.f.S.G., *Crystal structure of a putative thioesterase (pmt_2055) from prochlorococcus marinus str. Mit 9313 at 1.50 a resolution doi: 10.2210/pdb2hx5/pdb.* 2006.

[113.] Widhalm, J.R., C. van Oostende, F. Furt, and G.J. Basset, *A dedicated thioesterase of the hotdog-fold family is required for the biosynthesis of the naphthoquinone ring of vitamin k1.* Proc. Natl. Acad. Sci. USA, 2009. **106**(14): p. 5599-603.

[114.] Song, F., Z. Zhuang, L. Finci, D. Dunaway-Mariano, R. Kniewel, J.A. Buglino, et al., *Structure, function, and mechanism of the phenylacetate pathway hot dog-fold thioesterase paai.* J. Biol. Chem., 2006. **281**(16): p. 11028-38.

[115.] Gonzalez, C.F., A. Tchigvintsev, G. Brown, R. Flick, E. Evdokimova, X. Xu, et al., *Structure and activity of the pseudomonas aeruginosa hotdog-fold thioesterases pa5202 and pa2801.* Biochem. J, 2012. **444**(3): p. 445-55.

[116.] Su, X.-D., Hou, Q.M., Fan, X.X., Nan, J., Liu, X., *The crystal structure of smu.793 from streptococcus mutans ua159 doi: 10.2210/pdb3lbb/pdb.* 2011.

[117.] Khandokar, Y.B., N. Roman, K.M. Smith, P. Srivastava, and J.K. Forwood, *Expression, purification, crystallization and preliminary x-ray analysis of the paai-like thioesterase sav0944 from staphylococcus aureus.* Acta Crystallogr F Struct Biol Commun, 2014. **70**(Pt 2): p. 244-7.

[118.] Khandokar, Y.B., Srivastava, P., Forwood, J., *Crystal structure of mutant of (q32a) thioesterase enzyme sav0944 from staphylococcus aureus subsp. Aureus mu50 doi: 10.2210/pdb4ybv/pdb.* 2016.

[119.] Kunishima, N., Y. Asada, M. Sugahara, J. Ishijima, Y. Nodake, M. Sugahara, et al., *A novel induced-fit reaction mechanism of asymmetric hot dog thioesterase paai.* J. Mol. Biol., 2005. **352**(1): p. 212-28.

[120.] Shimizu, K., RIKEN Structural Genomics/Proteomics Initiative (RSGI), *Mutant n33d structure of phenylacetic acid degradation protein paai from thermus thermophilus hb8 doi: 10.2210/pdb2dsl/pdb.* 2006.

[121.] Teufel, R., V. Mascaraque, W. Ismail, M. Voss, J. Perera, W. Eisenreich, et al., *Bacterial phenylalanine and phenylacetate catabolic pathway revealed.* Proc. Natl. Acad. Sci. USA, 2010. **107**(32): p. 14390-5.

[122.] Teufel, R., C. Gantert, M. Voss, W. Eisenreich, W. Haehnel, and G. Fuchs, *Studies on the mechanism of ring hydrolysis in phenylacetate degradation a metabolic branching point.* J. Biol. Chem., 2011. **286**(13): p. 11021-34.

[123.] Nogales, J., R. Macchi, F. Franchi, D. Barzaghi, C. Fernández, J. García, et al., *Characterization of the last step of the aerobic phenylacetic acid degradation pathway.* Microbiology, 2007. **153**(2): p. 357-65.

[124.] Sassetti, C.M. and E.J. Rubin, *Genetic requirements for mycobacterial survival during infection.* Proc. Natl. Acad. Sci. U. S. A., 2003. **100**(22): p. 12989-94.

[125.] Sassetti, C.M., D.H. Boyd, and E.J. Rubin, *Genes required for mycobacterial growth defined by high density mutagenesis.* Mol. Microbiol., 2003. **48**(1): p. 77-84.

[126.] Maity, K., P. Bajaj, N. Surolia, A. Surolia, and K. Suguna, *Insights into the substrate specificity of a thioesterase rv0098 of mycobacterium tuberculosis through x-ray crystallographic and molecular dynamics studies.* Journal of Biomolecular Structure and Dynamics, 2012. **29**(5): p. 973-83.

[127.] Dias, M.V., F. Huang, D.Y. Chirgadze, M. Tosin, D. Spiteller, E.F. Dry, et al., *Structural basis for the activity and substrate specificity of fluoroacetyl-coa thioesterase flk.* J. Biol. Chem., 2010. **285**(29): p. 22495-504.

[128.] Weeks, A.M., S.M. Coyle, M. Jinek, J.A. Doudna, and M.C. Chang, *Structural and biochemical studies of a fluoroacetyl-coa-specific thioesterase reveal a molecular basis for fluorine selectivity.* Biochem., 2010. **49**(43): p. 9269-79.

[129.] Weeks, A.M., N.S. Keddie, K.D. Wadoux, D. O'Hagan, and M.C. Chang, *Molecular recognition of fluorine impacts substrate selectivity in the fluoroacetyl-coa thioesterase flk.* Biochem., 2014. **53**(12): p. 2053-63.

[130.] Zhuravleva, E., H. Gut, D. Hynx, D. Marcellin, C.K. Bleck, C. Genoud, et al., *Acyl coenzyme a thioesterase them5/acot15 is involved in cardiolipin remodeling and fatty liver development.* Mol. Cell. Biol., 2012. **32**(14): p. 2685-97.

[131.] Jones, A., H.M. Davies, and T.A. Voelker, *Palmitoyl-acyl carrier protein (acp) thioesterase and the evolutionary origin of plant acyl-acp thioesterases.* The Plant Cell Online, 1995. **7**(3): p. 359-71.

[132.] Salas, J.n.J. and J.B. Ohlrogge, *Characterization of substrate specificity of plant fata and fatb acyl-acp thioesterases.* Archives of Biochemistry and Biophysics, 2002. **403**(1): p. 25-34.

[133.] Pollard, M.R., L. Anderson, C. Fan, D.J. Hawkins, and H.M. Davies, *A specific acyl-acp thioesterase implicated in medium-chain fatty acid production in immature cotyledons of umbellularia californica.* Arch Biochem Biophys, 1991. **284**(2): p. 306-12.

[134.] Knaut, J. and H. Richtler, *Trends in industrial uses of palm and lauric oils.* Journal of the American Oil Chemists' Society, 1985. **62**(2): p. 317-27.

[135.] Kim, H.J., J.E. Silva, H.S. Vu, K. Mockaitis, J.-W. Nam, and E.B. Cahoon, *Toward production of jet fuel functionality in oilseeds: Identification of fatb acyl-acyl carrier protein thioesterases and*

evaluation of combinatorial expression strategies in camelina seeds. J. Exp. Bot., 2015. **66**(14): p. 4251-65.

[136.] Burgal, J., J. Shockey, C. Lu, J. Dyer, T. Larson, I. Graham, et al., *Metabolic engineering of hydroxy fatty acid production in plants: Rcdgat2 drives dramatic increases in ricinoleate levels in seed oil.* Plant Biotechnol. J., 2008. **6**(8): p. 819-31.

[137.] Jing, F., D.C. Cantu, J. Tvaruzkova, J.P. Chipman, B.J. Nikolau, M.D. Yandeau-Nelson, et al., *Phylogenetic and experimental characterization of an acyl-acp thioesterase family reveals significant diversity in enzymatic specificity and activity.* BMC Biochem., 2011. **12**(1): p. 44.

[138.] (JCSG), J.C.f.S.G., *Crystal structure of oleoyl thioesterase (putative) (np_784467.1) from lactobacillus plantarum at 2.00 a resolution doi: 10.2210/pdb2own/pdb.* 2007.

[139.] (JCSG), J.C.f.S.G., *Crystal structure of an acyl-acp thioesterase (np_810988.1) from bacteroides thetaiotaomicron vpi-5482 at 1.90 a resolution doi: 10.2210/pdb2ess/pdb.* 2006.

[140.] Chang, C., Wu, R., Endres, M., Joachimiak, A., Midwest Center for Structural Genomics (MCSG), *Crystal structure of acyl-acp thioesterase from spirosoma linguale doi: 10.2210/pdb4gak/pdb.* 2012.

[141.] Feng, Y., Y. Wang, J. Liu, Y. Liu, X. Cao, and S. Xue, *Structural insight into acyl-acp thioesterase toward substrate specificity design.* ACS Chem. Biol., 2012. **7**(11): p. 2830-6.

[142.] Hellyer, A., P.F. Leadlay, and A.R. Slabas, *Induction, purification and characterisation of acyl-acp thioesterase from developing seeds of oil seed rape (brassica napus).* Plant Mol. Biol., 1992. **20**(5): p. 763-80.

[143.] McKeon, T.A. and P.K. Stumpf, *Purification and characterization of the stearoyl-acyl carrier protein desaturase and the acyl-acyl carrier protein thioesterase from maturing seeds of safflower.* J. Biol. Chem., 1982. **257**(20): p. 12141-7.

[144.] Jing, F., M.D. Yandeau-Nelson, and B.J. Nikolau, *Identification of active site residues implies a two-step catalytic mechanism for acyl-acp thioesterase.* Biochem. J, 2018. **475**(23): p. 3861-73.

[145.] Kotaka, M., R. Kong, I. Qureshi, Q.S. Ho, H. Sun, C.W. Liew, et al., *Structure and catalytic mechanism of the thioesterase calicheamicin enediyne biosynthesis.* J. Biol. Chem., 2009. **284**(23): p. 15739-49.

[146.] Kim, Y., Bigelow, L., Bearden, J., Babnigg, J., Bingman, C.A., Yennamalli, R., Lohman, J., Ma, M., Shen, B., Phillips Jr., G.N., Joachimiak, A., Midwest Center for Structural Genomics (MCSG), Enzyme Discovery for Natural Product Biosynthesis (NatPro), *The structure of sgce10, the acp-polyene thioesterase involved in c-1027 biosynthesis doi: 10.2210/pdb4i4j/pdb.* 2012.

[147.] Liew, C.W., A. Sharma, M. Kotaka, R. Kong, H. Sun, I. Qureshi, et al., *Induced-fit upon ligand binding revealed by crystal structures of the hot-dog fold thioesterase in dynemicin biosynthesis.* J. Mol. Biol., 2010. **404**(2): p. 291-306.

[148.] Hinman, L.M., P.R. Hamann, R. Wallace, A.T. Menendez, F.E. Durr, and J. Upeslacis, *Preparation and characterization of monoclonal antibody conjugates of the calicheamicins: A novel and potent family of antitumor antibiotics.* Cancer Res., 1993. **53**(14): p. 3336-42.

[149.] Horsman, G.P., Y. Chen, J.S. Thorson, and B. Shen, *Polyketide synthase chemistry does not direct biosynthetic divergence between 9-and 10-membered enediynes.* Proc. Natl. Acad. Sci. USA, 2010. **107**(25): p. 11331-5.

[150.] Belecki, K., J.M. Crawford, and C.A. Townsend, *Production of octaketide polyenes by the calicheamicin polyketide synthase cale8: Implications for the biosynthesis of enediyne core structures.* J. Am. Chem. Soc., 2009. **131**(35): p. 12564-6.

[151.] Lenfant, N., T. Hotelier, Y. Bourne, P. Marchot, and A. Chatonnet, *Proteins with an alpha/beta hydrolase fold: Relationships between subfamilies in an ever-growing superfamily.* Chemico-biological interactions, 2013. **203**(1): p. 266-8.

[152.] Svensson, L.T., M. Wilcke, and S.E. Alexson, *Peroxisome proliferators differentially regulate long-chain acyl-coa thioesterases in rat liver.* Eur. J. Biochem., 1995. **230**(2): p. 813-20.
[153.] Lawson, D., U. Derewenda, L. Serre, S. Ferri, R. Szittner, Y. Wei, et al., *Structure of a myristoyl-acp-specific thioesterase from vibrio harveyi.* Biochem., 1994. **33**(32): p. 9382-8.
[154.] Ollis, D.L., E. Cheah, M. Cygler, B. Dijkstra, F. Frolow, S.M. Franken, et al., *The α/β hydrolase fold.* Protein Eng., 1992. **5**(3): p. 197-211.
[155.] Marchot, P. and A. Chatonnet, *Enzymatic activity and protein interactions in alpha/beta hydrolase fold proteins: Moonlighting versus promiscuity.* Protein and peptide letters, 2012. **19**(2): p. 132-43.
[156.] Röttig, M., M.H. Medema, K. Blin, T. Weber, C. Rausch, and O. Kohlbacher, *Nrpspredictor2—a web server for predicting nrps adenylation domain specificity.* Nucleic Acids Res., 2011: p. gkr323.
[157.] Yuzawa, S., W. Kim, L. Katz, and J.D. Keasling, *Heterologous production of polyketides by modular type i polyketide synthases in escherichia coli.* Curr. Opin. Biotechnol., 2012. **23**(5): p. 727-35.
[158.] Yu, X., T. Liu, F. Zhu, and C. Khosla, *In vitro reconstitution and steady-state analysis of the fatty acid synthase from escherichia coli.* Proc. Natl. Acad. Sci. USA, 2011. **108**(46): p. 18643-8.
[159.] Chakravarty, B., Z. Gu, S.S. Chirala, S.J. Wakil, and F.A. Quiocho, *Human fatty acid synthase: Structure and substrate selectivity of the thioesterase domain.* Proc. Natl. Acad. Sci. U. S. A., 2004. **101**(44): p. 15567-72.
[160.] Maier, T., M. Leibundgut, and N. Ban, *The crystal structure of a mammalian fatty acid synthase.* Science, 2008. **321**(5894): p. 1315-22.
[161.] Korman, T.P., J.M. Crawford, J.W. Labonte, A.G. Newman, J. Wong, C.A. Townsend, et al., *Structure and function of an iterative polyketide synthase thioesterase domain catalyzing claisen cyclization in aflatoxin biosynthesis.* Proc. Natl. Acad. Sci. USA, 2010. **107**(14): p. 6246-51.
[162.] Frueh, D.P., H. Arthanari, A. Koglin, D.A. Vosburg, A.E. Bennett, C.T. Walsh, et al., *Dynamic thiolation–thioesterase structure of a non-ribosomal peptide synthetase.* Nature, 2008. **454**(7206): p. 903-6.
[163.] Samel, S.A., B. Wagner, M.A. Marahiel, and L.-O. Essen, *The thioesterase domain of the fengycin biosynthesis cluster: A structural base for the macrocyclization of a non-ribosomal lipopeptide.* J. Mol. Biol., 2006. **359**(4): p. 876-89.
[164.] Siponen, M.I., Moche, M., Arrowsmith, C.H., Berglund, H., Bountra, C., Collins, R., Edwards, A.M., Flodin, S., Flores, A., Graslund, S., Hammarstrom, M., Johansson, A., Johansson, I., Kallas, A., Karlberg, T., Kraulis, P., Kotenyova, T., Kotzsch, A., Markova, N., Nielsen, T.K., Nordlund, P., Nyman, T., Persson, C., Roos, A.K., Schutz, P., Svensson, L., Thorsell, A.G., Tresaugues, L., Van Den Berg, S., Wahlberg, E., Weigelt, J., Welin, M., Wisniewska, M., Schuler, H., Structural Genomics Consortium (SGC), *Human acyl-coenzyme a thioesterase 4 doi: 10.2210/pdb3k2i/pdb.* 2009.
[165.] Mandel, C.R., B. Tweel, and L. Tong, *Crystal structure of human mitochondrial acyl-coa thioesterase (acot2).* Biochem. Biophys. Res. Commun., 2009. **385**(4): p. 630-3.
[166.] Durgan, D.J., J.K. Smith, M.A. Hotze, O. Egbejimi, K.D. Cuthbert, V. G. Zaha, et al., *Distinct transcriptional regulation of long-chain acyl-coa synthetase isoforms and cytosolic thioesterase 1 in the rodent heart by fatty acids and insulin.* American Journal of Physiology-Heart and Circulatory Physiology, 2006. **290**(6): p. H2480-H97.
[167.] Wilson, C., M. Tran, K. Salazar, M. Young, and H. Taegtmeyer, *Western diet, but not high fat diet, causes derangements of fatty acid metabolism and contractile dysfunction in the heart of wistar rats.* Biochem. J, 2007. **406**: p. 457-67.
[168.] Hunt, M.C., A. Rautanen, M.A. Westin, L.T. Svensson, and S.E. Alexson, *Analysis of the mouse and human acyl-coa thioesterase (acot) gene clusters shows that convergent, functional*

evolution results in a reduced number of human peroxisomal acots. FASEB J., 2006. **20**(11): p. 1855-64.

[169.] Park, I.H., J.D. Venable, C. Steckler, S.E. Cellitti, S.A. Lesley, G. Spraggon, et al., *Estimation of hydrogen-exchange protection factors from md simulation based on amide hydrogen bonding analysis.* J. Chem. Inf. Model., 2015. **55**(9): p. 1914-25.

[170.] Pemble, C.W., L.C. Johnson, S.J. Kridel, and W.T. Lowther, *Crystal structure of the thioesterase domain of human fatty acid synthase inhibited by orlistat.* Nat. Struct. Mol. Biol., 2007. **14**(8): p. 704-9.

[171.] Zhang, W., B. Chakravarty, F. Zheng, Z. Gu, H. Wu, J. Mao, et al., *Crystal structure of fas thioesterase domain with polyunsaturated fatty acyl adduct and inhibition by dihomo -γ-linolenic acid.* Proc. Natl. Acad. Sci. USA, 2011. **108**(38): p. 15757-62.

[172.] Gay, D.C., P.J. Spear, and A.T. Keatinge-Clay, *A double-hotdog with a new trick: Structure and mechanism of the trans-acyltransferase polyketide synthase enoyl-isomerase.* ACS Chem. Biol., 2014. **9**(10): p. 2374-81.

[173.] Liu, Y., T. Zheng, and S.D. Bruner, *Structural basis for phosphopantetheinyl carrier domain interactions in the terminal module of nonribosomal peptide synthetases.* Chem Biol, 2011. **18**(11): p. 1482-8.

[174.] Menendez, J.A. and R. Lupu, *Fatty acid synthase and the lipogenic phenotype in cancer pathogenesis.* Nature Reviews Cancer, 2007. **7**(10): p. 763-77.

[175.] Menendez, J.A., A. Vazquez-Martin, F.J. Ortega, and J.M. Fernandez-Real, *Fatty acid synthase: Association with insulin resistance, type 2 diabetes, and cancer.* Clin. Chem., 2009. **55**(3): p. 425-38.

[176.] Raymond, K.N., E.A. Dertz, and S.S. Kim, *Enterobactin: An archetype for microbial iron transport.* Proc. Natl. Acad. Sci. USA, 2003. **100**(7): p. 3584-8.

[177.] Huguenin-Dezot, N., D.A. Alonzo, G.W. Heberlig, M. Mahesh, D.P. Nguyen, M.H. Dornan, et al., *Trapping biosynthetic acyl-enzyme intermediates with encoded 2,3-diaminopropionic acid.* Nature, 2019. **565**(7737): p. 112-7.

[178.] Tsai, S.-C., L.J. Miercke, J. Krucinski, R. Gokhale, J.C.-H. Chen, P.G. Foster, et al., *Crystal structure of the macrocycle-forming thioesterase domain of the erythromycin polyketide synthase: Versatility from a unique substrate channel.* Proc. Natl. Acad. Sci. USA, 2001. **98**(26): p. 14808-13.

[179.] Tsai, S.-C., H. Lu, D.E. Cane, C. Khosla, and R.M. Stroud, *Insights into channel architecture and substrate specificity from crystal structures of two macrocycle-forming thioesterases of modular polyketide synthases.* Biochem., 2002. **41**(42): p. 12598-606.

[180.] Argyropoulos, P., F. Bergeret, C. Pardin, J.M. Reimer, A. Pinto, C.N. Boddy, et al., *Towards a characterization of the structural determinants of specificity in the macrocyclizing thioesterase for deoxyerythronolide b biosynthesis.* Biochim Biophys Acta, 2016. **1860**(3): p. 486-97.

[181.] Li, X., N. Sevillano, F. La Greca, J. Hsu, Mathews, II, T. Matsui, et al., *Discovery and characterization of a thioesterase-specific monoclonal antibody that recognizes the 6-deoxyerythronolide b synthase.* Biochem., 2018. **57**(43): p. 6201-8.

[182.] Scaglione, J.B., D.L. Akey, R. Sullivan, J.D. Kittendorf, C.M. Rath, E.S. Kim, et al., *Biochemical and structural characterization of the tautomycetin thioesterase: Analysis of a stereoselective polyketide hydrolase.* Angew. Chem., 2010. **122**(33): p. 5862-6.

[183.] Giraldes, J.W., D.L. Akey, J.D. Kittendorf, D.H. Sherman, J.L. Smith, and R.A. Fecik, *Structural and mechanistic insights into polyketide macrolactonization from polyketide-based affinity labels.* Nat. Chem. Biol., 2006. **2**(10): p. 531-6.

[184.] Akey, D.L., J.D. Kittendorf, J.W. Giraldes, R.A. Fecik, D.H. Sherman, and J.L. Smith, *Structural basis for macrolactonization by the pikromycin thioesterase.* Nat. Chem. Biol., 2006. **2**(10): p. 537-42.

[185.] Whicher, J.R., G. Florova, P.K. Sydor, R. Singh, M. Alhamadsheh, G.L. Challis, et al., *Structure and function of the redj protein, a thioesterase from the prodiginine biosynthetic pathway in streptomyces coelicolor.* J. Biol. Chem., 2011. **286**(25): p. 22558-69.

[186.] Claxton, H.B., D.L. Akey, M.K. Silver, S.J. Admiraal, and J.L. Smith, *Structure and functional analysis of rifr, the type ii thioesterase from the rifamycin biosynthetic pathway.* J. Biol. Chem., 2009. **284**(8): p. 5021-9.

[187.] Koglin, A., F. Löhr, F. Bernhard, V.R. Rogov, D.P. Frueh, E.R. Strieter, et al., *Structural basis for the selectivity of the external thioesterase of the surfactin synthetase.* Nature, 2008. **454**(7206): p. 907-11.

[188.] Kotowska, M. and K. Pawlik, *Roles of type ii thioesterases and their application for secondary metabolite yield improvement.* Applied microbiology and biotechnology, 2014. **98**(18): p. 7735-46.

[189.] Ohlemacher, S.I., Y. Xu, D.L. Kober, M. Malik, J.C. Nix, T.J. Brett, et al., *Ybtt is a low-specificity type ii thioesterase that maintains production of the metallophore yersiniabactin in pathogenic enterobacteria.* J. Biol. Chem., 2018. **293**(51): p. 19572-85.

[190.] Guntaka, N.S., A.R. Healy, J.M. Crawford, S.B. Herzon, and S.D. Bruner, *Structure and functional analysis of clbq, an unusual intermediate-releasing thioesterase from the colibactin biosynthetic pathway.* ACS Chem. Biol., 2017. **12**(10): p. 2598-608.

[191.] Wall, L. and E.A. Meighen, *Subunit structure of the fatty acid reductase complex from photobacterium phosphoreum.* Biochem., 1986. **25**(15): p. 4315-21.

[192.] Riendeau, D., A. Rodriguez, and E. Meighen, *Resolution of the fatty acid reductase from photobacterium phosphoreum into acyl protein synthetase and acyl-coa reductase activities. Evidence for an enzyme complex.* J. Biol. Chem, 1982. **257**(12): p. 6908-15.

[193.] Brodl, E., A. Winkler, and P. Macheroux, *Molecular mechanisms of bacterial bioluminescence.* Comput Struct Biotechnol J, 2018. **16**: p. 551-64.

[194.] Ferri, S. and E. Meighen, *A lux-specific myristoyl transferase in luminescent bacteria related to eukaryotic serine esterases.* J. Biol. Chem., 1991. **266**(20): p. 12852-7.

[195.] Li, J., B. Ahvazi, R. Szittner, and E. Meighen, *Mutation of the nucleophilic elbow of the lux-specific thioesterase from vibrio harveyi.* Biochem. Biophys. Res. Commun., 2000. **275**(2): p. 704-8.

[196.] Ulitzur, S. and J.W. Hastings, *Evidence for tetradecanal as the natural aldehyde in bacterial bioluminescence.* Proc. Natl. Acad. Sci. U. S. A., 1979. **76**(1): p. 265-7.

[197.] Bellizzi, J.J., 3rd, J. Widom, C. Kemp, J.Y. Lu, A.K. Das, S.L. Hofmann, et al., *The crystal structure of palmitoyl protein thioesterase 1 and the molecular basis of infantile neuronal ceroid lipofuscinosis.* Proc. Natl. Acad. Sci. U. S. A., 2000. **97**(9): p. 4573-8.

[198.] Calero, G., P. Gupta, M.C. Nonato, S. Tandel, E.R. Biehl, S.L. Hofmann, et al., *The crystal structure of palmitoyl protein thioesterase-2 (ppt2) reveals the basis for divergent substrate specificities of the two lysosomal thioesterases, ppt1 and ppt2.* J. Biol. Chem., 2003. **278**(39): p. 37957-64.

[199.] Martin, B.R., C. Wang, A. Adibekian, S.E. Tully, and B.F. Cravatt, *Global profiling of dynamic protein palmitoylation.* Nat. Methods, 2012. **9**(1): p. 84-9.

[200.] Gupta, P., A.A. Soyombo, A. Atashband, K.E. Wisniewski, J.M. Shelton, J.A. Richardson, et al., *Disruption of ppt1 or ppt2 causes neuronal ceroid lipofuscinosis in knockout mice.* Proc. Natl. Acad. Sci. USA, 2001. **98**(24): p. 13566-71.

[201.] Segal-Salto, M., T. Sapir, and O. Reiner, *Reversible cysteine acylation regulates the activity of human palmitoyl-protein thioesterase 1 (ppt1).* PLoS One, 2016. **11**(1): p. e0146466.

[202.] Rebecca, V.W., M.C. Nicastri, C. Fennelly, C.I. Chude, J.S. Barber-Rotenberg, A. Ronghe, et al., *Ppt1 promotes tumor growth and is the molecular target of chloroquine derivatives in cancer.* Cancer Discov., 2019. **9**(2): p. 220-9.

[203.] Bürger, M., T.J. Zimmermann, Y. Kondoh, P. Stege, N. Watanabe, H. Osada, et al., *Crystal structure of the predicted phospholipase lyplal1 reveals unexpected functional plasticity despite close relationship to acyl protein thioesterases.* J. Lipid Res., 2012. **53**(1): p. 43-50.

[204.] Devedjiev, Y., Z. Dauter, S.R. Kuznetsov, T.L. Jones, and Z.S. Derewenda, *Crystal structure of the human acyl protein thioesterase i from a single x-ray data set to 1.5 å.* Structure, 2000. **8**(11): p. 1137-46.

[205.] Pesaresi, A. and D. Lamba, *Insights into the fatty acid chain length specificity of the carboxylesterase pa3859 from pseudomonas aeruginosa: A combined structural, biochemical and computational study.* Biochimie, 2010. **92**(12): p. 1787-92.

[206.] Kim, K.K., H.K. Song, D.H. Shin, K.Y. Hwang, S. Choe, O.J. Yoo, et al., *Crystal structure of carboxylesterase from pseudomonas fluorescens, an α/β hydrolase with broad substrate specificity.* Structure, 1997. **5**(12): p. 1571-84.

[207.] Ma, J., L. Wu, F. Guo, J. Gu, X. Tang, L. Jiang, et al., *Enhanced enantioselectivity of a carboxyl esterase from rhodobacter sphaeroides by directed evolution.* Applied microbiology and biotechnology, 2013. **97**(11): p. 4897-906.

[208.] Filippova, E.V., L.A. Weston, M.L. Kuhn, B. Geissler, A.M. Gehring, N. Armoush, et al., *Large scale structural rearrangement of a serine hydrolase from francisella tularensis facilitates catalysis.* J. Biol. Chem., 2013. **288**(15): p. 10522-35.

[209.] Sadeghi, R.S., K. Kulej, R.S. Kathayat, B.A. Garcia, B.C. Dickinson, D.C. Brady, et al., *Wnt5a signaling induced phosphorylation increases dpt1 activity and promotes melanoma metastatic behavior.* Elife, 2018. **7**.

[210.] Kong, E., S. Peng, G. Chandra, C. Sarkar, Z. Zhang, M.B. Bagh, et al., *Dynamic palmitoylation links cytosol-membrane shuttling of acyl-protein thioesterase-1 and acyl-protein thioesterase-2 with that of proto-oncogene h-ras products and growth-associated protein-43.* J. Biol. Chem., 2013. **288**(13): p. 9112-25.

[211.] Tian, L., H. McClafferty, H.-G. Knaus, P. Ruth, and M.J. Shipston, *Distinct acyl protein transferases and thioesterases control surface expression of calcium-activated potassium channels.* J. Biol. Chem., 2012. **287**(18): p. 14718-25.

[212.] Kim, M.H., B.S. Kang, S. Kim, K.J. Kim, C.H. Lee, B.C. Oh, et al., *The crystal structure of the esta protein, a virulence factor from streptococcus pneumoniae.* Proteins: Structure, Function, and Bioinformatics, 2008. **70**(2): p. 578-83.

[213.] van Straaten, K.E., C.F. Gonzalez, R.B. Valladares, X. Xu, A.V. Savchenko, and D.A. Sanders, *The structure of a putative s-formylglutathione hydrolase from agrobacterium tumefaciens.* Protein Sci., 2009. **18**(10): p. 2196-202.

[214.] Chen, N.H., R.M. Couñago, K.Y. Djoko, M.P. Jennings, M.A. Apicella, B. Kobe, et al., *A glutathione-dependent detoxification system is required for formaldehyde resistance and optimal survival of neisseria meningitidis in biofilms.* Antioxidants & redox signaling, 2013. **18**(7): p. 743-55.

[215.] Lemak, S., A. Tchigvintsev, P. Petit, R. Flick, A.U. Singer, G. Brown, et al., *Structure and activity of the cold-active and anion-activated carboxyl esterase olei01171 from the oil-degrading marine bacterium oleispira antarctica.* Biochem. J, 2012. **445**(2): p. 193-203.

[216.] Alterio, V., V. Aurilia, A. Romanelli, A. Parracino, M. Saviano, S. D'Auria, et al., *Crystal structure of an s-formylglutathione hydrolase from pseudoalteromonas haloplanktis tac125.* Biopolymers: Original Research on Biomolecules, 2010. **93**(8): p. 669-77.

[217.] Legler, P.M., D. Kumaran, S. Swaminathan, F.W. Studier, and C.B. Millard, *Structural characterization and reversal of the natural organophosphate resistance of a d-type esterase, saccharomyces cerevisiae s-formylglutathione hydrolase.* Biochem., 2008. **47**(36): p. 9592-601.

[218.] Legler, P.M., D.H. Leary, W.J. Hervey IV, and C.B. Millard, *A role for his-160 in peroxide inhibition of s. Cerevisiae s-formylglutathione hydrolase: Evidence for an oxidation sensitive motif.* Archives of biochemistry and biophysics, 2012. **528**(1): p. 7-20.

[219.] Wu, D., Y. Li, G. Song, D. Zhang, N. Shaw, and Z.-J. Liu, *Crystal structure of human esterase d: A potential genetic marker of retinoblastoma.* FASEB J., 2009. **23**(5): p. 1441-6.

[220.] Cummins, I., K. McAuley, A. Fordham-Skelton, R. Schwoerer, P.G. Steel, B.G. Davis, et al., *Unique regulation of the active site of the serine esterase s-formylglutathione hydrolase.* J. Mol. Biol., 2006. **359**(2): p. 422-32.

[221.] Frydman, M., B. Bonné-Tamir, L.A. Farrer, P.M. Conneally, A. Magazanik, S. Ashbel, et al., *Assignment of the gene for wilson disease to chromosome 13: Linkage to the esterase d locus.* Proc. Natl. Acad. Sci. USA, 1985. **82**(6): p. 1819-21.

[222.] Sparkes, R.S., A.L. Murphree, R.W. Lingua, M.C. Sparkes, L.L. Field, S.J. Funderburk, et al., *Gene for hereditary retinoblastoma assigned to human chromosome 13 by linkage to esterase d.* Science, 1983. **219**(4587): p. 971-3.

[223.] Mullins, E.A. and T.J. Kappock, *Crystal structures of acetobacter aceti succinyl-coenzyme a (coa): Acetate coa-transferase reveal specificity determinants and illustrate the mechanism used by class i coa-transferases.* Biochem., 2012. **51**(42): p. 8422-34.

[224.] Forouhar, F., Neely, H., Seetharaman, J., Yong, W., Ho, C.K., Fang, Y., Cunningham, K., Ma, L.-C., Xiao, R., Liu, J., Baran, M.C., Acton, T.B., Rost, B., Montelione, G.T., Hunt, J.F., Tong, L., Northeast Structural Genomics Consortium (NESG), *Crystal structure of the putative acetyl-coa hydrolase/transferase pg1013 from porphyromonas gingivalis, northeast structural genomics target pgr16. Doi: 10.2210/pdb2nqv/pdb.* 2007.

[225.] Chang, C., Evdokimova, E., Kudritska, M., Savchenko, A., Edwards, A., Joachimiak, A., Midwest Center for Structural Genomics (MCSG), *Crystal structure of coenzyme a transferase from pseudomonas aeruginosa doi: 10.2210/pdb2g39/pdb.* 2006.

[226.] Mullins, E.A., J.A. Francois, and T.J. Kappock, *A specialized citric acid cycle requiring succinyl-coenzyme a (coa): Acetate coa-transferase (aarc) confers acetic acid resistance on the acidophile acetobacter aceti.* J. Bacteriol., 2008. **190**(14): p. 4933-40.

[227.] White, H. and W.P. Jencks, *Mechanism and specificity of succinyl-coa: 3-ketoacid coenzyme a transferase.* J. Biol. Chem., 1976. **251**(6): p. 1688-99.

[228.] Torres, R., B. Lan, Y. Latif, N. Chim, and C.W. Goulding, *Structural snapshots along the reaction pathway of yersinia pestis ripa, a putative butyryl-coa transferase.* Acta Crystallogr. Sect. D. Biol. Crystallogr., 2014. **70**(4): p. 0-.

[229.] Murphy, J.R., E.A. Mullins, and T.J. Kappock, *Functional dissection of the bipartite active site of the class i coenzyme a (coa)-transferase succinyl-coa: Acetate coa-transferase.* Frontiers in chemistry, 2016. **4**: p. 23.

[230.] Lo, Y.-C., S.-C. Lin, J.-F. Shaw, and Y.-C. Liaw, *Crystal structure of escherichia coli thioesterase i/protease i/lysophospholipase l1: Consensus sequence blocks constitute the catalytic center of sgnh-hydrolases through a conserved hydrogen bond network.* J. Mol. Biol., 2003. **330**(3): p. 539-51.

[231.] Brzuszkiewicz, A., E. Nowak, Z. Dauter, M. Dauter, H. Cieslinski, A. Dlugolecka, et al., *Structure of esta esterase from psychrotrophic pseudoalteromonas sp. 643a covalently inhibited by monoethylphosphonate.* Acta Crystallogr. Sect. F Struct. Biol. Cryst. Commun., 2009. **65**(Pt 9): p. 862-5.

[232.] Kovacic, F., J. Granzin, S. Wilhelm, B. Kojic-Prodic, R. Batra-Safferling, and K.E. Jaeger, *Structural and functional characterisation of tesa - a novel lysophospholipase a from pseudomonas aeruginosa.* PLoS One, 2013. **8**(7): p. e69125.

[233.] Cho, H. and J.E. Cronan, Jr., *Escherichia coli thioesterase i, molecular cloning and sequencing of the structural gene and identification as a periplasmic enzyme.* J. Biol. Chem., 1993. **268**(13): p. 9238-45.

[234.] Ichihara, S., Y. Matsubara, C. Kato, K. Akasaka, and S. Mizushima, *Molecular cloning, sequencing, and mapping of the gene encoding protease i and characterization of proteinase and proteinase-defective escherichia coli mutants.* J. Bacteriol., 1993. **175**(4): p. 1032-7.

[235.] Karasawa, K., K. Yokoyama, M. Setaka, and S. Nojima, *The escherichia coli pldc gene encoding lysophospholipase l1 is identical to the apea and tesa genes encoding protease i and thioesterase i, respectively.* J. Biochem., 1999. **126**(2): p. 445-8.

[236.] Spencer, A., Greenspan, AD & Cronan, JE, *Thioesterases i and ii of escherichia coli.* The Journal of Biological Chemistry, 1978. **253**(17): p. 5922-6.

[237.] Shin, K.S., S. Kim, and S.K. Lee, *Improvement of free fatty acid production using a mutant acyl-coa thioesterase i with high specific activity in escherichia coli.* Biotechnol Biofuels, 2016. **9**: p. 208.

[238.] Cho, H. and J.E. Cronan, Jr., *"Protease i" of escherichia coli functions as a thioesterase in vivo.* J. Bacteriol., 1994. **176**(6): p. 1793-5.

[239.] Grisewood, M.J., N.J. Hernandez Lozada, J.B. Thoden, N.P. Gifford, D. Mendez-Perez, H.A. Schoenberger, et al., *Computational redesign of acyl-acp thioesterase with improved selectivity toward medium-chain-length fatty acids.* ACS Catal, 2017. **7**(6): p. 3837-49.

[240.] Dixon, D.P., L. Cummins, D.J. Cole, and R. Edwards, *Glutathione-mediated detoxification systems in plants.* Curr. Opin. Plant Biol., 1998. **1**(3): p. 258-66.

[241.] Inoue, Y. and A. Kimura, *Methylglyoxal and regulation of its metabolism in microorganisms.* Adv. Microb. Physiol., 1995. **37**: p. 177-227.

[242.] Rai, S., S. Yadav, R. Rai, A. Chatterjee, S. Singh, and L.C. Rai, *Molecular and biochemical characterization of all0580 as a methylglyoxal detoxifying glyoxalase ii of anabaena sp. Pcc7120 that confers abiotic stress tolerance in e. Coli.* Int. J. Biol. Macromol., 2019. **124**: p. 981-93.

[243.] Michalska, K., Chhor, G., Mandel, M.E., Bearden, J., Joachimiak, A., Midwest Center for Structural Genomics (MCSG), *Crystal structure of alicyclobacillus acidocaldarius protein with beta-lactamase and rhodanese domains doi: 10.2210/pdb3tp9/pdb.* 2011.

[244.] Stamp, A.L., P. Owen, K. El Omari, C.E. Nichols, M. Lockyer, H.K. Lamb, et al., *Structural and functional characterization of salmonella enterica serovar typhimurium ycbl: An unusual type ii glyoxalase.* Protein Sci., 2010. **19**(10): p. 1897-905.

[245.] Campos-Bermudez, V.A., J. Moran-Barrio, A.J. Costa-Filho, and A.J. Vila, *Metal-dependent inhibition of glyoxalase ii: A possible mechanism to regulate the enzyme activity.* J. Inorg. Biochem., 2010. **104**(7): p. 726-31.

[246.] Marasinghe, G.P., I.M. Sander, B. Bennett, G. Periyannan, K.W. Yang, C.A. Makaroff, et al., *Structural studies on a mitochondrial glyoxalase ii.* J. Biol. Chem., 2005. **280**(49): p. 40668-75.

[247.] Levin, E.J., D.A. Kondrashov, G.E. Wesenberg, and G.N. Phillips, Jr., *Ensemble refinement of protein crystal structures: Validation and application.* Structure, 2007. **15**(9): p. 1040-52.

[248.] McCoy, J.G., C.A. Bingman, E. Bitto, M.M. Holdorf, C.A. Makaroff, and G.N. Phillips, Jr., *Structure of an ethe1-like protein from arabidopsis thaliana.* Acta Crystallogr. D Biol. Crystallogr., 2006. **62**(Pt 9): p. 964-70.

[249.] Sousa Silva, M., L. Barata, A.E. Ferreira, S. Romão, A.M. Tomás, A. Ponces Freire, et al., *Catalysis and structural properties of leishmania infantum glyoxalase ii: Trypanothione specificity and phylogeny.* Biochem., 2008. **47**(1): p. 195-204.

[250.] Cameron, A.D., M. Ridderström, B. Olin, and B. Mannervik, *Crystal structure of human glyoxalase ii and its complex with a glutathione thiolester substrate analogue.* Structure, 1999. **7**(9): p. 1067-78.
[251.] Schilling, O., N. Wenzel, M. Naylor, A. Vogel, M. Crowder, C. Makaroff, et al., *Flexible metal binding of the metallo-β-lactamase domain: Glyoxalase ii incorporates iron, manganese, and zinc in vivo.* Biochem., 2003. **42**(40): p. 11777-86.
[252.] Limphong, P., R.M. McKinney, N.E. Adams, C.A. Makaroff, B. Bennett, and M.W. Crowder, *The metal ion requirements of arabidopsis thaliana glx2-2 for catalytic activity.* J. Biol. Inorg. Chem., 2010. **15**(2): p. 249-58.
[253.] Ghosh, A., A. Pareek, S.K. Sopory, and S.L. Singla-Pareek, *A glutathione responsive rice glyoxalase ii, osglyii-2, functions in salinity adaptation by maintaining better photosynthesis efficiency and anti-oxidant pool.* Plant J., 2014. **80**(1): p. 93-105.
[254.] Thornalley, P.J., *Protein and nucleotide damage by glyoxal and methylglyoxal in physiological systems--role in ageing and disease.* Drug Metabol. Drug Interact., 2008. **23**(1-2): p. 125-50.
[255.] Hanssen, N.M.J., C.D.A. Stehouwer, and C.G. Schalkwijk, *Methylglyoxal stress, the glyoxalase system, and diabetic chronic kidney disease.* Curr. Opin. Nephrol. Hypertens., 2019. **28**(1): p. 26-33.
[256.] Hasanuzzaman, M., K. Nahar, T.I. Anee, and M. Fujita, *Glutathione in plants: Biosynthesis and physiological role in environmental stress tolerance.* Physiol Mol Biol Plants, 2017. **23**(2): p. 249-68.
[257.] Sankaranarayanan, S., M. Jamshed, A. Kumar, L. Skori, S. Scandola, T. Wang, et al., *Glyoxalase goes green: The expanding roles of glyoxalase in plants.* Int. J. Mol. Sci., 2017. **18**(4).
[258.] Lee, C. and C. Park, *Bacterial responses to glyoxal and methylglyoxal: Reactive electrophilic species.* Int. J. Mol. Sci., 2017. **18**(1).

Figure 1. Thioesterases act on a wide range of different substrate types, including acyl-CoA (red), acyl-ACP (green), protein substrates (purple), and acyl-glutathione (orange) and mediate a wide variety of functions.

Figure 2. An overview of the domain types present in different thioesterases. Hotdog domains (blue) are present in acyl-CoA thioesterases and acyl-ACP thioesterases. The α/β hydrolase domains (green) are present in acyl-CoA thioesterases, acyl-ACP thioesterases, protein thioesterases, and glutathione thioesterases. Lactamase (purple) domains are present only in flavodoxin-like domains, while NagB (orange), and Flavodoxin-like (red) are present only in acyl-CoA thioesterases.

Figure 3. Overview of the domain organization present in different thioesterases. Domain coloring is preserved from Figure 2, with hotdog domains in blue, α/β hydrolase domains in green, lactamase domains in purple, flavodoxin-like domain in red, and NagB domains in orange. Domains shown with full outlines have structures determined, while dotted lines indicate missing structures. Completely missing domains indicated that these thioesterase familes are not present in respective prokaryote or eukaryote genome.

Figure 4. TE4 family members harbour a double hotdog fold arranged in the form of a tetramer (or octamer of hotdog domains). The active site is comprised of Asp, Thr, and Gln, and the structure of PDB 1C8U is presented with a topology of α1-β1-β2-α2-β3-β4-β5-β6-*α3-β7-β8-α4-β9-β10-β11-β12* where the hotdog domain boundary is indicated by italics. β-strands are presented as yellow arrows, α-helices are red rectangles, and loops in green. The position of the active site residues are presented in both 3D form and on the topology.

Figure 5. TE5 family members possess a single hotdog domain arranged as a tetramer. The Asp residue positioned after the first alpha-helical turn is likely to be crucial for catalysis. The structure of PDB 1NJK is presented with an associated topology of β1-α1-α2-α3-β2-β3-β4-β5-α4. The β-strands are presented as yellow arrows, α-helices are red rectangles, and loops in green. The position of the active site residue is presented on both the 3D fold and the topology depiction.

Figure 6. TE6 family members exhibit a domain duplication in eukaryotes compared with prokaryotes. Prokaryotes possess a single hotdog domain arranged as a hexamer, while eukaryotes possess two hotdog domains arranged as a trimer. The overall structures are highly similar. An Asp residue on the a-helix is common to all TE6 family members, and share a similar topology of β1-α1-β2-β3-β4-β5-α2 in each domain. In eukaryotes, this domain is extended by *-β6-α3-β7-β8-β9-β10-α4*. The structure of a prokaryotic TE6 member is represented by PDB 1YLI, while the structure of a eukaryotic PDB is represented by 4ZV3. The β-strands are presented as yellow arrows, α-helices are red rectangles, and loops in green. The position of the active site residue is presented on both the 3D fold and the topology depiction.

Figure 7. Structure of ACOT12, a TE6 family member. The protein possesses a dual hotdog domain and a C-terminal START domain (pink). These assemble into a trimer, with each domain depicted I, II, and III. Activity is regulated by a nucleotide dependent binding loop, shown in blue. The structure is described in Swarbrick et al., JBC. 2014. doi: 10.1074.

Figure 8. A homology model of ACOT9, a TE7 family member. Based on sequence conservation, it is proposed to be arranged as a trimer. The active site for this family remains to determined experimentally. The predicted topology is β1-α1-β2-β3-β4-β5-α2-*β6-α3-β3-β7-β8-*

β9-β10-α4. The β-strands are presented as yellow arrows, α-helices are red rectangles, and loops in green.

Figure 9. TE8 family members possess a single hotdog domain arranged as a tetramer. The active site is comprised of Asp, Asn, Ser, with the Asp residue positioned in the middle of the α-helix. The structure of PDB 2F0X is presented with the topology of α1-β1-β2-α2-β3-β4-β5-β6. The β-strands are presented as yellow arrows, α-helices are red rectangles, and loops in green. The position of the active site residue is presented on both the 3D fold and the topology depiction.

Figure 10. TE9 family members possess a single hotdog domain arranged as a tetramer. The active site is comprised of Tyr, Asp, His. The structure of PDB 1S5U is presented with the topology of β1-α1-α2-α3-β2-β3-β4-β5-β6-α4. The β-strands are presented as yellow arrows, α-helices are red rectangles, and loops in green. The position of the active site residue is presented on both the 3D fold and the topology depiction.

Figure 11. TE10 family members possess a single hotdog domain arranged as a tetramer. An Asp residue positioned between β1-α1 is critical for activity. The structure of PDB 1BVQ is presented with the topology of β1-α1-α2-α3-β2-β3-β4-β5-β6-β7-β8-α4. The β-strands are presented as yellow arrows, α-helices are red rectangles, and loops in green. The position of the active site residue is presented on both the 3D fold and the topology depiction.

Figure 12. TE11 family members possess a single hotdog domain arranged as a tetramer. A Glu residue positioned on the central α4 is critical for activity. The structure of PDB 1Q4S is presented with the topology of α1-α2-β1-β2-α3-α4-α5-β3-β4-β5-β6. The β-strands are presented as yellow arrows, α-helices are red rectangles, and loops in green. The position of the active site residue is presented on both the 3D fold and the topology depiction.

Figure 13. TE12 family members possess a single hotdog domain arranged as a tetramer. An Asp residue positioned on the loop between β1 and α1 is critical for activity. The structure of PDB 2HX5 is presented with the topology of α1-β1-α2-α3-α4-β2-β3-β4-β5-β6-β7-α5. The β-strands are presented as yellow arrows, α-helices are red rectangles, and loops in green. The position of the active site residue is presented on both the 3D fold and the topology depiction.

Figure 14. TE13 family members possess a single hotdog domain arranged as a tetramer with the β-sheets arranged in a "back-to-back" configuration. Residues important for catalysis are positioned on the central α-helix, and comprise Asp, Asn and Thr. The structure of PDB 1PSU is presented with the topology of α1-β1-β2-α2-α3-β3-β4-β5-β6. The β-strands are presented as yellow arrows, α-helices are red rectangles, and loops in green. The position of the active site residue is presented on both the 3D fold and the topology depiction.

Figure 15. TE24 family members possess a single hotdog domain arranged as a hexamer in a trimer of dimers configuration. Residues important for catalysis are positioned on the α1-helix and a loop connecting β2 and α3. The structure of PDB 2PFC is presented with the topology of α1-β1-β2-α2-α3-β3-β4-β5-β6. The β-strands are presented as yellow arrows, α-helices are red rectangles, and loops in green. The position of the active site residue is presented on both the 3D fold and the topology depiction.

Figure 16. TE25 family members possess a single hotdog domain arranged as a homodimer. Residues important for catalysis are positioned on the α2-helix and a loop connecting β2 and β3.

The structure of PDB 3KU7 is presented with the topology of β1-α1-α2-β2-β3-β4-β5-α3. The β-strands are presented as yellow arrows, α-helices are red rectangles, and loops in green. The position of the active site residue is presented on both the 3D fold and the topology depiction.

Figure 17. TE26 family members possess a single hotdog domain arranged as a homodimer. Residues important for catalysis are positioned on the α2-helix, the loop preceding the α2 helix, and a Thr residue on a loop connecting α2 and β3. The structure of PDB 4AE7 is presented with the topology of α1-β1-β2-α2-β3-β4-β5-β6. The β-strands are presented as yellow arrows, α-helices are red rectangles, and loops in green. The position of the active site residue is presented on both the 3D fold and the topology depiction.

Figure 18. TE14 family members possess two fused hotdog domains which bind as homodimers to form a tetramer of double hotdog domains with the β-sheets arranged in a "face-to-face" configuration. Residues important for catalysis are pictured on both the topology and 3D image and comprise Glu, His, Asp, and Asn. The structure of PDB 5X04 is presented with the topology of α1-α2-β1-α3-α4-α5-β2-β3-β4-β5-α6-α7-α8-β6-α9-α10-α11-β7-β8-β9-β10. The β-strands are presented as yellow arrows, α-helices are red rectangles, and loops in green.

Figure 19. TE15 family members possess a single hotdog domain and form a tetramer with the β-sheets arranged in a "face-to-face" configuration. Residues important for catalysis are pictured on both the topology and 3D image and comprise Tyr and Arg residues located on the central α2 helix. The structure of PDB 2W3X is presented with the topology of β1-α1-α2-α3-β2-β3-β4-β5-α4. The β-strands are presented as yellow arrows, α-helices are red rectangles, and loops in green.

Figure 20. TE2 family members possess a single α/β hydrolase fold with an N-terminal β-sandwich. The structure of PDB 3HLK is presented with the topology of β1-β2-β3-α1-β4-α2-β5-α3-β6-β7-α4-β8-α5. The β-strands are presented as yellow arrows, α-helices are red rectangles, and loops in green. The position of the active site residue is presented on both the 3D fold and the topology depiction.

Figure 21. TE16 family members possess a single α/β hydrolase fold. Residues important for catalysis are positioned on the α3- and α7-helices, and a loop connecting β5 and α4. The structure of PDB 2CB9 is presented with the topology of β1-β2-α1-β3-α2-β4-α3-β5-α4-β6-α5-α6-β7-α7-α8. The β-strands are presented as yellow arrows, α-helices are red rectangles, and loops in green. The position of the active site residue is presented on both the 3D fold and the topology depiction.

Figure 22. TE17 family members possess a single α/β hydrolase fold which associated to form a homodimer. Residues important for catalysis are positioned on loop regions connecting β6-α5 and β9-α8, and at the end of β7. The structure of PDB 1MO2 is presented with the topology of α1-β1-β2-β3-α2-α3-β4-β5-α4-β6-α5-β7-α6-α7-β8-β9-α8. The β-strands are presented as yellow arrows, α-helices are red rectangles, and loops in green. The position of the active site residue is presented on both the 3D fold and the topology depiction.

Figure 23. TE18 family members possess a single α/β hydrolase fold which associated to form a homodimer. Residues important for catalysis are positioned on loop regions connecting β5-α11 and β6-α12 and at start of α4. The structure of PDB 3QMV is presented with the topology of α1-β1-α2-α3-β2-α4-α5-β3-α6-β4-α7-α8-α9-α10-β5-α11-β6-α12-α13. The β-strands are presented as yellow arrows, α-helices are red rectangles, and loops in green. The position of the active site residue is presented on both the 3D fold and the topology depiction.

Figure 24. TE19 family members possess a single α/β hydrolase fold which associated to form a homodimer. Residues important for catalysis are positioned on loop regions connecting β6-α4, β9-α8, and β10-α9. The structure of PDB 1THT is presented with the topology of β1-β2-β3-α1-α2-β4-α3-β5-α4-β6-α5-β7-β8-α6-α7-β9-α8-β10-α9-α10-β11. The β-strands are presented as yellow arrows, α-helices are red rectangles, and loops in green. The position of the active site residue is presented on both the 3D fold and the topology depiction.

Figure 25. TE20 family members possess a single α/β hydrolase fold and are monomeric. Residues important for catalysis, Ser111, Asp228 and His283, are labelled in the inset. The structure of PDB 1PJA is presented with the topology of β1-α1-β2-α2-β3-α3-β4-α4-α5-α6-α7-α8-α9-α10-β5-α11-β6-β7-α12-α13-α14-β8-α15-α16. The β-strands are presented as yellow arrows, α-helices are red rectangles, and loops in green. The position of the active site residue is presented on both the 3D fold and the topology depiction.

Figure 26. TE21 family members possess a single α/β hydrolase fold which associated to form a homodimer. Residues important for catalysis are positioned on α5 and loop regions connecting β8-α7 and β9-α8. The structure of PDB 1FJ2 is presented with the topology of β1-β2-α1-β3-β4-α2-β5-α3-α4-β6-α5-β7-α6-β8-α7-β9-α8. The β-strands are presented as yellow arrows, α-helices are red rectangles, and loops in green. The position of the active site residue is presented on both the 3D fold and the topology depiction.

Figure 27. TE22 family members possess a single α/β hydrolase fold which associated to form a homodimer. Residues important for catalysis Ser120, position on are positioned on α6, Asp202 positioned on a looped connecting β7-α11, and His231, positioned on a loop connecting β8-α12. The structure of PDB 2UZ0 is presented with the topology of β1-β2-β3-α1-α2-β4-α3-α4-α5-β5-α6-β6-α7-α8-α9-α10-β7-α11-β8-α12. The β-strands are presented as yellow arrows, α-helices are red rectangles, and loops in green. The position of the active site residue is presented on both the 3D fold and the topology depiction.

Figure 28. TE1 family members possess a double NagB fold which associated to form a homodimer. The structure of PDB 4EUD is presented with the topology of α1-α2-β1-α3-β2-α4-β3-α5-β4-α6-α7-β5-β6-β7-α8-β8-α9-β9-α10-β10-α11-β11-α12-β12-β13-α13-β14-β15-α14-α15-β16-α16-α17-β17-β18-β19-β20-α18-β21-α19-β22-β23-α20-β24-β25-α21-β26-β27-α22-α23-α24. The β-strands are presented as yellow arrows, α-helices are red rectangles, and loops in green. The position of the active site residue is presented on both the 3D fold and the topology depiction.

Figure 29. TE3 family members possess a monomeric flavodoxin-like fold and residues important for catalysis include Ser10, positioned on α1, and Asp154 and His157 positioned on the loop connecting α6 and α7. The structure of PDB 1IVN is presented with the topology of β1-α1-α2-β2-α3-β3-α4-β4-α5-β5-α6-α7. The β-strands are presented as yellow arrows, α-helices are red rectangles, and loops in green. The position of the active site residue is presented on both the 3D fold and the topology depiction.

Figure 30. TE23 family members possess a GlyoxaslaseII fold. The structure of 1QH3 is presented with the topology of β1-β2-β3-α1-β4-α2-α3-β5-β6-β7-β8-β9-β10-β11-β12-α4-β13-α5-α6-β14-α7-α8-α9. The β-strands are presented as yellow arrows, α-helices are red rectangles, and loops in green. The position of the active site residue is presented on both the 3D fold and the topology depiction.

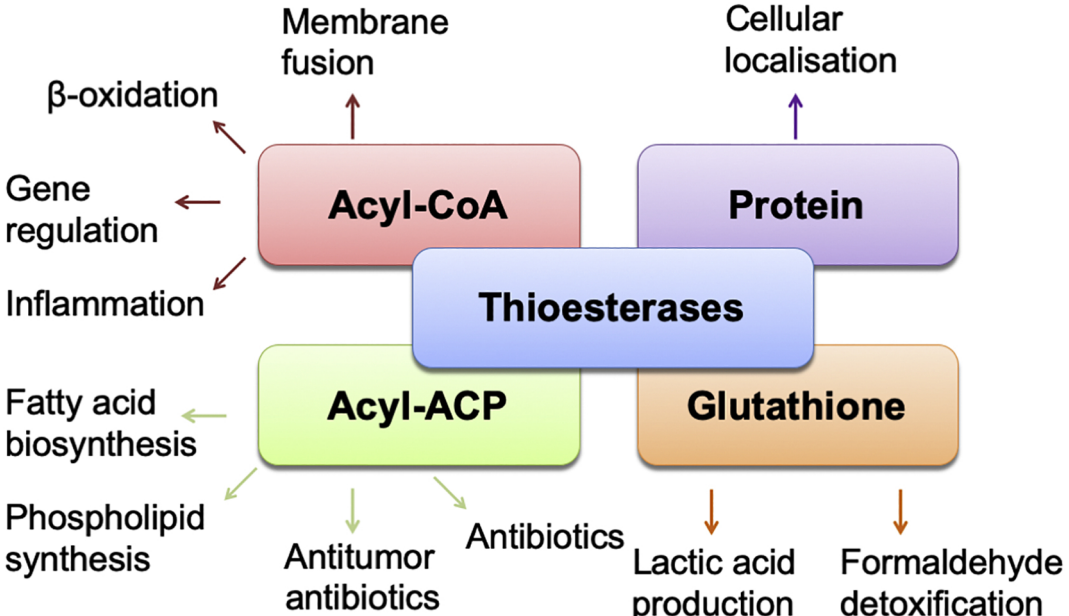
Membrane fusion
Cellular localisation
β-oxidation
Gene regulation
Inflammation
Acyl-CoA
Protein
Thioesterases
Fatty acid biosynthesis
Acyl-ACP
Glutathione
Phospholipid synthesis
Antitumor antibiotics
Antibiotics
Lactic acid production
Formaldehyde detoxification

Figure 1

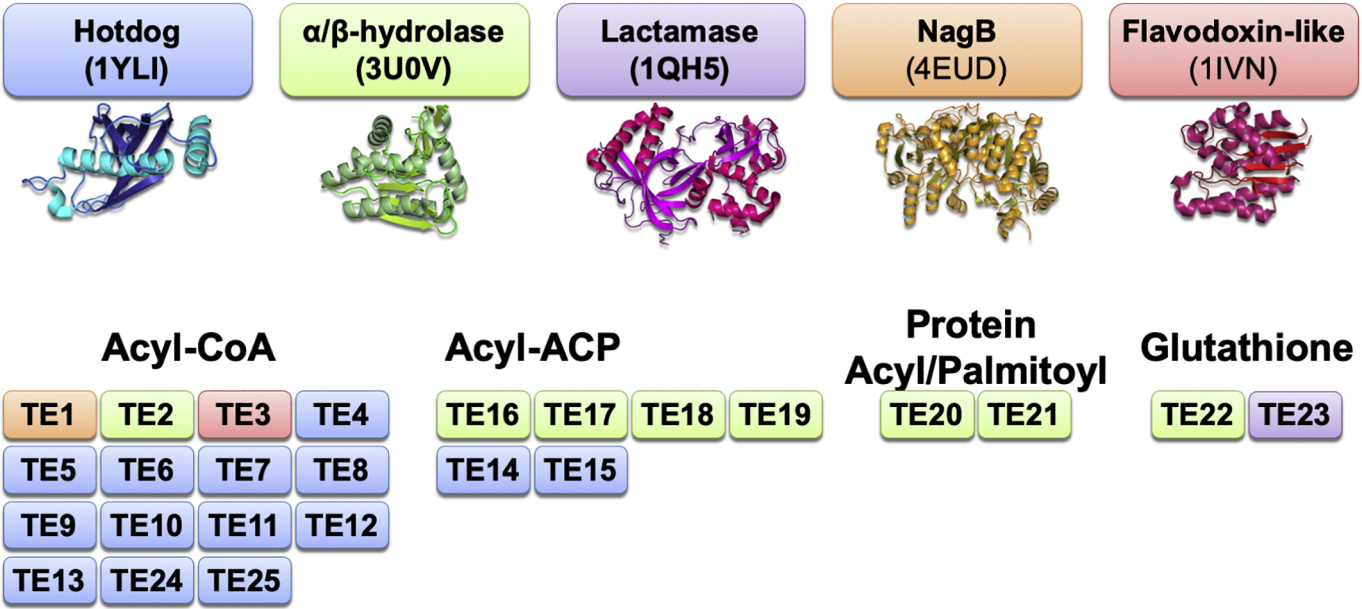
Hotdog
(1YLI)
α/β-hydrolase
(3U0V)
Lactamase
(1QH5)
NagB
(4EUD)
Flavodoxin-like
(1IVN)
Acyl-CoA
TE1
TE2
TE3
TE4
TE5
TE6
TE7
TE8
TE9
TE10
TE11
TE12
TE13
TE24
TE25
Acyl-ACP
TE16
TE17
TE18
TE19
TE14
TE15
Protein
Acyl/Palmitoyl
TE20
TE21
Glutathione
TE22
TE23

Figure 2

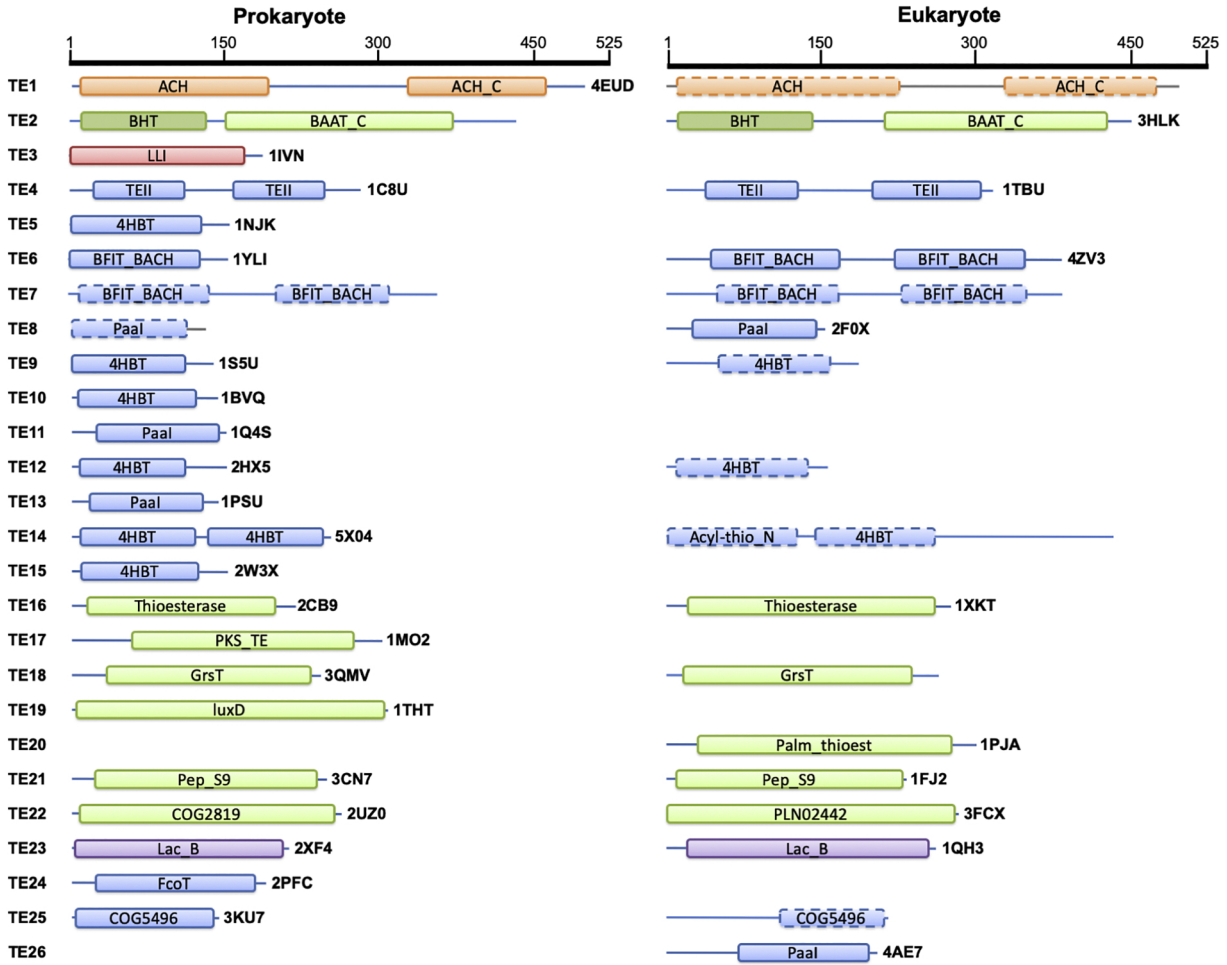
Prokaryote
1
150
300
450
525
TE1
ACH
ACH_C
4EUD
TE2
BHT
BAAT_C
TE3
LLI
1IVN
TE4
TEII
TEII
1C8U
TE5
4HBT
1NJK
TE6
BFIT_BACH
1YLI
TE7
BFIT_BACH
BFIT_BACH
TE8
PaaI
TE9
4HBT
1S5U
TE10
4HBT
1BVQ
TE11
PaaI
1Q4S
TE12
4HBT
2HX5
TE13
PaaI
1PSU
TE14
4HBT
4HBT
5X04
TE15
4HBT
2W3X
TE16
Thioesterase
2CB9
TE17
PKS_TE
1MO2
TE18
GrsT
3QMV
TE19
luxD
1THT
TE20
TE21
Pep_S9
3CN7
TE22
COG2819
2UZ0
TE23
Lac_B
2XF4
TE24
FcoT
2PFC
TE25
COG5496
3KU7
TE26
Eukaryote
1
150
300
450
525
ACH
ACH_C
BHT
BAAT_C
3HLK
TEII
TEII
1TBU
BFIT_BACH
BFIT_BACH
4ZV3
BFIT_BACH
BFIT_BACH
PaaI
2F0X
4HBT
4HBT
Acyl-thio_N
4HBT
Thioesterase
1XKT
GrsT
Palm_thioest
1PJA
Pep_S9
1FJ2
PLN02442
3FCX
Lac_B
1QH3
COG5496
PaaI
4AE7

Figure 3

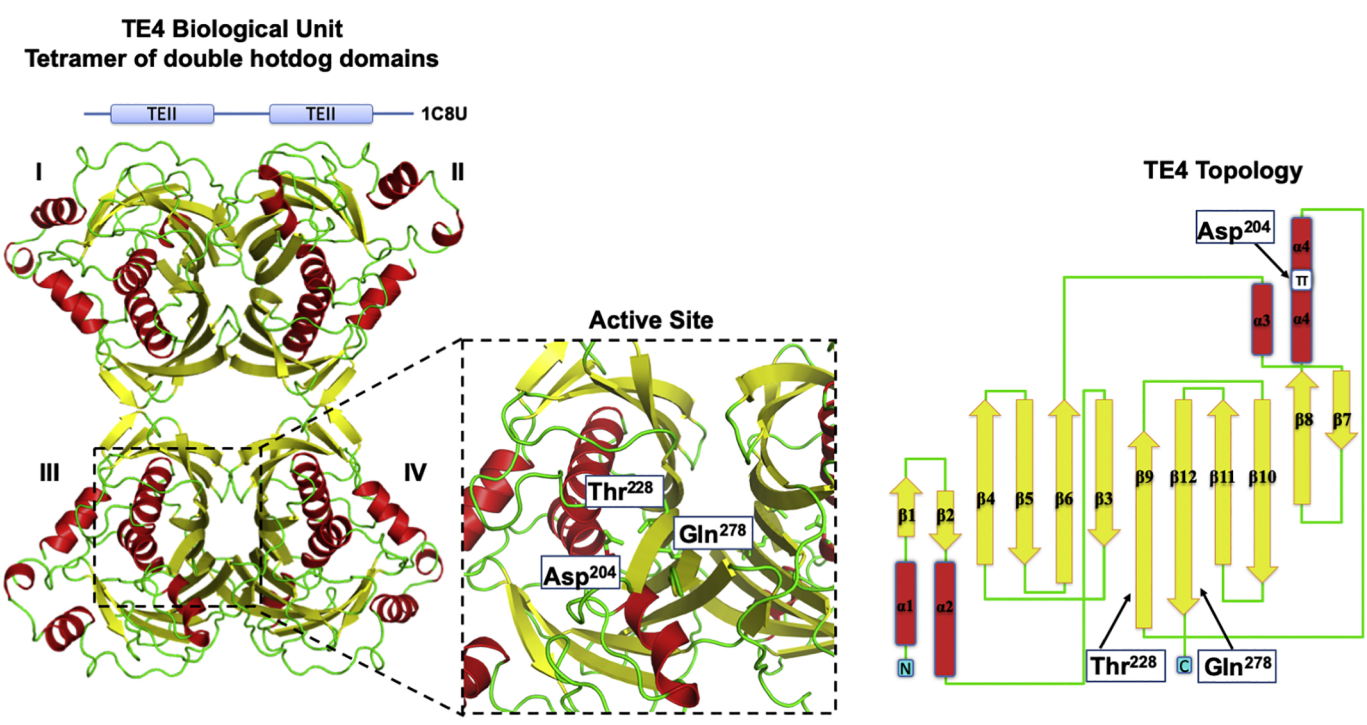
TE4 Biological Unit
Tetramer of double hotdog domains
TEII
TEII
1C8U
I
II
III
IV
Active Site
Thr228
Gln278
Asp204
TE4 Topology
Asp204
α4
TT
α3
α4
β8
β7
β1
β2
β4
β5
β6
β3
β9
β12
β11
β10
α1
α2
N
C
Thr228
Gln278

Figure 4

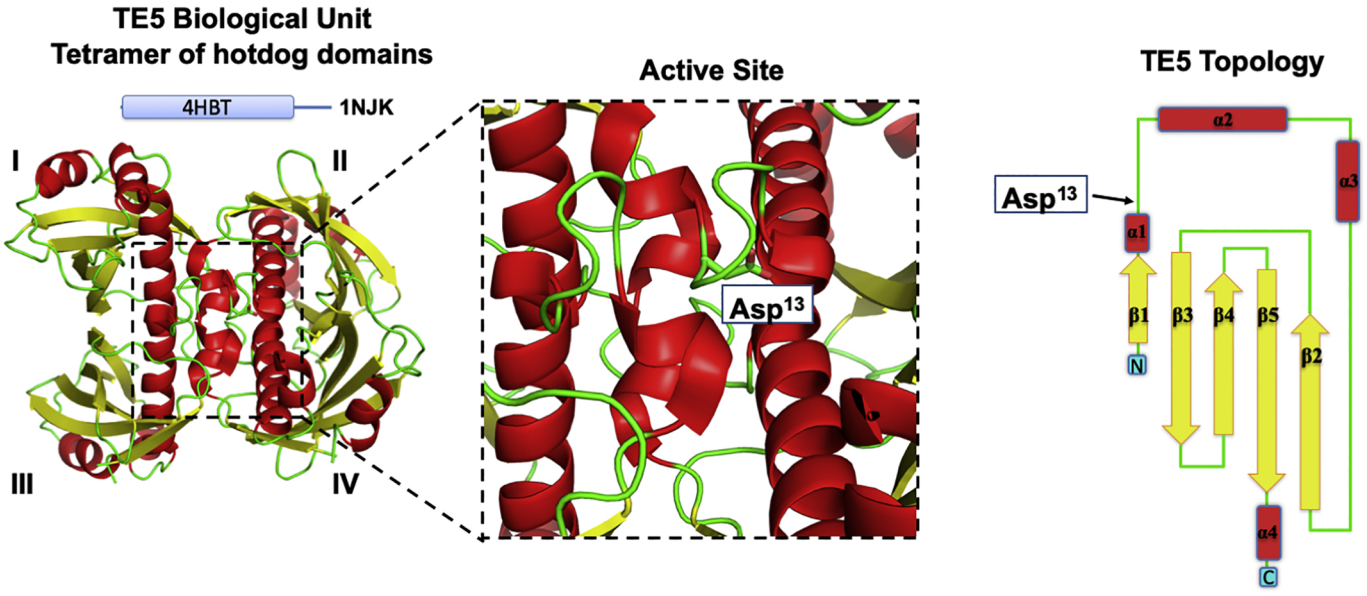
TE5 Biological Unit
Tetramer of hotdog domains
4HBT
1NJK
I
II
III
IV
Active Site
Asp13
TE5 Topology
Asp13
α1
α2
α3
α4
β1
β2
β3
β4
β5
N
C

Figure 5

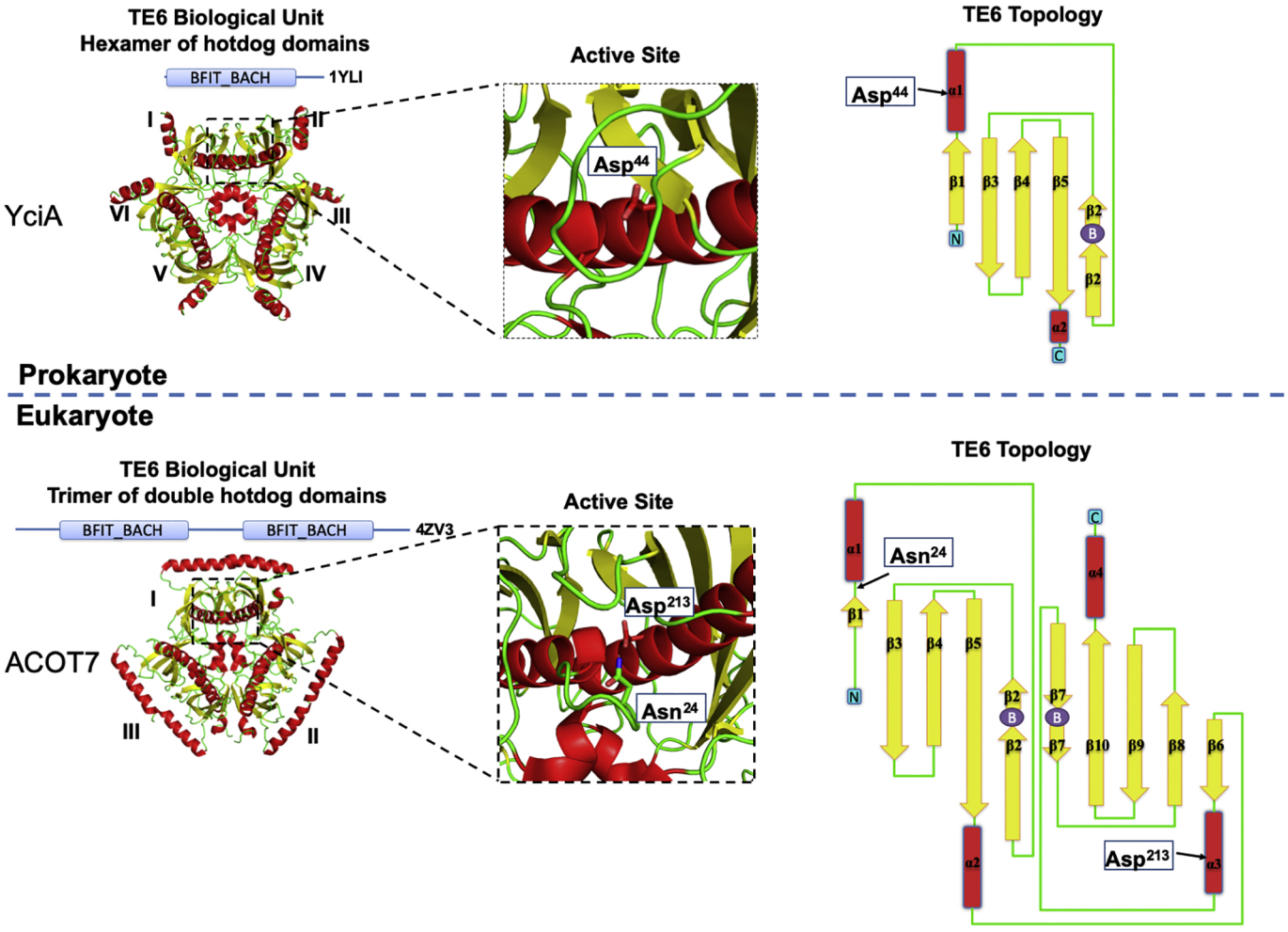
TE6 Biological Unit
Hexamer of hotdog domains
BFIT_BACH
1YLI
YciA
I
II
III
IV
V
VI
Active Site
Asp44
TE6 Topology
Asp44
α1
β1
β3
β4
β5
β2
β2
α2
N
C
Prokaryote
Eukaryote
TE6 Biological Unit
Trimer of double hotdog domains
BFIT_BACH
BFIT_BACH
4ZV3
ACOT7
I
II
III
Active Site
Asp213
Asn24
TE6 Topology
Asn24
α1
β1
β3
β4
β5
β2
β2
α2
α4
β7
β7
β10
β9
β8
β6
Asp213
α3
N
C

Figure 6

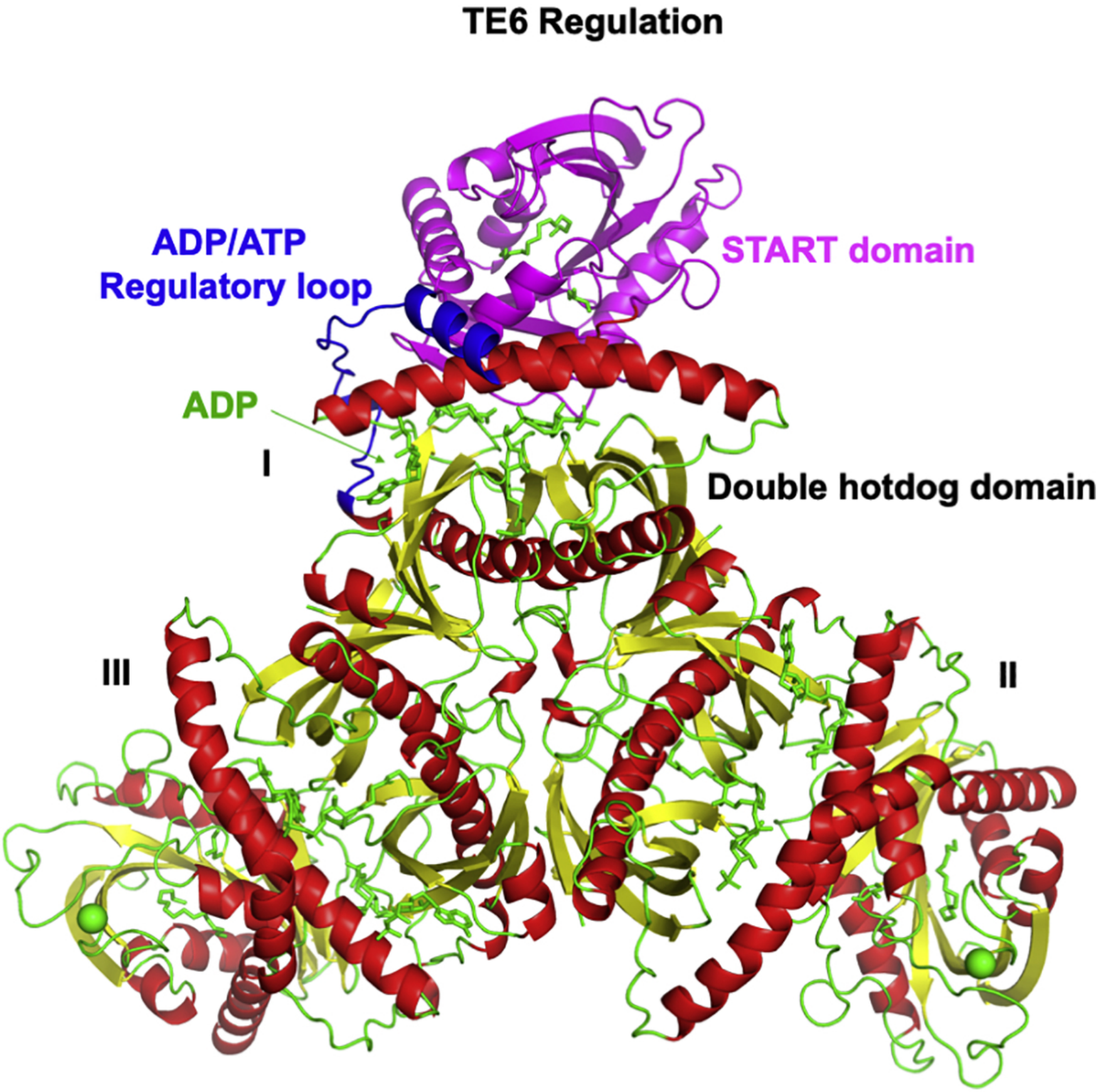
TE6 Regulation
ADP/ATP
Regulatory loop
START domain
ADP
I
Double hotdog domain
III
II

Figure 7

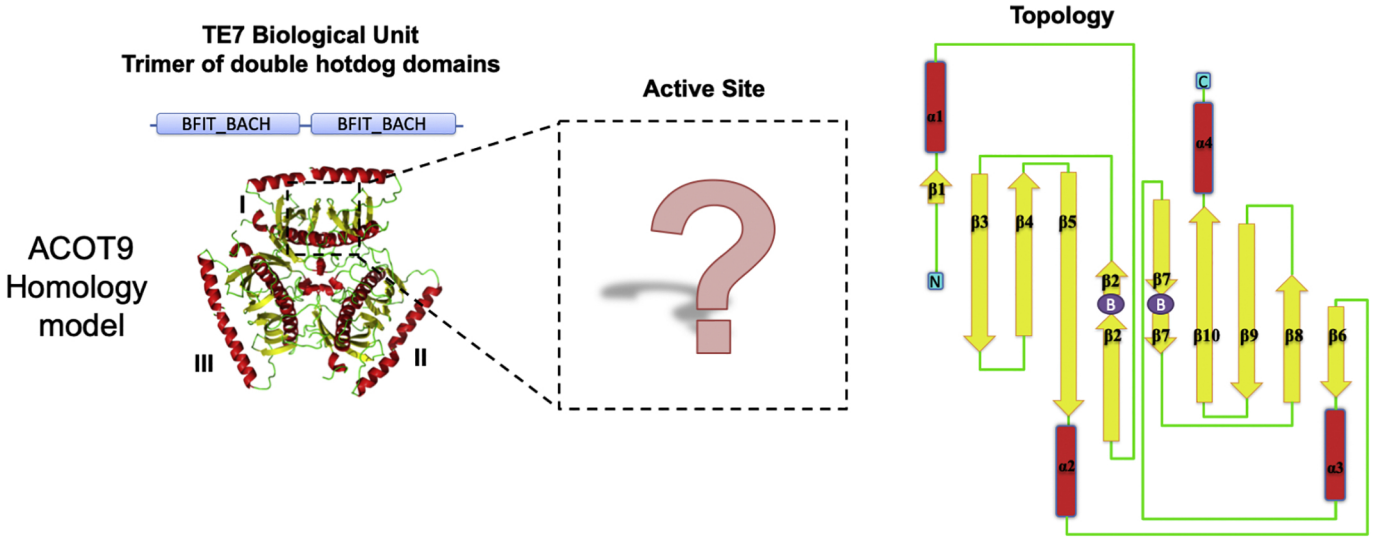
TE7 Biological Unit
Trimer of double hotdog domains
BFIT_BACH
BFIT_BACH
ACOT9
Homology
model
I
II
III
Active Site
?
Topology
α1
β1
N
β3
β4
β5
α2
β2
B
β2
β7
B
β7
C
α4
β10
β9
β8
β6
α3

Figure 8

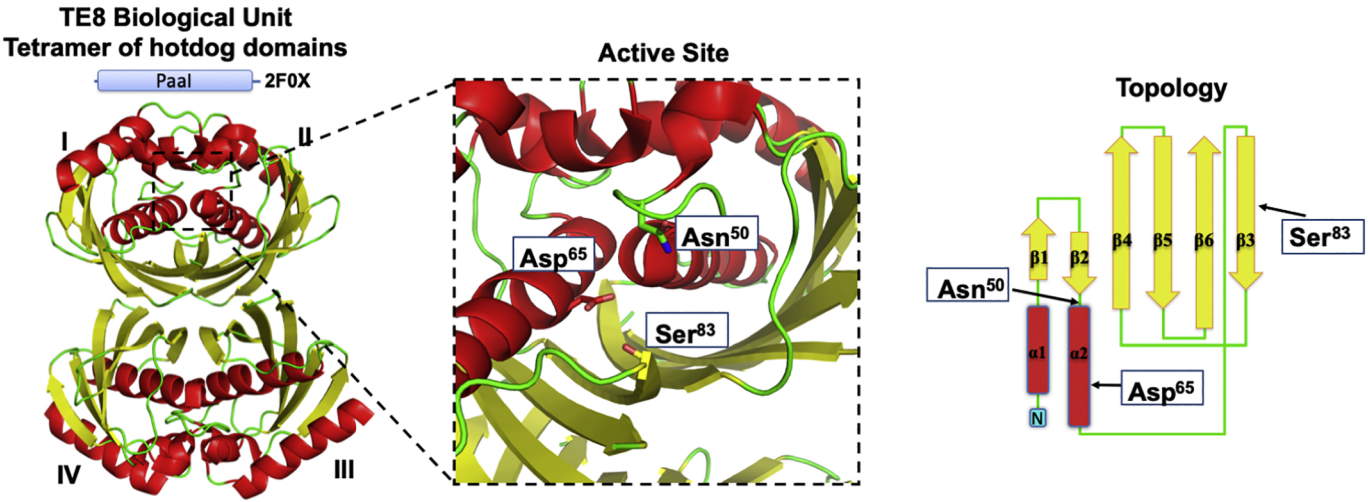
TE8 Biological Unit
Tetramer of hotdog domains
PaaI
2F0X
I
II
IV
III
Active Site
Asp65
Asn50
Ser83
Topology
β1
β2
β4
β5
β6
β3
Ser83
Asn50
α1
α2
Asp65
N

Figure 9

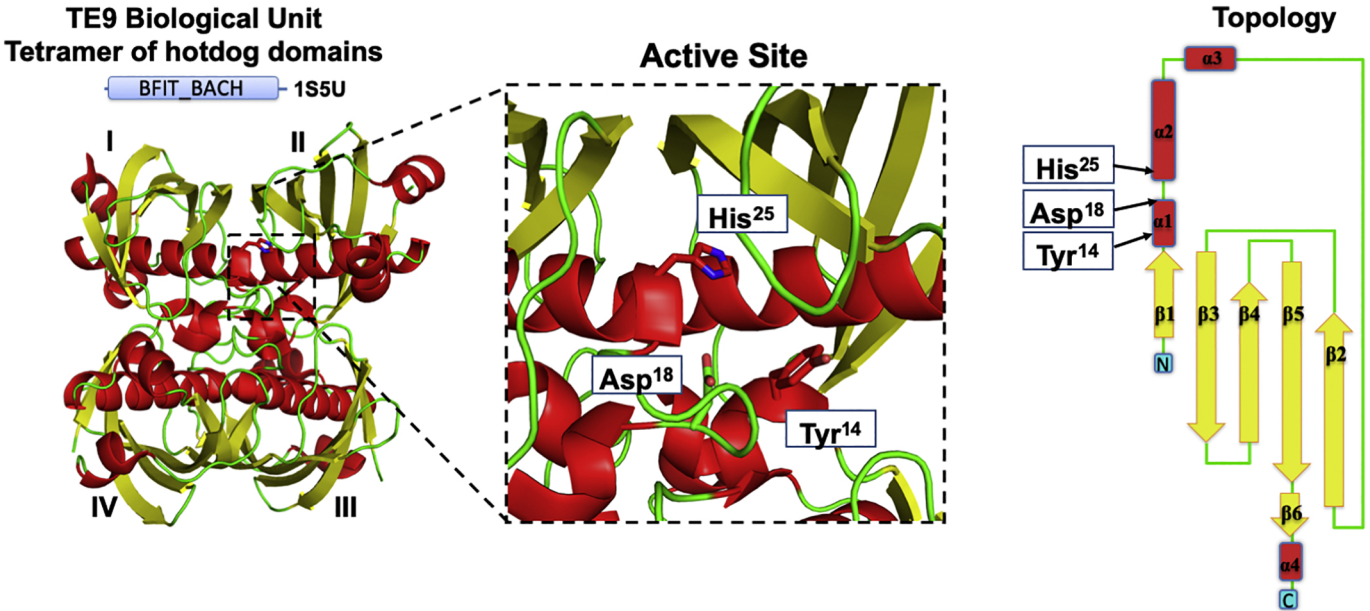
TE9 Biological Unit
Tetramer of hotdog domains
BFIT_BACH
1S5U
I
II
IV
III
Active Site
His25
Asp18
Tyr14
Topology
α3
α2
α1
His25
Asp18
Tyr14
β1
β3
β4
β5
β2
β6
α4
N
C

Figure 10

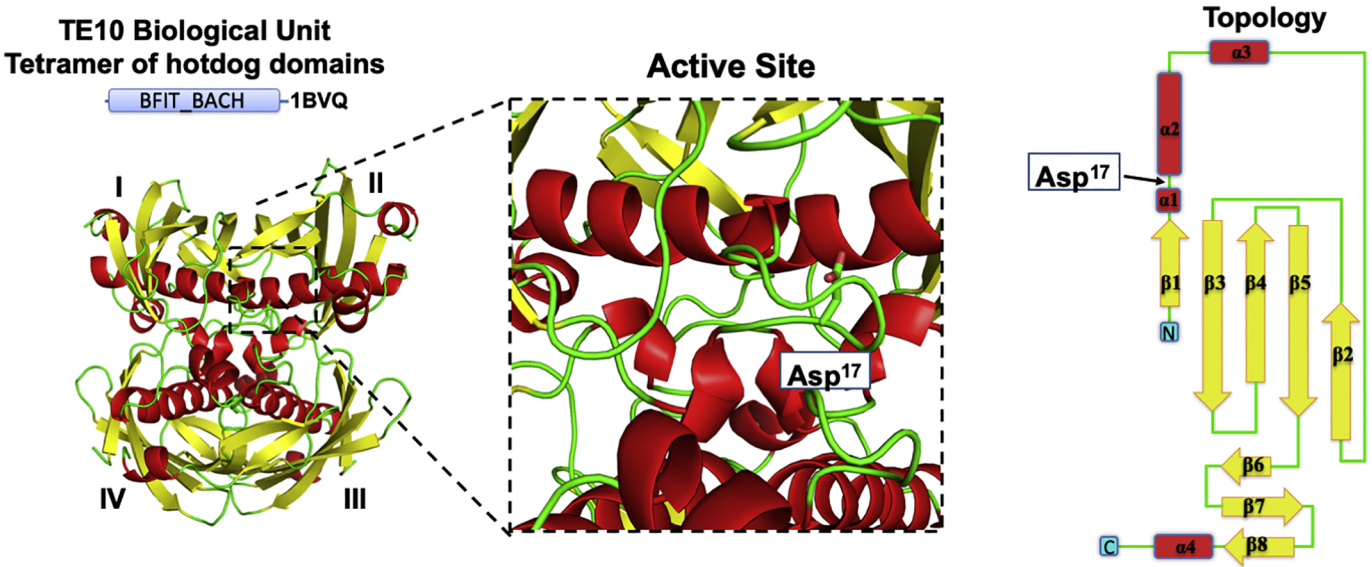
TE10 Biological Unit
Tetramer of hotdog domains
BFIT_BACH
1BVQ
I
II
IV
III
Active Site
Asp17
Topology
α3
α2
Asp17
α1
β1
β3
β4
β5
β2
N
β6
β7
C
α4
β8

Figure 11

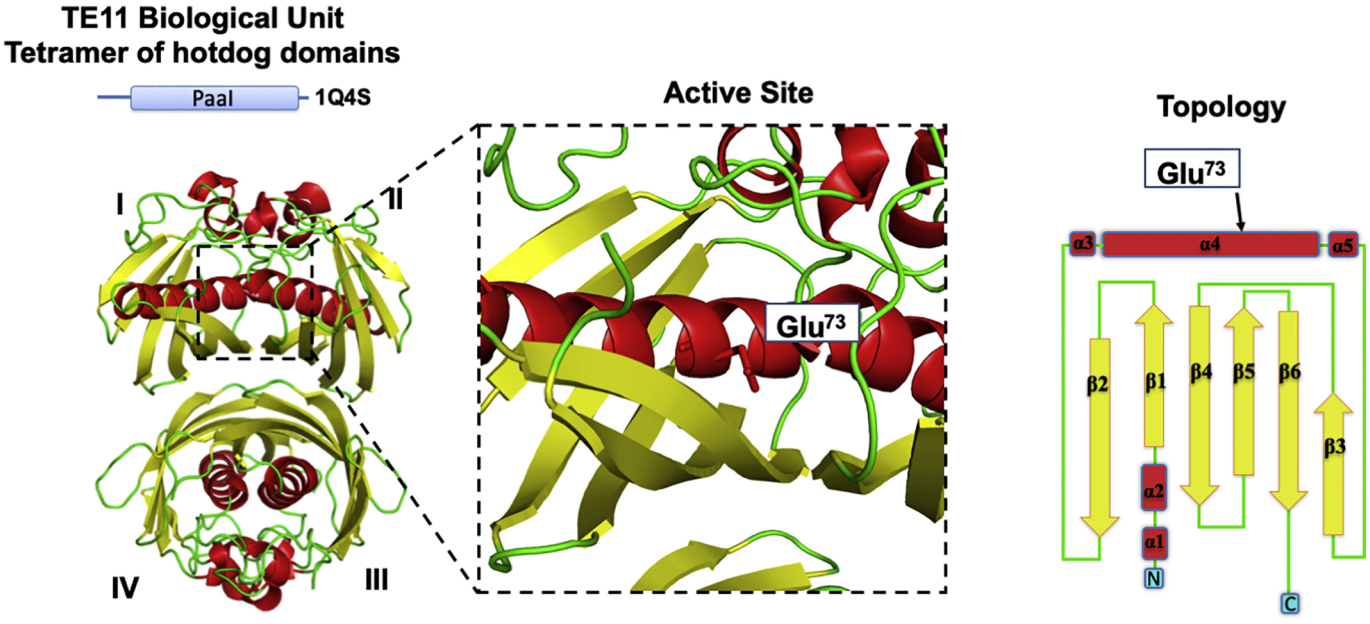
TE11 Biological Unit
Tetramer of hotdog domains
PaaI
1Q4S
I
II
III
IV
Active Site
Glu73
Topology
Glu73
α3
α4
α5
β2
β1
β4
β5
β6
β3
α2
α1
N
C

Figure 12

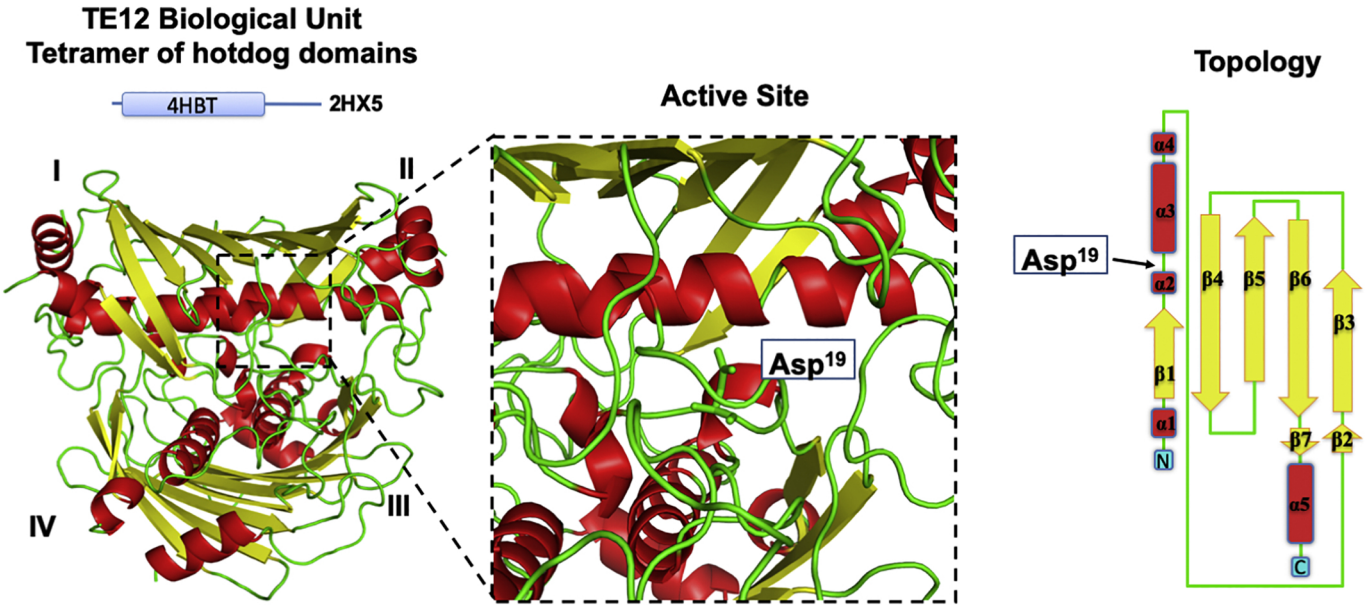
TE12 Biological Unit
Tetramer of hotdog domains
4HBT
2HX5
I
II
III
IV
Active Site
Asp19
Topology
Asp19
α4
α3
α2
β1
α1
N
β4
β5
β6
β3
β7
β2
α5
C

Figure 13

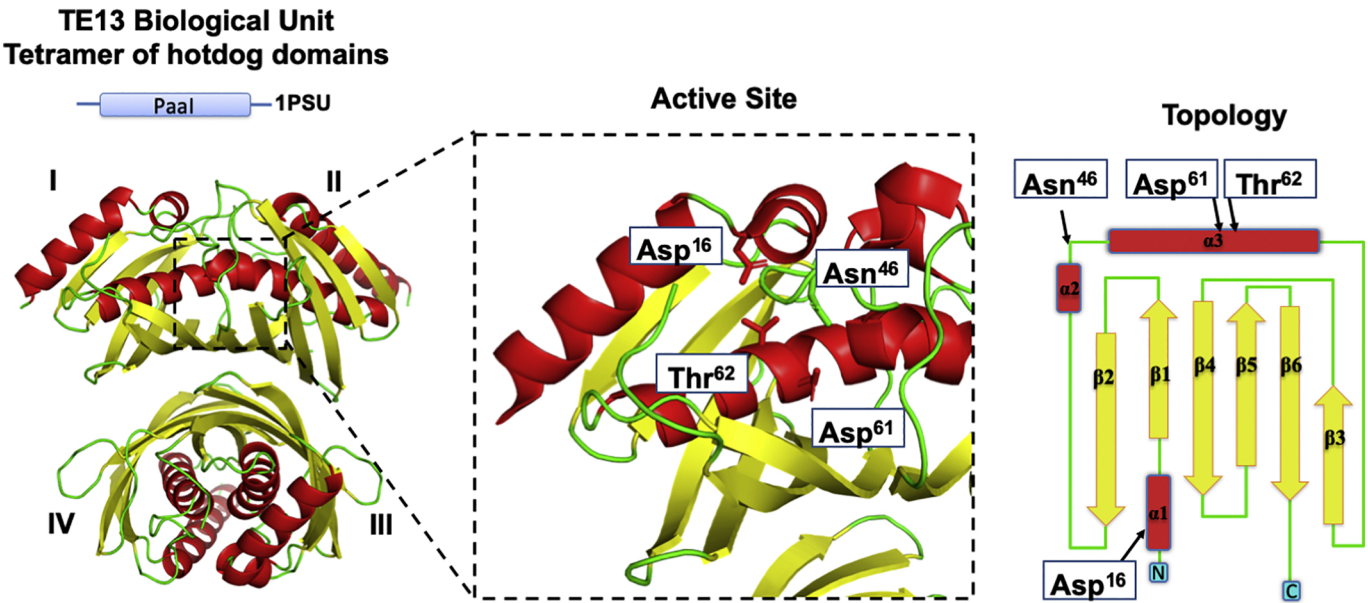
TE13 Biological Unit
Tetramer of hotdog domains
PaaI
1PSU
I
II
III
IV
Active Site
Asp16
Asn46
Thr62
Asp61
Topology
Asn46
Asp61
Thr62
α3
α2
β2
β1
β4
β5
β6
β3
α1
N
C
Asp16

Figure 14

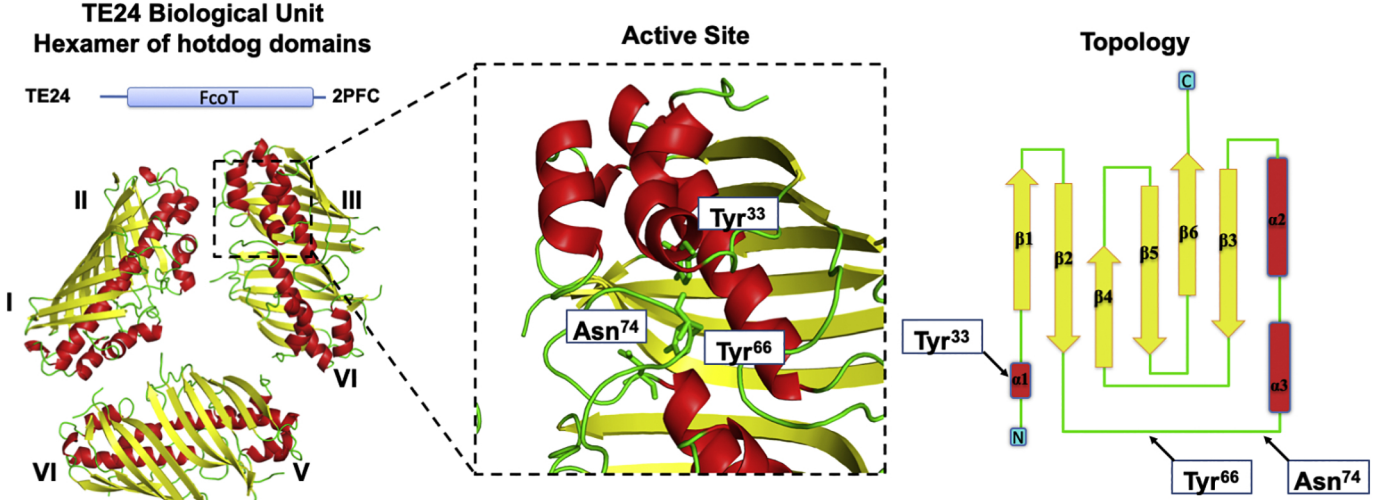
TE24 Biological Unit
Hexamer of hotdog domains
TE24
FcoT
2PFC
I
II
III
VI
VI
V
Active Site
Tyr33
Asn74
Tyr66
Topology
C
N
β1
β2
β4
β5
β6
β3
α1
α2
α3
Tyr33
Tyr66
Asn74

Figure 15

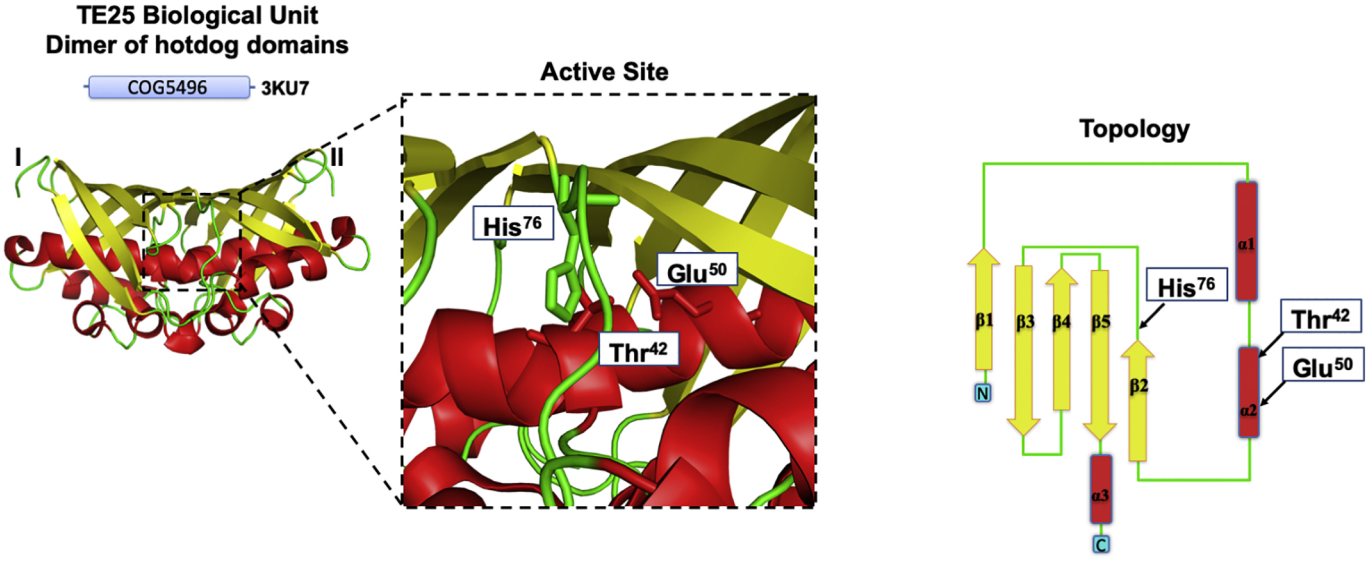
TE25 Biological Unit
Dimer of hotdog domains
COG5496
3KU7
I
II
Active Site
His76
Glu50
Thr42
Topology
β1
β3
β4
β5
β2
α1
α2
α3
N
C
His76
Thr42
Glu50

Figure 16

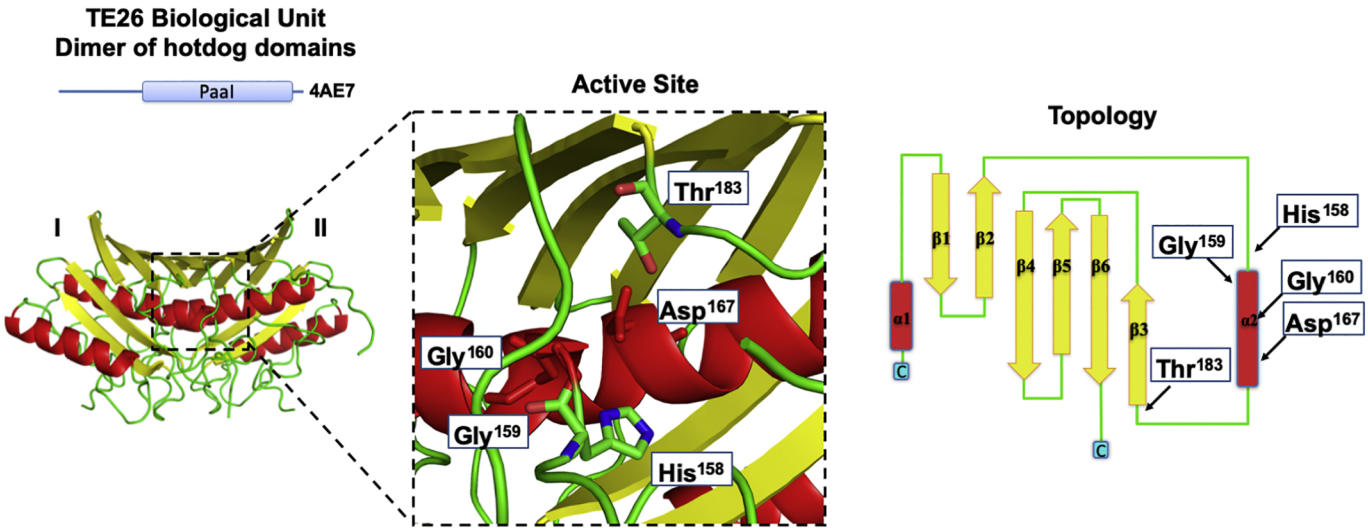
TE26 Biological Unit
Dimer of hotdog domains
PaaI
4AE7
I
II
Active Site
Thr183
Asp167
Gly160
Gly159
His158
Topology
β1
β2
β4
β5
β6
β3
α1
α2
C
C
His158
Gly159
Gly160
Asp167
Thr183

Figure 17

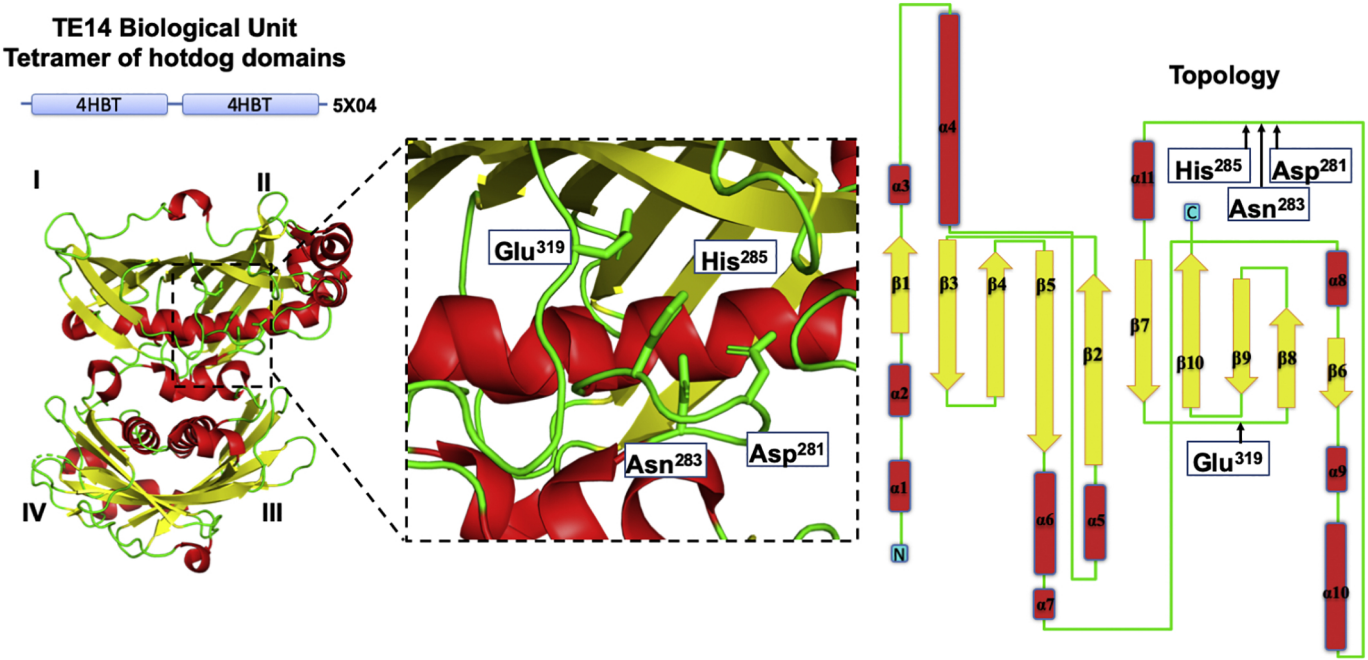
TE14 Biological Unit
Tetramer of hotdog domains
4HBT
4HBT
5X04
I
II
III
IV
Glu319
His285
Asn283
Asp281
Topology
α4
α3
β1
β3
β4
β5
β2
α2
α1
N
α6
α5
α7
α11
His285
Asp281
Asn283
C
β7
β10
β9
β8
α8
β6
Glu319
α9
α10

Figure 18

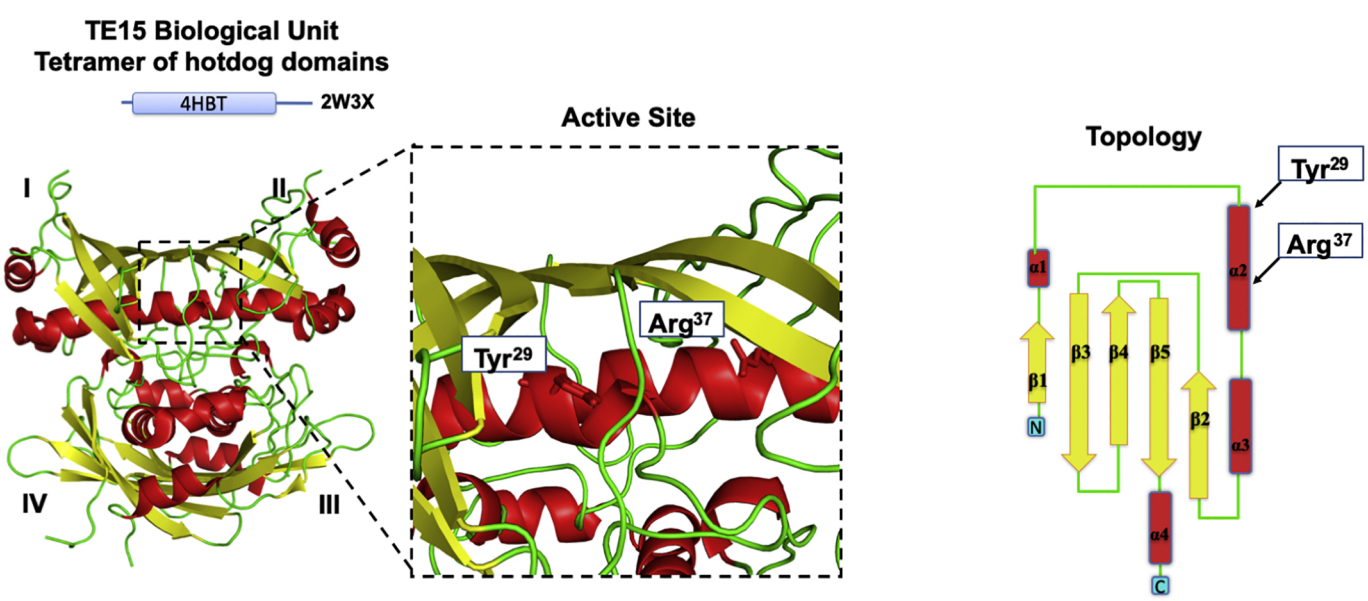
TE15 Biological Unit
Tetramer of hotdog domains
4HBT
2W3X
I
II
III
IV
Active Site
Tyr29
Arg37
Topology
Tyr29
Arg37
α1
α2
β1
β3
β4
β5
β2
α3
α4
N
C

Figure 19

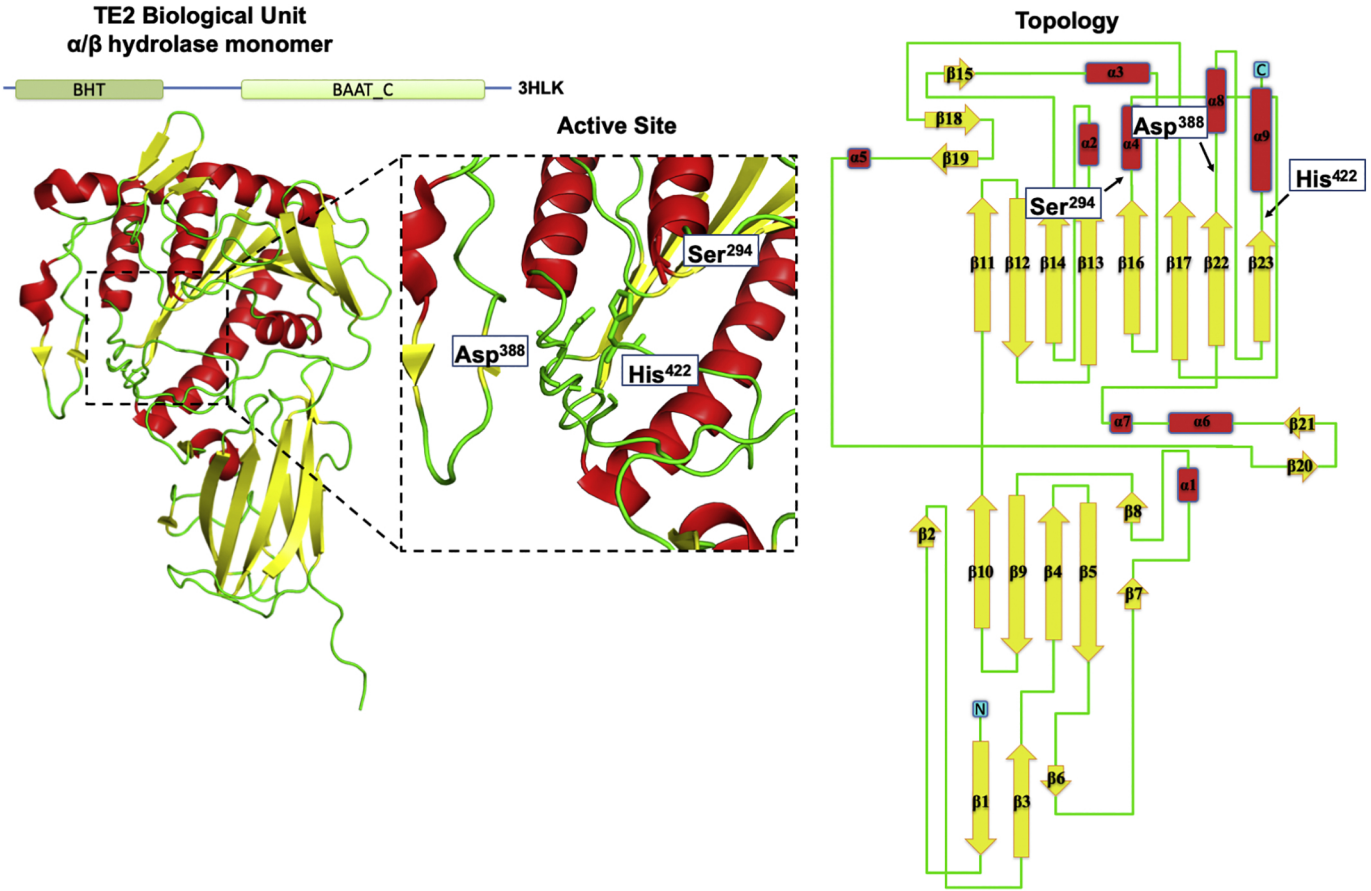
TE2 Biological Unit
α/β hydrolase monomer
BHT
BAAT_C
3HLK
Active Site
Ser294
Asp388
His422
Topology
β15
α3
β18
α2
α4
Asp388
α8
α9
C
α5
β19
Ser294
His422
β11
β12
β14
β13
β16
β17
β22
β23
α7
α6
β21
β20
α1
β2
β8
β10
β9
β4
β5
β7
N
β1
β3
β6

Figure 20

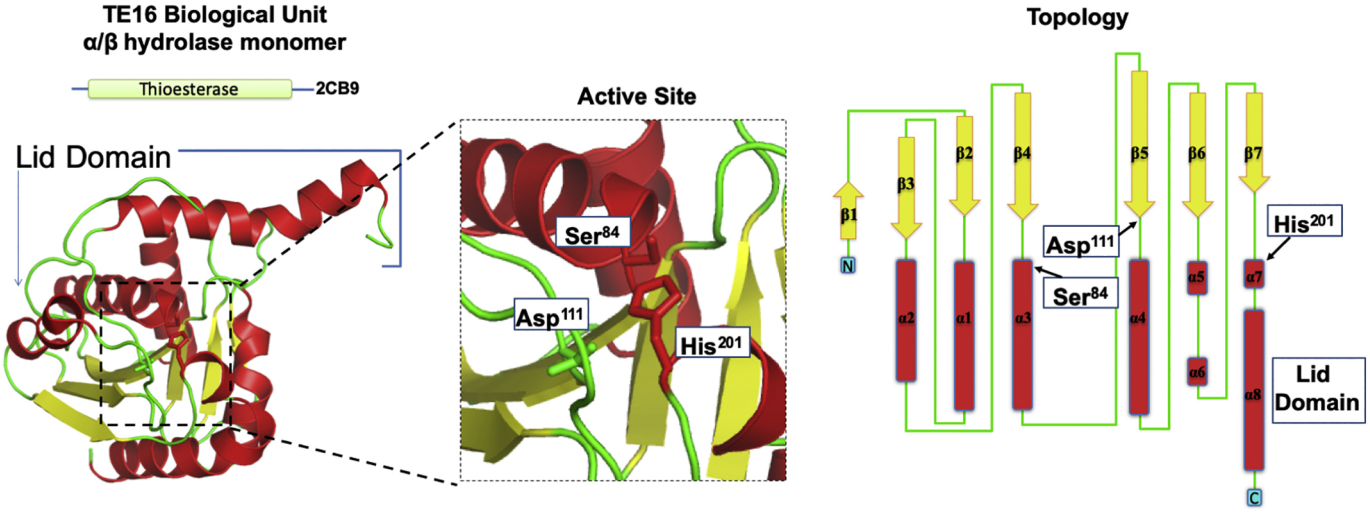
TE16 Biological Unit
α/β hydrolase monomer
Thioesterase
2CB9
Lid Domain
Active Site
Ser84
Asp111
His201
Topology
β1
β3
β2
β4
β5
β6
β7
N
α2
α1
α3
α4
α5
α6
α7
α8
Asp111
Ser84
His201
Lid Domain
C

Figure 21

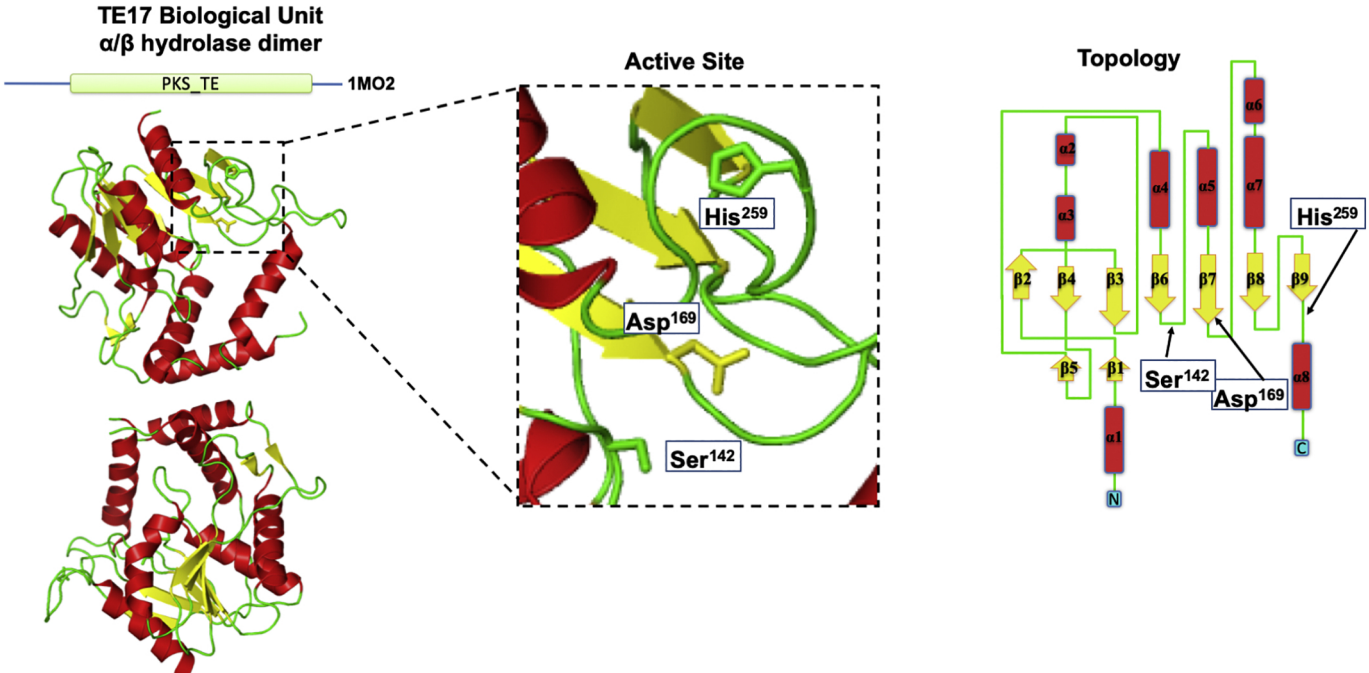
TE17 Biological Unit
α/β hydrolase dimer
PKS_TE
1MO2
Active Site
His259
Asp169
Ser142
Topology
α2
α3
α4
α5
α6
α7
α8
β1
β2
β3
β4
β5
β6
β7
β8
β9
His259
Ser142
Asp169
N
C

Figure 22

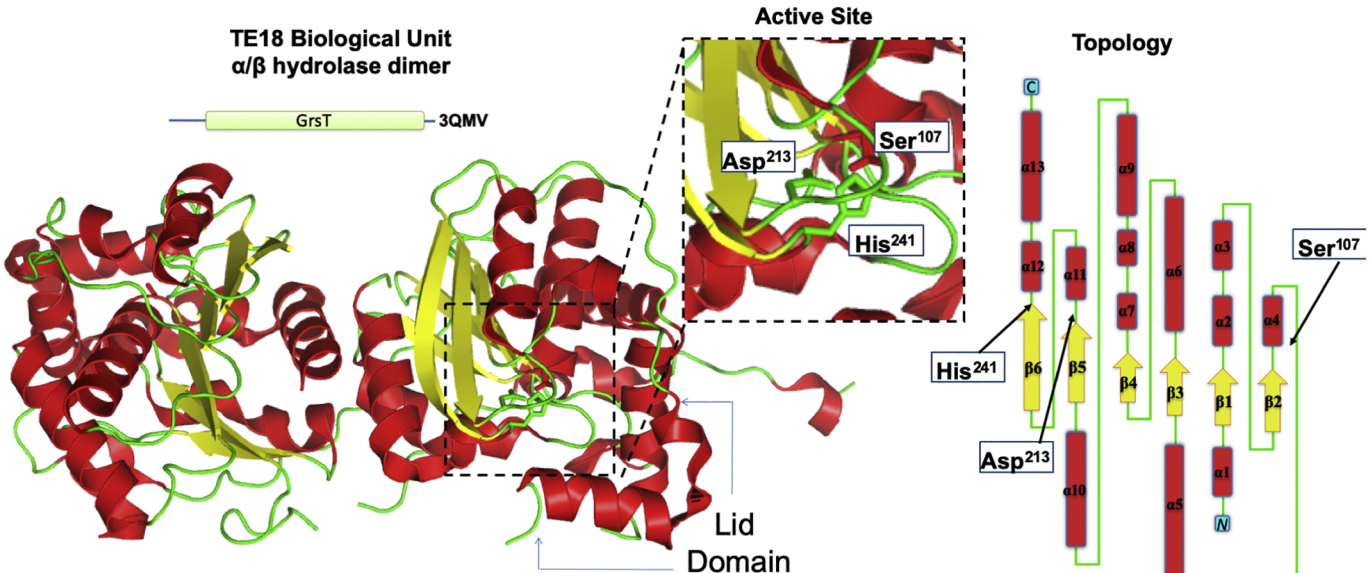
TE18 Biological Unit
α/β hydrolase dimer
GrsT
3QMV
Active Site
Asp213
Ser107
His241
Lid
Domain
Topology
C
α13
α12
α11
α9
α8
α7
α6
α3
α2
α4
Ser107
His241
β6
β5
β4
β3
β1
β2
Asp213
α10
α5
α1
N

Figure 23

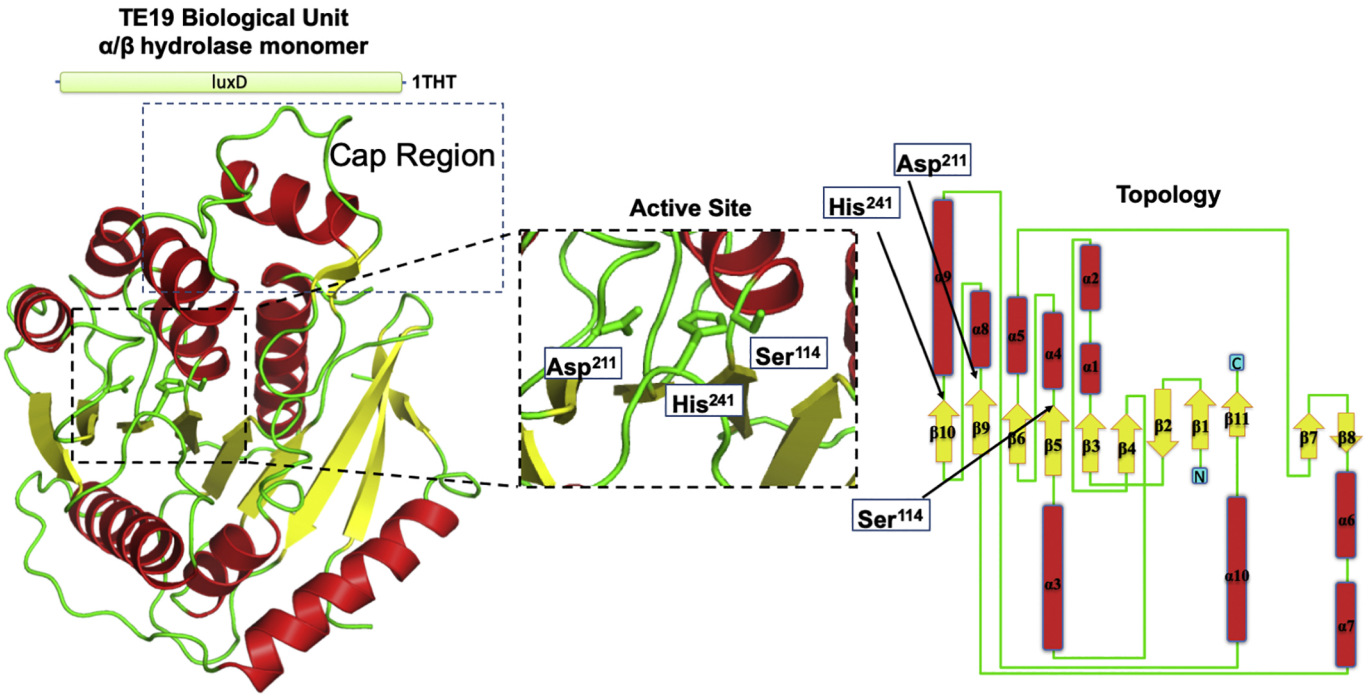
TE19 Biological Unit
α/β hydrolase monomer
luxD
1THT
Cap Region
Active Site
Asp211
Ser114
His241
Asp211
His241
Ser114
Topology
α9
α8
α5
α4
α2
α1
β10
β9
β6
β5
β3
β4
β2
β1
C
N
β11
β7
β8
α6
α3
α10
α7

Figure 24

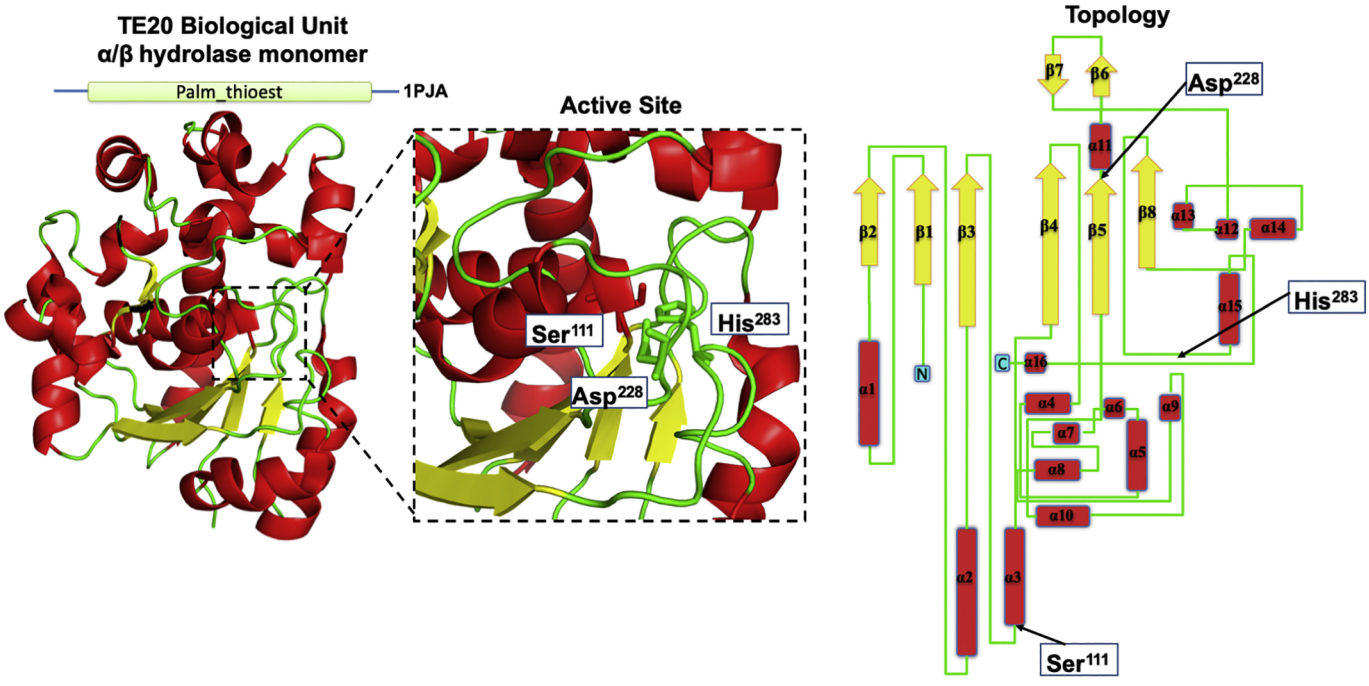
TE20 Biological Unit
α/β hydrolase monomer
Palm_thioest
1PJA
Active Site
Ser111
His283
Asp228
Topology
β7
β6
Asp228
α11
β2
β1
β3
β4
β5
β8
α13
α12
α14
α15
His283
α1
N
C
α16
α4
α6
α9
α7
α5
α8
α10
α2
α3
Ser111

Figure 25

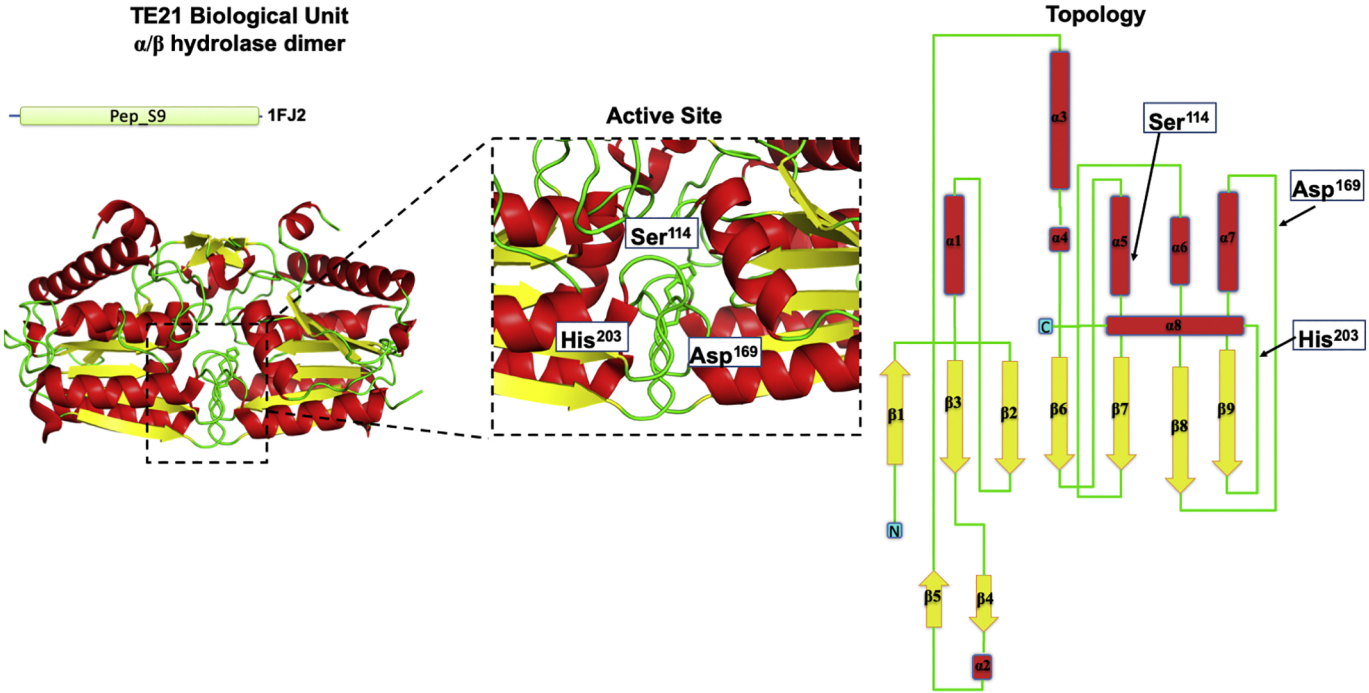
TE21 Biological Unit
α/β hydrolase dimer
Pep_S9
1FJ2
Active Site
Ser114
His203
Asp169
Topology
α3
Ser114
Asp169
α1
α4
α5
α6
α7
C
α8
His203
β1
β3
β2
β6
β7
β8
β9
N
β5
β4
α2

Figure 26

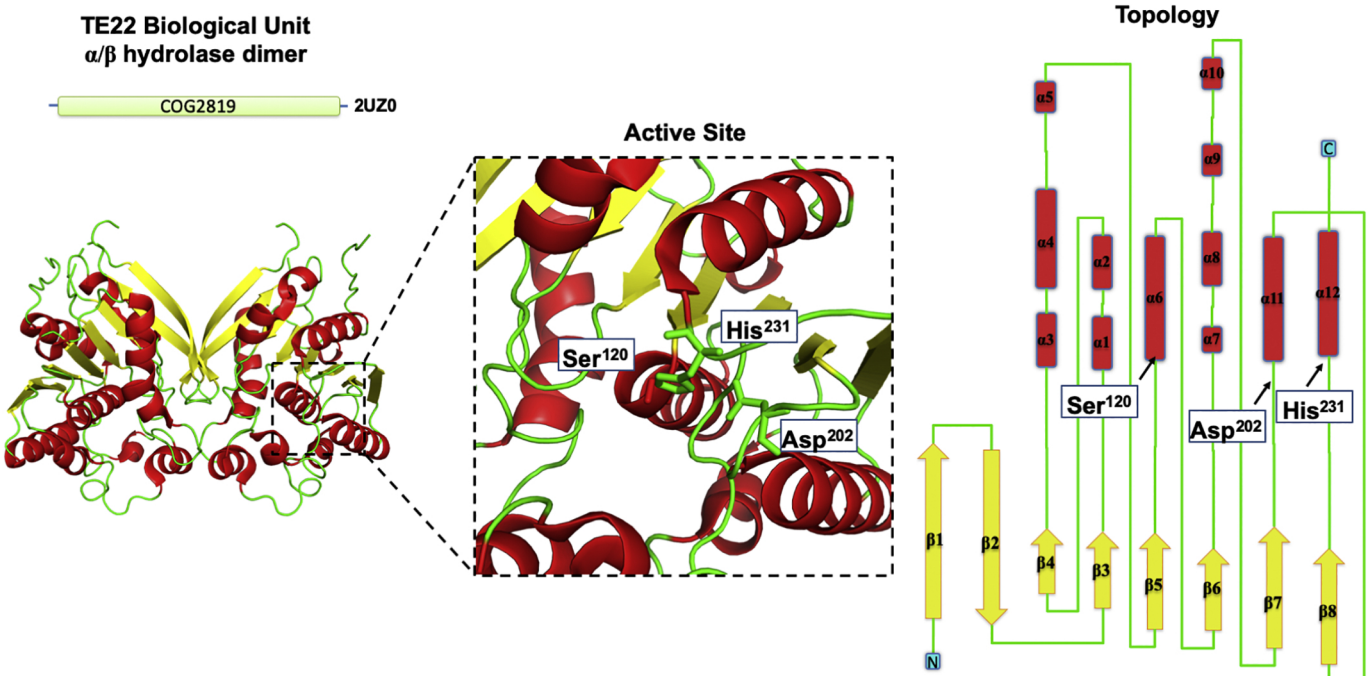
TE22 Biological Unit
α/β hydrolase dimer
COG2819
2UZ0
Active Site
Ser120
His231
Asp202
Topology
α5
α10
α9
C
α4
α2
α6
α8
α11
α12
α3
α1
α7
Ser120
Asp202
His231
β1
β2
β4
β3
β5
β6
β7
β8
N

Figure 27

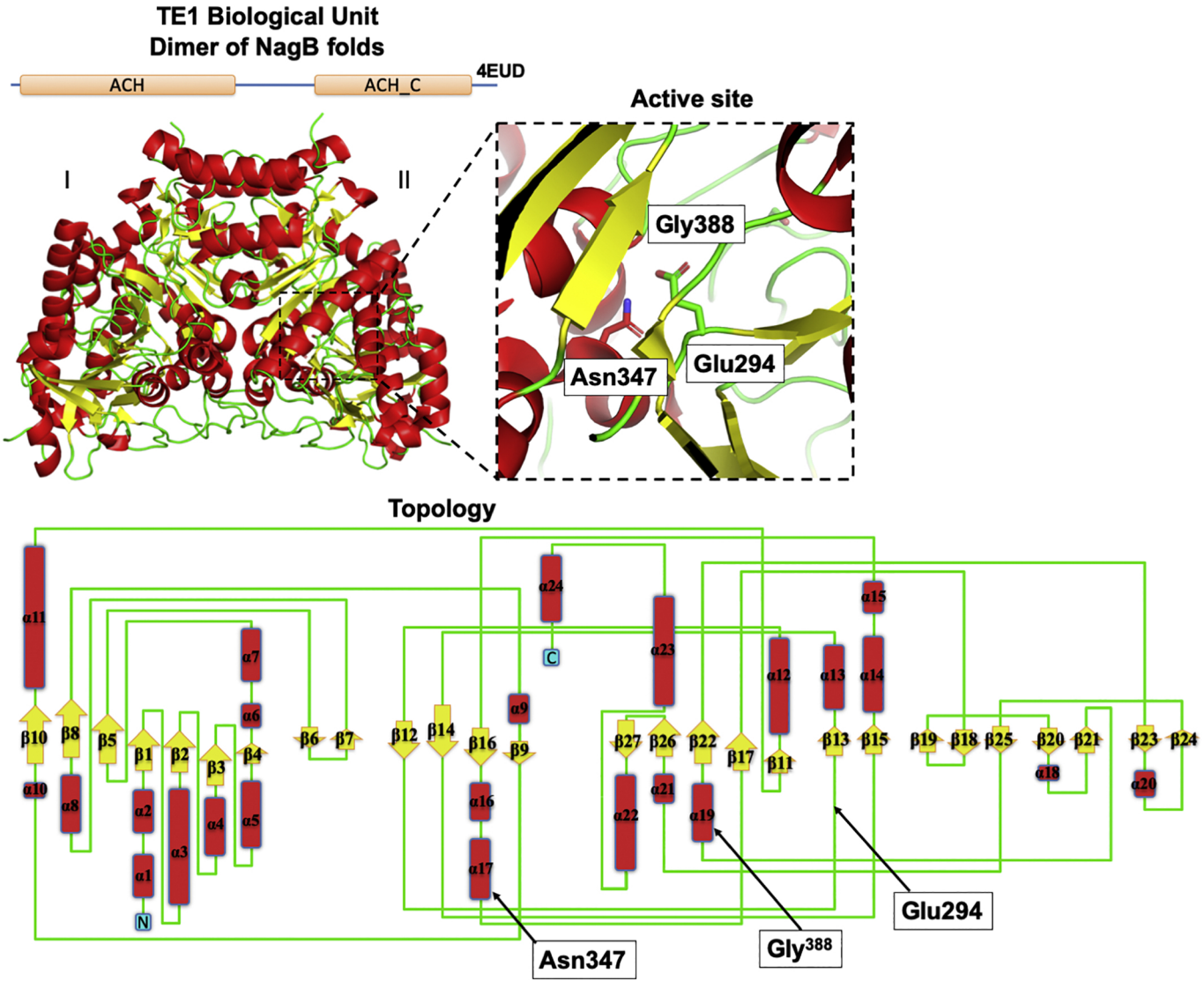
TE1 Biological Unit
Dimer of NagB folds
ACH
ACH_C
4EUD
I
II
Active site
Gly388
Asn347
Glu294
Topology
α11
β10
α10
β8
α8
β5
β1
α2
α1
N
β2
α3
β3
α4
α7
α6
β4
α5
β6
β7
α24
C
β12
β14
β16
α16
α17
α9
β9
α23
β27
β26
α21
α22
β22
α19
β17
α12
β11
α15
α13
α14
β13
β15
β19
β18
β25
α18
β20
β21
α20
β23
β24
Asn347
Gly388
Glu294

Figure 28

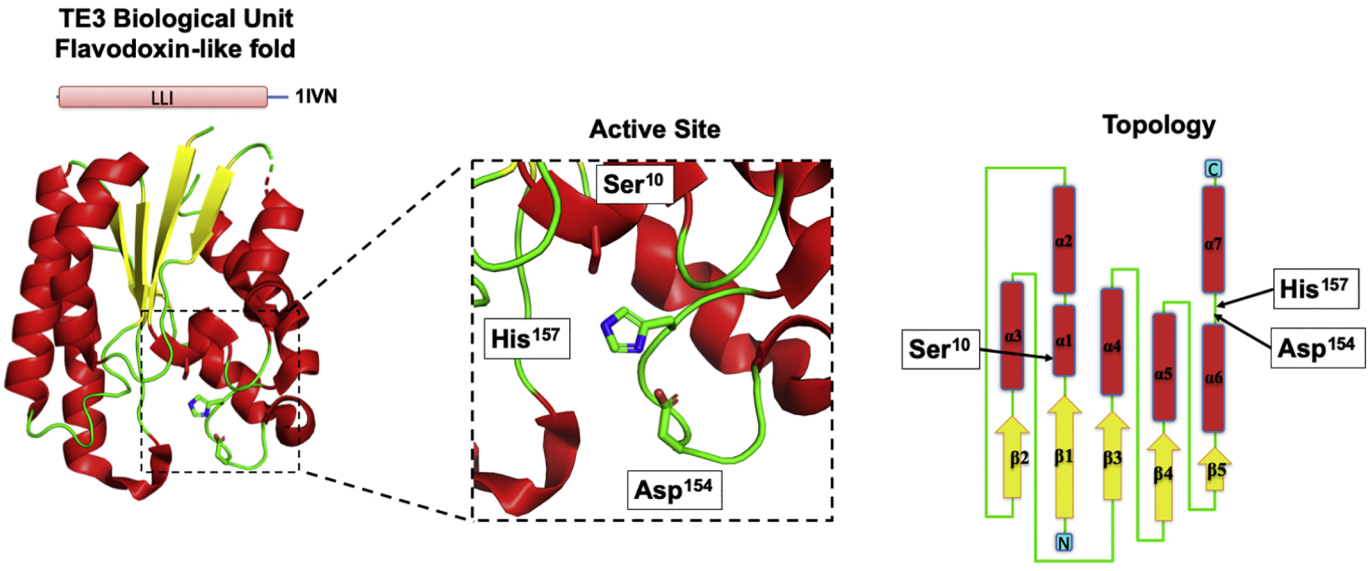
TE3 Biological Unit
Flavodoxin-like fold
LLI
1IVN
Active Site
Ser10
His157
Asp154
Topology
C
N
α1
α2
α3
α4
α5
α6
α7
β1
β2
β3
β4
β5
Ser10
His157
Asp154

Figure 29

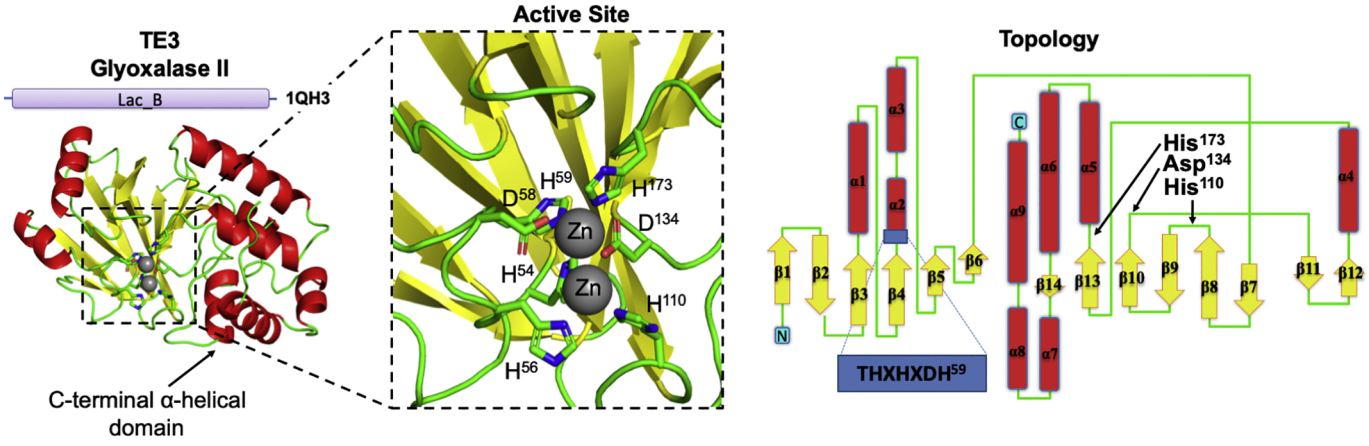
TE3
Glyoxalase II
Lac_B
1QH3
C-terminal α-helical domain
Active Site
D58
H59
H173
D134
H54
Zn
Zn
H110
H56
Topology
α1
α2
α3
α4
α5
α6
α7
α8
α9
β1
β2
β3
β4
β5
β6
β7
β8
β9
β10
β11
β12
β13
β14
N
C
His173
Asp134
His110
THXHXDH59

Figure 30